Photocatalytic Transformations Catalyzed by Inorganic Semiconductors and Iridium Complexes

Dissertation

Zur Erlangung des Doktorgrades der Naturwissenschaften

(Dr. rer. nat.)

an der Naturwissenschaftlichen Fakultät IV

- Chemie und Pharmazie -

der Universität Regensburg

vorgelegt von

Maria Cherevatskaya

aus Usinsk (Russische Föderation)

October 2013

The experimental part of this work was carried out between April 2010 and April 2013 under the supervision of Prof. Dr. Burkhard König at the Institute of Organic Chemistry, University of Regensburg.

The thesis was submitted on:		20.09.2013
Date of the colloquium:		23.10.2013
Board of examiners:	Prof. Dr. Robert Wolf	(chairman)
	Prof. Dr. Burkhard König	(1st referee)
	Prof. Dr. Arno Pfitzner	(2nd referee)
	Prof. Dr. Axel Jacobi von Wangelin	(examiner)

Dedicated to

Vitalik and our boy

&

My Parents and Sisters

“Success is a journey,

not a destination.

The doing is often more important

than the outcome.”

-Arthur Ashe

Table of Contents

CHAPTER 1

1. HETEROGENEOUS PHOTOCATALYSTS IN ORGANIC SYNTHESIS *

* This chapter was submitted to *Russian Chemical Reviews* as Review.

Inorganic semiconductors have found applications as heterogeneous photocatalysts in organic synthesis. Although the majority of reported reactions still aim at the photocatalytic decomposition of organic compounds, the number of examples in synthetic applications is growing. We begin our survey with the discussion of principal mechanisms of heterogeneous semiconductor photocatalysis. The selected examples are limited to inorganic semiconductors and the discussion is divided by the required excitation wavelength, either UV or visible light, and by the bond forming reaction that is catalyzed, either carbon-carbon bonds or carbon-heteroatom bonds. Although we are just beginning to understand the mechanistic details of the reactions, the use of heterogeneous inorganic semiconductors has potential for a broader application in the photocatalyzed synthesis of organic compounds.

1.1 INTRODUCTION

The idea of using photochemical processes to synthesize useful organic chemicals was mentioned already long ago in Giacomo Ciamician´s report in *Science* in 1912 where he raised the question "*Would it not be advantageous to make better use of radiant energy?*" He predicted the rapid development of methods that use abundant and renewable solar energy instead of harmful reagents in organic synthesis.[1a]

Photochemistry has since then developed into a mature field of chemistry. The majority of the experiments use direct excitation of molecules by UV light. Sensitization or photocatalytic methods, in contrast, apply dye molecules, which are excited by visible light irradiation and transfer energy or an electron from the excited state to the molecule to be converted. Such photocatalysts or sensitizers can be either soluble in the reaction media or insoluble leading to homogeneous or heterogeneous reaction mixtures. Widely used homogeneous visible light absorbing photocatalysts are organic dyes, such as Eosin Y, Rose Bengal, Nile Red or Rhodamine B and ruthenium(II), iridium(III) or copper(I) metal complexes. Typical heterogeneous photocatalysts are organic and inorganic semiconductors. We discuss in this review synthetically useful C-C and C-heteroatom bond formation methods mediated by heterogeneous inorganic photocatalysts (Figure 1).

Most early applications of heterogeneous photocatalysis aim for the degradation of organic pollutants or dyes in wastewater streams, water or air or for the photocatalytic splitting of water into hydrogen and oxygen. Only recently heterogeneous photocatalysis was more widely applied to the organic synthesis of fine chemicals.[1b]

We include in our survey the application of UV and visible light absorbing semiconductors. Typical UV absorbing semiconductors are TiO_2, ZnS, and ZnO. Their wide band gap makes them both strong oxidizing and strong reducing agents. Examples of visible light absorbing semiconductors are CdS, surface modified TiO_2 or $PbBiO_2Br$. The redox potential of all heterogeneous semiconductors is pH-dependent in water and again different in organic solvents. Figure 2 summarizes the redox potentials of some common semiconductors.

1.2 TYPICAL REACTION MECHANISMS OF HETEROGENEOUS PHOTOCATALYSIS

The mechanism of inorganic semiconductor (SC) photocatalyzed reactions involves several key steps given in equations 1-3 and is illustrated in Figure 1. Light absorption induces the electron/hole separation (eq. 1). This could be followed by back electron transfer to the valence band, thus regenerating the semiconductor ground state (eq. 2) or the electron-hole pair may undergo subsequent redox reactions with suitable electron donor and acceptor molecules (eq. 3).

$$SC \xrightarrow{h\nu} SC^*(e^-, h^+) \quad (1)$$

$$SC^*(e^-, h^+) \longrightarrow SC + h\nu/\text{heat} \quad (2)$$

$$SC^*(e^-, h^+) + A + D \longrightarrow SC + A^{\bullet -} + D^{\bullet +} \quad (3)$$

A successful organic synthesis using inorganic semiconductor photocatalysts therefore depends on several parameters:

1. The band gap of the semiconductor determines its absorption wavelength. Only a photon with the appropriate energy can excite an electron from the valence band (VB) to the conduction band (CB). The wavelength λ must have larger or equal energy as compared to the band gap energy (E_{BG}):

$$h \cdot v = \frac{h \cdot c}{\lambda} \geq E_{BG},$$

where *h* is the Planck constant, *v* the frequency of the photon and *c* is the speed of light.

The photon energy together with the oxidation potential of the valence band allows an estimation, which chemical processes as half reactions may be feasible (Figure 1). The generated hole at the valence band (VB) corresponds to the available oxidation potential energy. The reduction potential of the excited electron, in turn, is determined by the potential of the CB and can be calculated using the band gap (BG) value:

$$E_{CB}[V] = E_{VB}[V] + \frac{E_{BG}[eV]}{e^0[e]};$$

E_{CB} is the potential of the CB, E_{VB} is the potential of the VB, e^0 corresponds to the number of excited electrons, and E_{BG} is the band gap energy.[2]

2. The redox potentials of the reaction partners are crucial. An appropriate electron acceptor ($A/A^{\cdot-}$) should have a reduction potential lower than the conduction band (CB) of the semiconductor-photocatalyst. On the other hand the electron donor ($D/D^{\cdot+}$) oxidized by the excited photocatalyst should be higher in energy as the photocatalyst's valence band (VB). Using the Rehm-Weller equation one can calculate the Gibbs free energy indicating if the reaction is thermodynamically allowed.

3. When planning a synthesis based on heterogeneous semiconductor photocatalysis, the challenge is to translate the *transient* charge separation into an irreversible and selective reaction. After the semiconductor excitation we can expect different ways how the system loses the obtained energy (eq. 2-3). The easiest way for the excited electron on the CB is to recombine back to the VB (eq. 2) and after this recombination the electron and the hole are lost for a redox reaction. However, the desired way is the interfacial electron/hole transfer at the solid/liquid or solid/gas interface and consecutive redox reactions. In general, the electron/hole recombination time is dependent on the nature of the material and is in the range of ns to µs. In the case of TiO_2 the recombination process is very fast and takes place in about 30 ps.

To classify the bond formation reactions arising from primary redox species ($A^{\cdot -}$ and $D^{\cdot +}$) the group of Kisch suggested the terms of *Photocatalysis type A* and *Photocatalysis type B*. The *Photocatalysis type A* affords two different products – one reduced and one oxidized (eq. 4), while *Photocatalysis type B* leads to one single addition product via an intermolecular bond formation (eq. 5).[3]

$$A + D \xrightarrow[h\nu]{SC} B_{red} + C_{ox} \qquad (4) \qquad \textit{Phototcatalysis type A}$$

$$A + D \xrightarrow[h\nu]{SC} A\text{-}D \qquad (5) \qquad \textit{Photocatalysis type B}$$

It is commonly assumed that species A and D are adsorbed at the semiconductor (SC) surface to allow for electron transfer at high rates, but there are cases where the substrates cannot contact the semiconductor surface. These are examples of aerobic oxidations reactions where the electron transfers to and from adsorbed oxygen and water generates short-lived reactive intermediates that diffuse to the substrates.

Figure 1. Redox reactions of a light-excited semiconductor with electron donor (D) and electron acceptor (A) molecules.

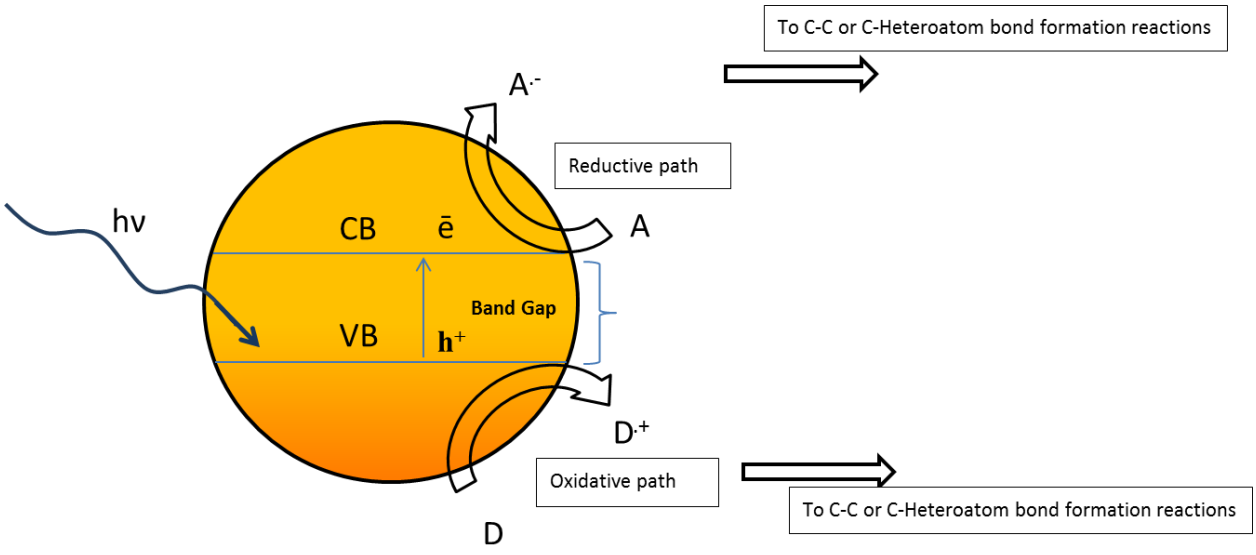

Figure 2. Redox potentials of common semiconductors and redox active sensitizers.

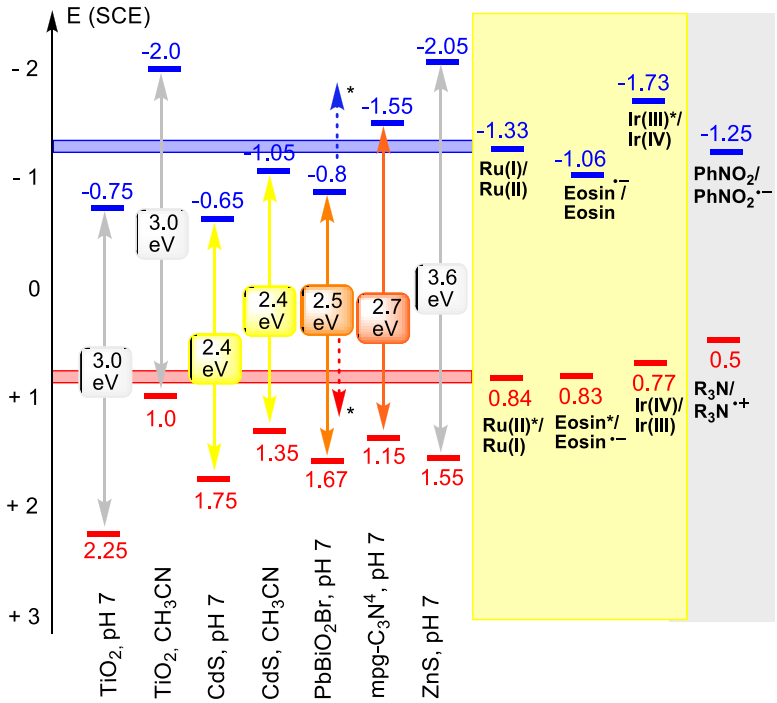

A key feature of photocatalyzed bond formation reactions is that they proceed often under *mild* conditions and allow the conversion of non-activated precursors. Photocatalysis therefore serves as a worthy alternative to thermal processes.

1.3 UV LIGHT MEDIATED HETEROGENEOUS PHOTOCATALYSIS

1.3.1 CARBON-CARBON BOND FORMING REACTIONS

The functionalization of C-H bonds is an ambitious task. Electrochemically[4,5] and thermally generated radicals[6,7,8] have been used, but photocatalytically generated radicals seem to be a promising alternative due to the rapidly growing achievements in this field. Successful examples of such transformations used the UV light absorbing homogeneous photocatalyst tetrabutylammonium decatungstate (TBADT) in the alkylation of α,β-unsaturated ketones or alkenes and other examples.[9,10,11,12,13]

The heterogeneous photocatalyst TiO_2 is widely used in water and air purification. It absorbs light up to 405 nm and is a very strong oxidant (+2.25 V, pH7, SCE; +1.0 V, CH3CN, SCE). The

anatase modification of TiO_2 turned out to be essential in the photocatalytic C-H functionalization of amides.[14] The Caronna group irradiated the semiconductor with sunlight and the electron/hole pair is able to oxidize formamide, N, N-dimethylformamide and N, N-dimethylacetamide via single electron transfer from the amide to the valence band of TiO_2. The one electron oxidation is followed by deprotonation of the amides giving the corresponding radicals, which then reacted with heterocycles. The example with formamide is shown in Scheme 1. The method was further extended to the functionalization of heterocycles using cyclic ethers as shown in Scheme 2.[15]

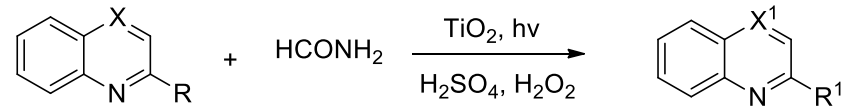

(1) X = CH, R = H
(2) X = CH, R = CH3
(3) X = C-CH3, R = H
(4) X = N, R = H

(5) X^1 = CH, R^1 = $CONH_2$
(6) X^1 = C-$CONH_2$, R^1 = CH_3
(7) X^1 = C-CH_3, R^1 = $CONH_2$
(8) X^1 = N, R^1 = $CONH_2$

GC yields, %:
(5) 90
(6) 100
(7) 69
(8) 42

Scheme 1. Functionalization of nitrogen heterocycles with formamide using TiO_2 photocatalysis.

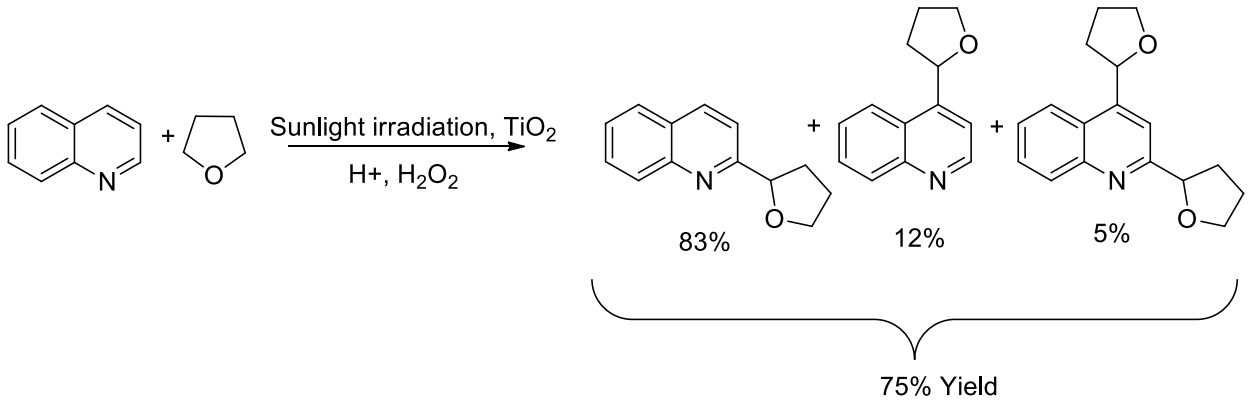

Scheme 2. Quinoline functionalization with photocatalytically oxidized ethers.

The oxidation of THF and other unsaturated cyclic ethers by UV light excited ZnS (1.82 V vs. NHE, pH 7) was reported by the Kisch group.[16] An unsaturated cyclic ether, 2, 5-dihydrofuran, undergoes the ZnS photocatalyzed one-electron oxidation and deprotonation 10 times faster compared to the photocatalytic THF oxidation. Both substrates form dimers as shown in Scheme 3.

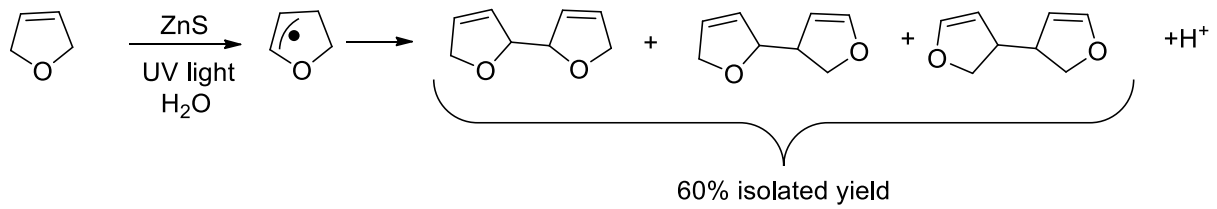

Scheme 3. ZnS-photocatalyzed 2,5-dihydrofurane dimerization.

Another example of TiO_2 heterogeneous photoredox catalysis is the C-C bond formation between an electrophilic alkene and adamantane.[17] Within 24 h irradiation time the target product was formed in only 35% yield (Scheme 4, path 1). By adding silver sulfate as a sacrificial electron acceptor, the yield increased to 75% (Scheme 4, path 1). As in the previously discussed examples, the single electron transfer oxidation of adamantane is followed by deprotonation leading to the 1-adamantyl radical that couples with isopropylydenmalonitrile (IPMN) (Scheme 4, path 1). Without the presence of the coupling reagent, 1-adamantyl radical dimerizes in trace amounts (Scheme 4, path 2) or couples with CH_3CN used as a solvent leading to 1-adamantyl methyl ketone (14% yield) via the iminyl radical (Scheme 4, path 3).

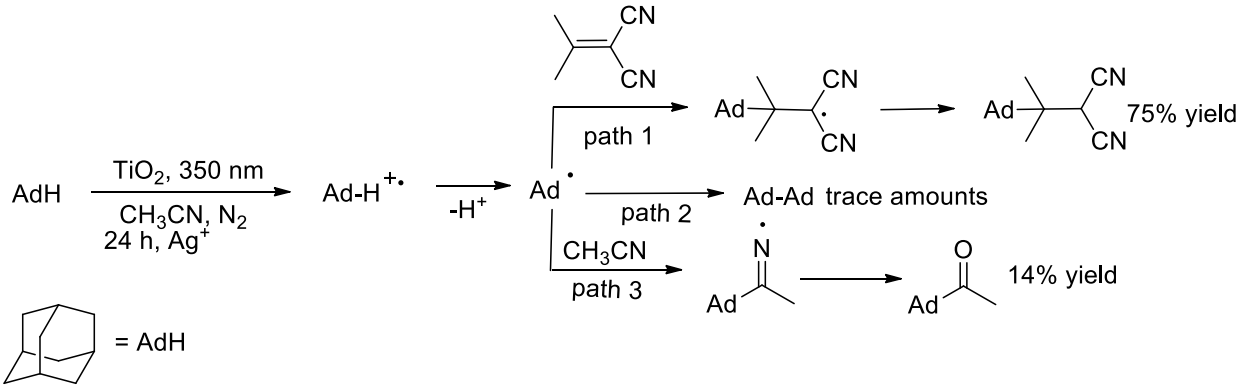

Scheme 4. C-C bond formation with adamantane by TiO_2 photocatalysis.

Easier than C-H activation is the activation of Si-C bonds, for example in R-TMS groups. As a good electrofugal group, trimethylsilyl is prone to leave the molecule after one-electron photooxidation by a suitable heterogeneous semiconductor. This principle was implemented in the radical alkylation of electrophilic olefins.[18] 4-Methoxybenzyl(trimethyl)silane (E_{ox} = 1.31 V *vs*. SCE in CH_3CN) serves as a single electron donor to the valence band of excited TiO_2. The electrophilic olefin plays the role of either a radical trap (Scheme 5, path 1) or electron acceptor

from the conduction band of TiO_2 (Scheme 5, path 2). This in turn facilitates the reaction course to the desired product (E_{red} = -0.84 V vs. SCE in CH_3CN for maleic acid or maleic anhydride). 4-Methoxybenzyl radical is reduced by the radical anion (Scheme 5, path 3) or by electron transfer from the conduction band of the TiO_2 semiconductor (Scheme 5, path 4), and protonated by water present in the solvent to give the final products. The isolated product yields in the case of these two radical traps were similar and in the range of 65%.

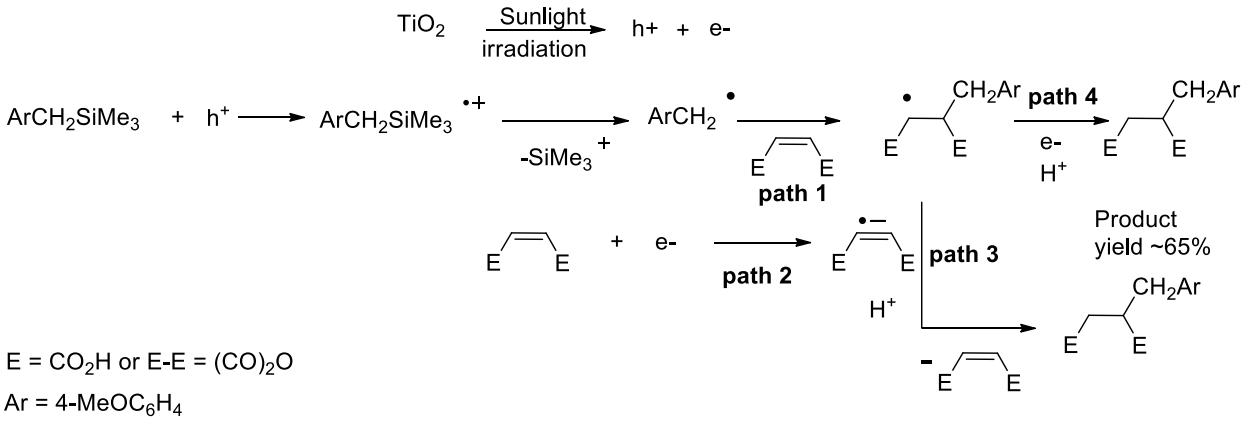

Scheme 5. Radical alkylation of electrophilic alkenes.

UV-light absorbing semiconductor TiO_2 proved to be an alternative to homogeneous photoredox-active organic dyes that were used in Aza-Henry and Mannich reactions, in C-P and other C-C bond formation reactions (Scheme 6).[19] The reaction starts with the easy oxidation of the tertiary amines, here tetrahydroisoquinolines (THIQ) that form highly reactive iminium ion intermediates after one-electron oxidation by a photoexcited semiconductor. The heterogeneous photocatalysts can be reused. They proved to be effective even after five consecutive photocatalytic reactions in case of the Aza-Henry reaction with TiO_2.

Oxidative Aza-Henry reaction

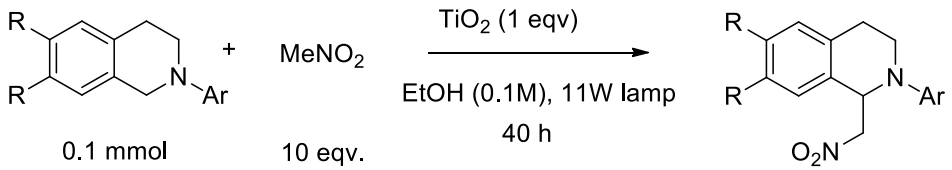

0.1 mmol

10 eqv.

R = H, OMe

Ar = phenyl, 4-MeO-phenyl, 4-F-phenyl, 2-Me-phenyl, 2-naphtyl and 4 more examples

Isolated yields 61 - 96%

Oxidative Mannich reaction

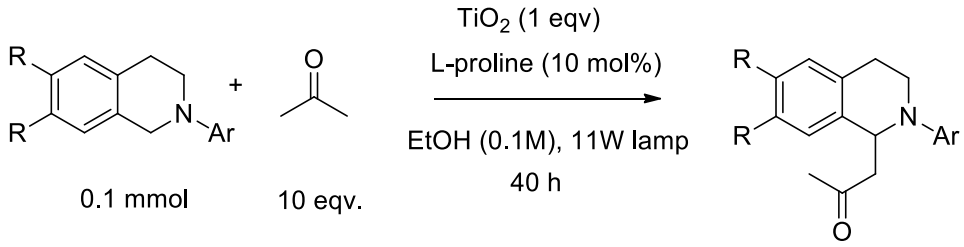

0.1 mmol

10 eqv.

R = H, OMe

Ar = phenyl, 4-MeO-phenyl, 4-F-phenyl, 4-Me-phenyl, 3-MeO-phenyl and 3 more examples

Isolated yields 54 - 98%

Oxidative cyanation reactions

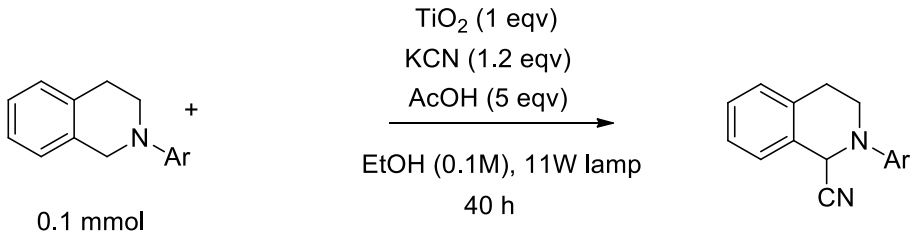

0.1 mmol

Ar = phenyl, 4-MeO-phenyl, 4-F-phenyl, 3-MeO-phenyl and 2 more examples

Isolated yields 79 - 99%

Scheme 6. TiO_2 mediated in C-C bond forming photocatalysis with tetrahydroisoquinolines.

Chiral metal-organic frameworks (MOFs) merge the properties of photoredox catalyst and organocatalyst.[20] Two independent units of L- or D-pyrrolidin-2-ylimidazole (PYI) serve as organocatalysts and triphenylamine is incorporated as photoredox active group into a solid framework that makes the system heterogeneous. The new porous metal-organic framework consists of a two-dimensional brick wall layered structure built from three connected binuclear zinc nodes and 4,4′,4″-nitrilotribenzoate bridges. Two investigated metal-organic frameworks Zn-PYI1 and Zn-PYI2 are mirror images that give identical products with inverse configuration. When producing these MOFs L-N-*tert*-butoxycarbonyl-2-(imidazole)-1-pyrrolidine was used for Zn-PYI1 and D-N-*tert*-butoxycarbonyl-2-(imidazole)-1-pyrrolidine was used for Zn-PYI2. The two heterogeneous photo-organocatalysts absorp at 350 nm and the redox potential of the excited-state Zn−PYI1+/Zn−PYI1* (or Zn−PYI2+/Zn−PYI2*) couple was estimated as −2.12 V *vs.* SCE being more negative than diethyl 2-bromomalonate (E^0 = -0.49 V) a well-known α-alkylation agent.[21] The successful reaction between diethyl 2-bromomalonate and phenylpropylaldehyde (**1**), octaldehyde (**2**), or (E)-non-6-enal (**3**) gave 74% (92%), 65% (86%) and 84% (92%) yield (*ee*), respectively (Scheme 7, aldehydes **1**, **2**, **3**). The pore size of the Zn-PYI1 catalyst is large enough to allow all these substrates to pass through, but the more bulky aldehyde **4** (Scheme 7, aldehyde **4**) larger than the pore size of Zn−PYI1 gave only gave 7% of α-alkylation product reaction under the same reaction conditions. The size selectivity of the substrate indicates that the alkylation reactions occurred mostly in the channel of the catalyst, but not on the external surface.

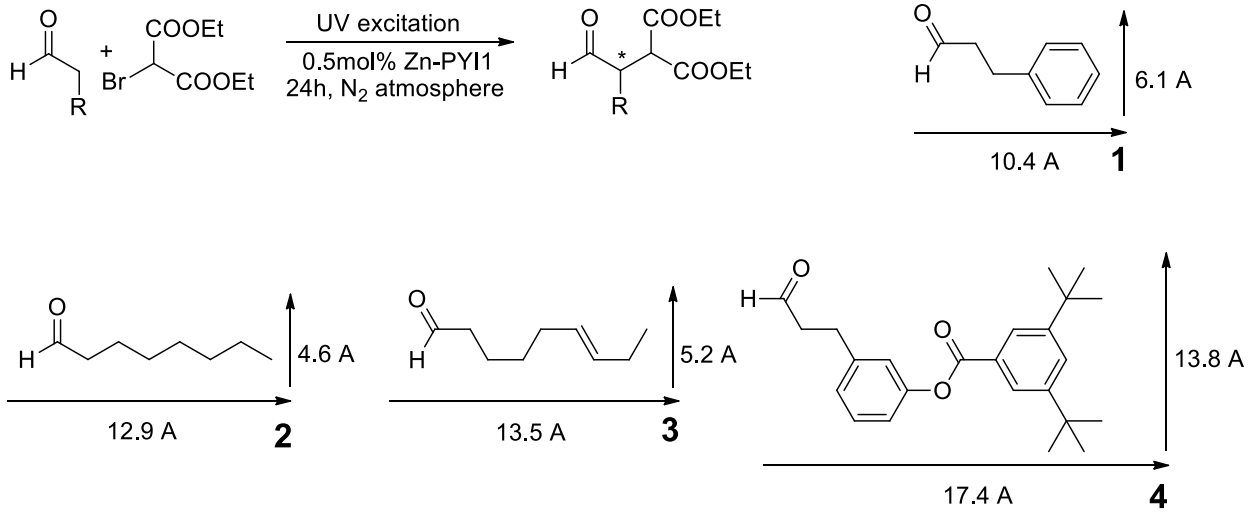

Scheme 7. MOF photocatalytically driven α-alkylation of aldehydes 1, 2, 3, 4.

1.3.2 CARBON-HETEROATOM BOND FORMING REACTIONS

1.3.2.1 C-P bond forming reactions

ZnO is another well-known UV-light absorbing semiconductor. The material was used to catalyze a C-P bond formation reactions described previously by the König group.[22] As discussed above, the one-electron oxidation of the tertiary amine tetrahydroisoquinoline by ZnO under irradiation allows coupling with diethyl phosphonate (Scheme 8).[23] Recycling experiments showed that the photocatalyst is effective for four subsequent reaction cycles.

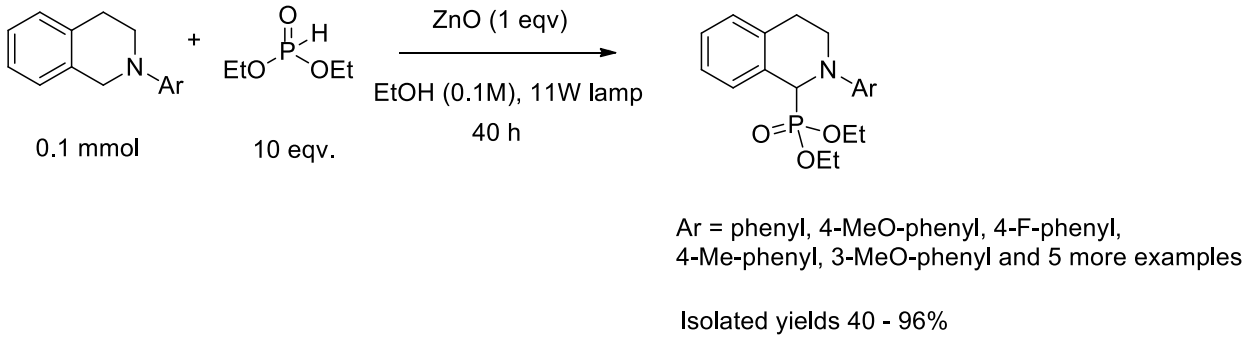

Scheme 8. Zinc oxide mediated oxidative phosphonylation reactions.

1.3.2.2 C-N bond forming reactions

In a modification of the above mentioned ZnS photocatalyzed dimerization of 2,5-dihydrofuran (described in section 3.1) the reactive radical intermediates were trapped by azobenzene to form a C-N bond yielding an allylhydrazine.[24] This method of photocatalyzed C-N bond formation is suitable for a range of 1,2-diazenes in combination with cyclic allyl or enol ethers and olefins as shown in Scheme 9. Difficulties in the purification process of the compounds led to low isolated yields (10-40 %) compared to the yields determined via HPLC analysis. A strong solvent dependence was observed for this photocatalytic process; the reaction proceeds fast in pure methanol or mixtures of methanol or water with n-hexane or THF while no reaction could be observed in dry solvents. The irradiation was performed with a high-pressure mercury lamp. In the case of 1-*tert*-butyl-2-phenyldiazene only one product isomer could be observed, which

can be explained by the higher stability of the phenyl substituted hydrazyl radical compared to the ^{t}Bu substituted one. The investigations by the Kisch group lead to the mechanistic proposal given in Scheme 10.[24] The first excitation step leads to an electron hole pair formation in the semiconductor. The allyl, enol or olefin radical in the oxidative part can be formed stepwise from the initial radical cation by deprotonation or via a simultaneous process where electron transfer is coupled with deprotonation. The hydrazyl radical in the reductive part forms via electron transfer to 1,2-diazene coupled with protonation. The reaction is a typical example of a *type B* heterogeneous photocatalysis.

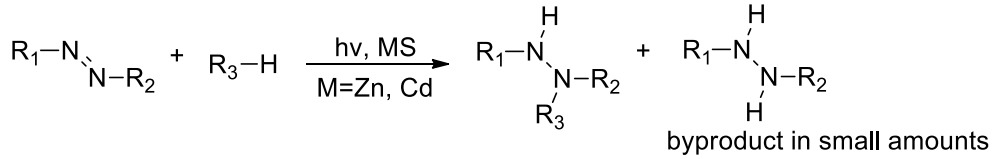

R_1	Ph	*p*-MeC_6H_4	^{t}Bu
R_2	Ph	*p*-MeC_6H_4	Ph

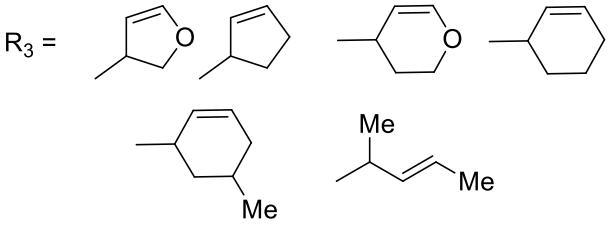

Scheme 9. Photocatalyzed C-N bond formation through the addition of cyclic allyl/enol ethers and olefins to 1,2-diazenes.

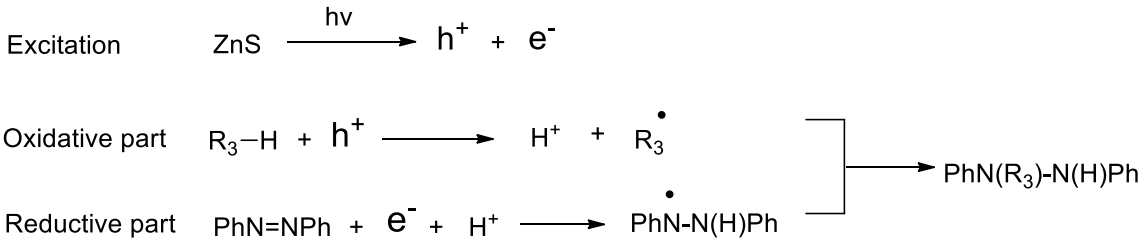

Scheme 10. Mechanism of photocatalyzed C-N bond formation

Another principle of C-N bond construction was implemented when mixtures of primary alcohols and primary amines were irradiated with UV-light in the presence of TiO_2 loaded with Pd[25] or Au[26] nanoparticles.

The mechanism as proposed by Stibal et. al.(Scheme 11)[26] for the formation of secondary amines using Au/TiO_2 and Pd/TiO_2 and includes one electron oxidation of the primary alcohol and subsequent condensation of the resulting aldehyde and amine, which is not photocatalytic. The alcohol oxidation can proceed via direct oxidation by holes from the valence band of the photocatalyst or indirectly via $OH^{\cdot}$ radicals, formed from the reaction of OH^- ions with surface holes. Further hydrogenation of the imine double bond proceeds via molecular hydrogen that is formed from protons on Au or Pd nanoparticles and electrons from the conduction band of the excited TiO_2. Particle size is crucial for the successful process with the optimum being around 5 nm for Au nanoparticles and around 2.5 nm for Pd nanoparticles. Scheme 12 represents the scope of the substrates when palladium nanoparticles are used and Scheme 13 for gold nanoparticles. Moreover the Au/TiO_2 photocatalyzed cyclization of 5-aminopentanol resulted in an acceptable yield of δ-valerolactam (Scheme 14), which shows that the method can in principle be applied to the synthesis of commercially valuable lactams and heterocyclic amines.

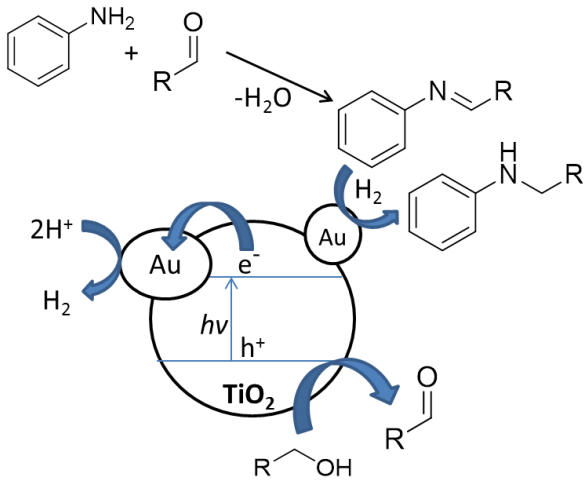

Scheme 11. Mechanism of photocatalytic secondary amine formation.

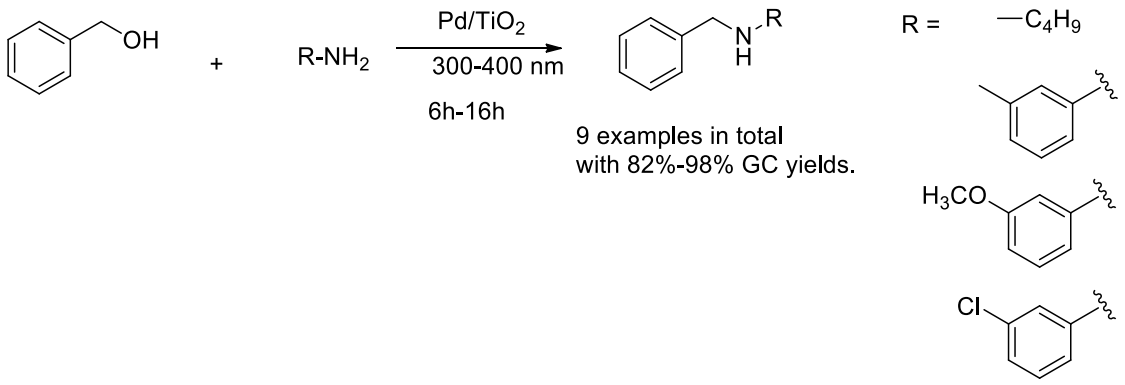

Scheme 12. Secondary amine formation by Pd/TiO_2 photocatalysis.

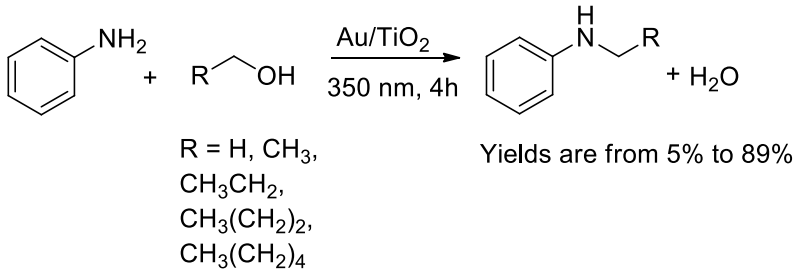

Scheme 13. Secondary amine formation over Au/TiO_2 photocatalysis.

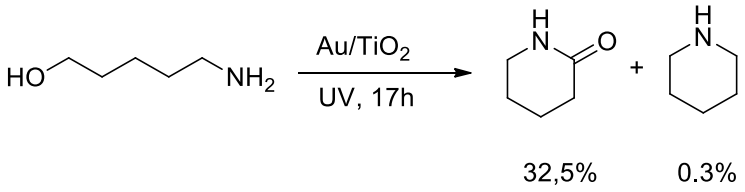

Scheme 14. Au/TiO_2 photocyclization of 5-aminopentanol.

1.3.2.3 C-O bond forming reactions

To pursuit the synthesis of fine chemicals the group of Matsumuro investigated photocatalytic epoxidation of olefins over TiO_2 and UV light irradiation, as epoxides are valuable intermediates for polymer synthesis.[27] The C-O bonds construction requires the presence of O_2 in the reaction

mixture. The epoxydation of 1-hexene, 1-decene and 1-hexadecene occurred to be selective giving the corresponding epoxides as almost single products when TiO_2 in the anatase modification is used as photocatalyst. This could be explained by the high capability of anatase TiO_2 to adsorb oxygen as component for a successful photocatalytic process. The chemical yield of the epoxide products increases with shorter olefin chains, in the case of 1-hexene it reached 79% while 1-decene gave 68% and 1-hexadecene gave 42% of the corresponding 1,2-epoxides. According to the oxidation potentials of starting olefins that are in the range of 0.98 – 1.0 V vs. Ag/AgCl (CH_3CN) the photogenerated holes on the valence band of TiO_2 are able to oxidize them to the corresponding radical cations with subsequent oxidation by oxygen yielding the desired epoxides.

1.4 VISIBLE LIGHT MEDIATED HETEROGENEOUS PHOTOCATALYSIS

1.4.1 PHOTOREDUCTION OF NITRO GROUPS

The photocatalytic reduction of nitrobenzene derivatives has been investigated in detail including visible light mediated heterogeneous photocatalysis. This N-H bond formation from N-O bonds is a 6 electron plus 6 proton reaction process (Scheme 15). Different heterogeneous photocatalysts such as Ru(II) dye sensitized metal deposited TiO_2,[28] Ru(II) dye sensitized urea modified TiO_2[29] and $PbBiO_2X$ (X = Br, Cl, I)[30] were applied for the photocatalytic reductions of nitrobenzene derivatives to the corresponding anilines.

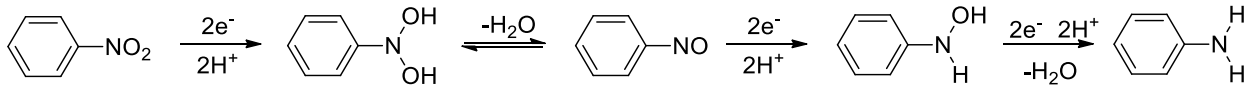

Scheme 15. Reduction of nitrobenzene to anilin.

Ru(II) dye sensitized TiO_2 is the active part of the Grätzel solar cell[31] and possesses an absorption maximum in the green region of the solar spectrum that has the highest intensity. This heterogeneous semiconductor mediates the reduction reaction well if the appropriate amount and particle size transition metal nanoparticles are present. The metal nanoparticles are obtained by photocatalytic reduction of Pt(II), Pt(IV), Pd(II), Ag(I) or Au(III) salts.[28] The formed clusters serve 1) as electron acceptors for the conduction band of the excited dye-sensitized TiO_2 (Scheme 16) and further generate dihydrogen by proton reduction provided

from the photocatalytically oxidized triethanol amine (TEOA) that closes the photocatalytic cycle by reducing the redox active dye and 2) as hydrogenation catalysts for the organic substrates. Systematic variation of the transition metals, their amounts and the method of their reduction revealed a relationship between the nature of the metal and the optimal catalytic amount. The most promising results with almost quantitative nitrobenzene conversion gave Pt colloids in the range of 10^{-1} – 10^{-6} mol%, Au(III) salts in the range of 10^{-1} and 10^{-4} mol% and 0.5 – 0.01 mol% of Pt(II) and Pd(II) salts (Scheme 16). The amount of the metal nanoparticle catalyst with a concentration of more than 1 mol% led to small conversions in all metal salts cases. An investigation of the morphology of the formed transition metal particles by transition electron microscopy revealed that the catalytically active particles have a typical size below 20 nm.

Using one of the best working catalysts precursors, K_2PtO_6, the substrate scope was extended to the photocatalytic reduction of aldehydes. The experiments indicated that it is necessary to optimize the salt concentration according to every substrate: ethyl 4-nitrobenzoate, 4-nitrobenzonitril, 4-nitrobenzaldehyde, 4-bromonitrobenzene, 1,4-dinitrobenzene, 1,2-dinitrobenzene, 2-nitroacetophenone and 4 more examples.

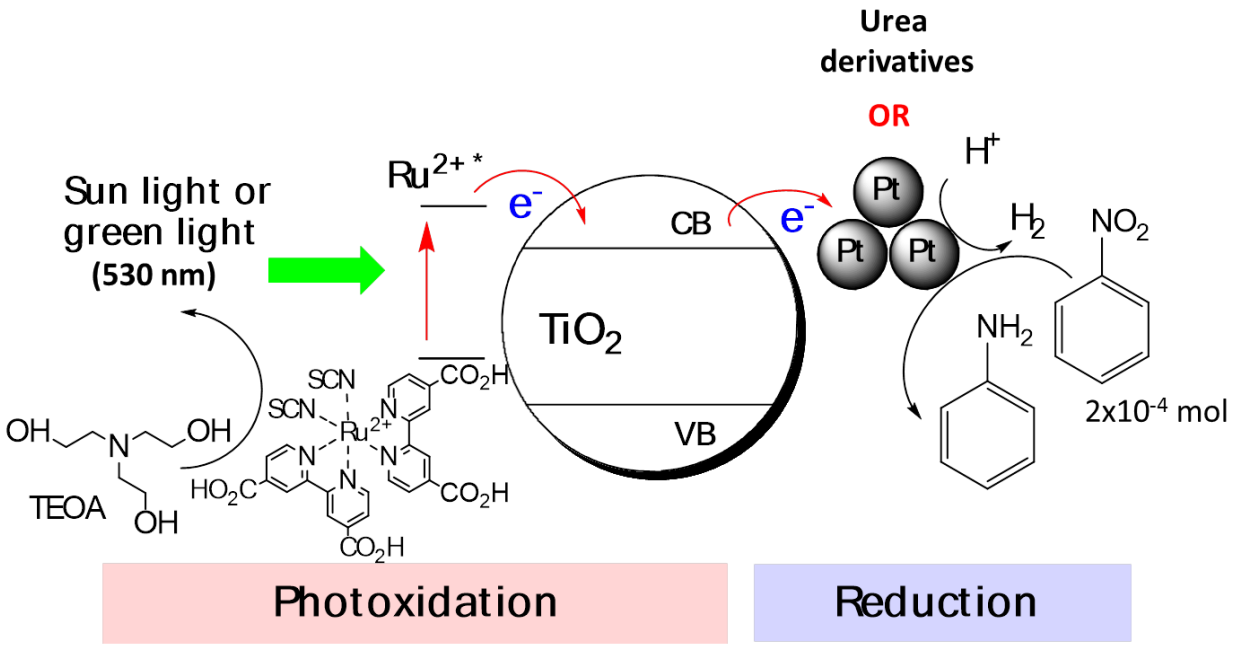

Scheme 16. The photocatalytic nitrobenzene reduction giving aniline as the main product is dependent on the amount of metal salts or urea derivative additives. The immobilized Ru(II) catalyst corresponds to 2 mol% with respect to nitrobenzene.

Later an enhanced photocatalytic activity of Ru(II)/TiO_2 heterogeneous photocatalyst in the nitroarenes reductions was found if urea derivatives are present.[29] Urea itself serves as proton transfer mediator. The oxidation of TEOA by the photocatalyst provides the electrons and protons necessary for the nitrobenzene reduction. Their transfer to the nitroarene substrate may be the rate determining step. The investigation showed that the addition of urea derivatives accelerates the proton transfer thus facilitating the use of TiO_2 based photocatalysts in nitroarene reductions. It was found that urea, thiourea, N, N-dimethylurea and tetramethylurea in 10^{-4} mol% (with respect to nitrobenzene) lead to almost quantitative conversion of nitrobenzene in the photocatalytic system (Scheme 16). The method also enhances the conversion of 4-cyano, 4-bromo and 4-COOEt nitrobenzenes to the corresponding anilines when using 10^{-4} mol% thiourea in the reaction mixture.

Semiconductors of the composition $PbBiO_2X$ (X = Br, Cl) were also used for the photocatalytic reduction of nitrobenzene derivatives under visible-light irradiation. The heterogeneous semiconductor is colored and absorbs visible-light without any additional sensitization.[30] The visible-light absorption is caused by the narrow band gap of the materials that is in range of 2.47 – 2.55 eV (Figure 2). These solid materials have a layered structure which consist of covalent metal oxygen layers $^{2}_{\infty}[PbBiO_2^{+}]$ separated by halide layers. The metal atoms reach the outer crystal surface and become therefore accessible for the catalytic process. Used for the same photocatalytic nitrobenzene reduction with blue light irradiation $PbBiO_2Br$ and $PbBiO_2Cl$ promoted almost a full conversion of nitrobenzene to aniline as the single main product (monitored by gas chromatography); no urea derivatives or metal nanoparticle are required in the process. Moreover the recycled $PbBiO_2Br$ semiconductor promoted the nitrobenzene photocatalytic reduction for up to 5 cycles without any lose in efficacy and is applicable for photocatalytic reduction of a wide range of nitrobenzene derivatives *e.g.* 4-OH, -COOEt, -CN, -NO_2, -CHO nitrobenzenes (overall 12 examples reported) with moderate to excellent conversions.

1.4.2 CARBON-CARBON BOND FORMING REACTIONS

The material most used in reactions of this type is the semiconductor CdS. With an appropriate band gap (2.4 eV) and oxidation potential (+1.5 V vs. SCE, CH_3CN) this semiconductor was thoroughly investigated by Kisch et al. A limitation of the semiconductor is its easy

photocorrosion. The dimerization of 2, 5-dihydrofuran by one-electron oxidation via excited ZnS was already mentioned in section 3.1 (Scheme 3). Substituting ZnS with CdS allows the excitation by visible light. The product distribution is unchanged.

The 2,5-dihydrofuryl radical could be further employed in C-C heterocoupling reactions with imines. Moreover the substrates that undergo one electron oxidation include different allyl/enol ethers and olefins. The resulting homoallylimines could be obtained in 30-75% yield when trisubstituted imines were used in the photocatalytic cycle (Scheme 17). Disubstituted imines in the same photocatalytic reaction with cyclopentene give the hydrodimer along with the desired homoallylamine as shown in Scheme 18. Its formation suggests a parallel one-electron reduction process from the conduction band of the excited photocatalyst to the imine affording the α-aminodiphenymethyl radical that couples with an allylic radical formed via the oxidative electron transfer.

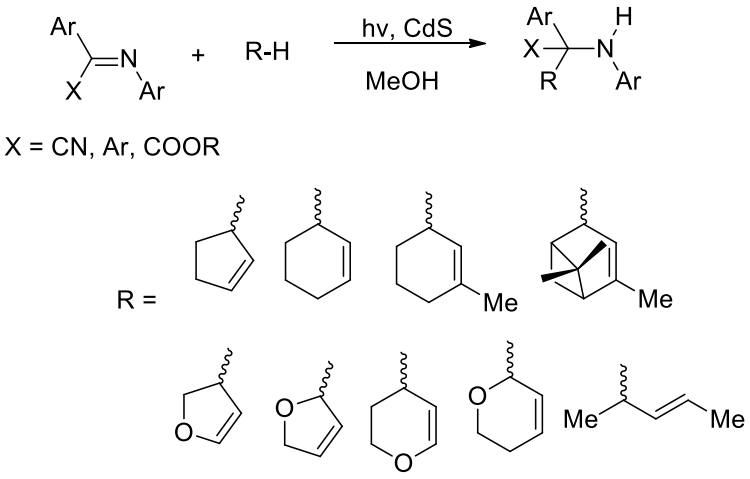

Scheme 17. Synthesis of homoallylimines from trisubstituted imines via visible-light photocatalysis with CdS.

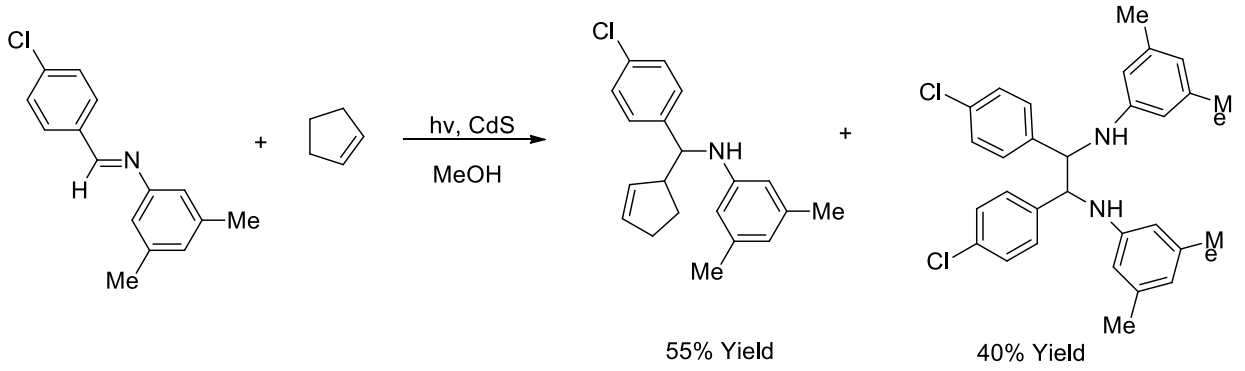

Scheme 18. Photocatalytic addition of disubstituted imine to cyclopentene. Yields of isolated products are given.

In another example polycrystalline CdS was found to be effective in the oxidative coupling of a series of benzyl alcohols with benzyl amines.[32] Irradiation of an oxygen-free suspension of CdS and primary benzyl alcohol derivatives dissolved in acetonitrile with blue light for 24 h gave substituted benzaldehyde, hydrobenzoin and benzoin as products (Scheme 19). As a byproduct, hydrogen is produced on the conduction band of the excited CdS using the remaining electrons of the photocatalytic cycle. Previous studies reported hydrogen gas formation at Pt nanoparticles on platinized CdS converting protons with the help of accumulated electrons from the conduction band.[33] The photocatalytic reaction is strongly dependent on temperature and initial primary benzyl alcohol concentration. When secondary benzyl alcohols were employed under the same photocatalytic conditions there was no formation of such product as benzoin, e.g. methylbenzyl alcohol gave a diastereomeric mixture of 1,2-diols in 75% yield and acetophenone (23%) as a byproduct (Scheme 20, a). In the photocatalytic conversion of para-methoxybenzyl alcohol-methyl ester with CdS, the homocoupling product forms almost exclusively with 89% yield (Scheme 20, b).

When the same reaction conditions were applied to N, N-dimethylbenzyl amine it was converted to 1,2-diphenyl-N,N,N,N-tetramethylethylendiamine and benzaldehyde. Other benzyl amine derivatives gave the desired C-C homocoupling products with benzaldehyde or imine as byproducts (Scheme 21).

As the photocatalytic homocoupling of benzyl amines and benzyl alcohols gave promising results it was interesting to combine them with the aim of obtaining cross-coupling 1,2-aminoalcohol products (Scheme 22). Along with the desired cross-coupling product,

homocoupling products from benzyl amine and benzyl alcohol were found. The reaction requires further optimization to become applicable to a wider range of starting materials.

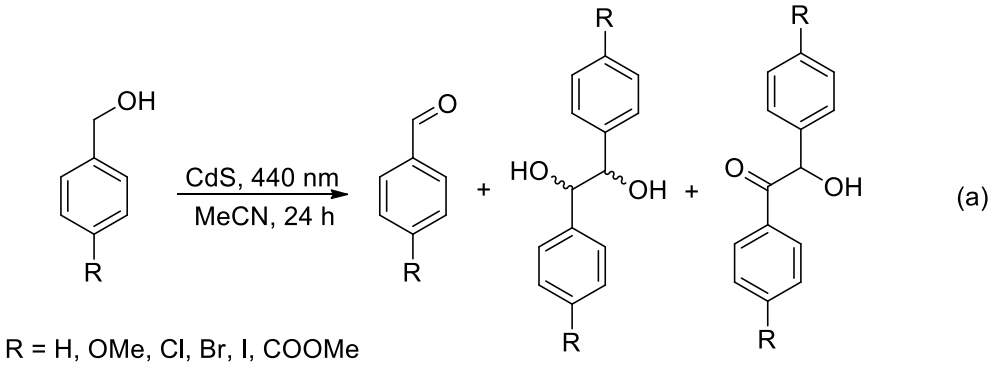

(a)

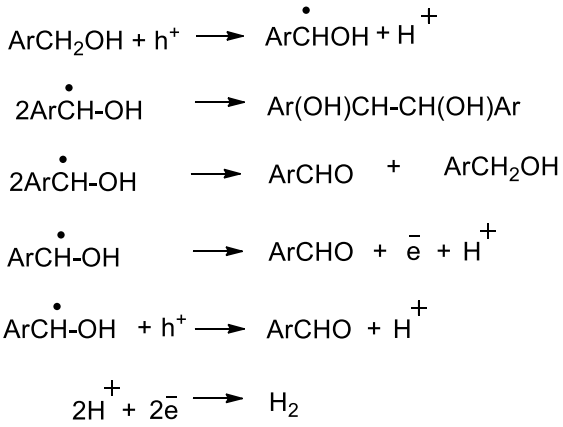

(b)

Scheme 19. (a) CdS visible light photocatalyzed conversion of benzylic alcohols. (b) Mechanism of CdS visible light photocatalytic products formation from benzylic alcohols and hydrogen evolution.

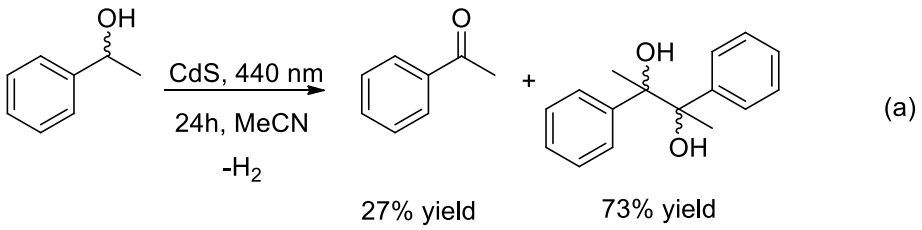

(a)

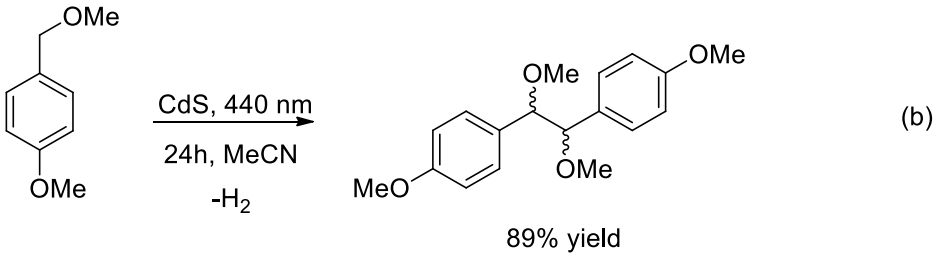

(b)

Scheme 20. Visible light irradiated CdS photooxidation of the α-methylbenzyl alcohol (a) and *para*-methoxybenzyl alcohol methyl ester (b).

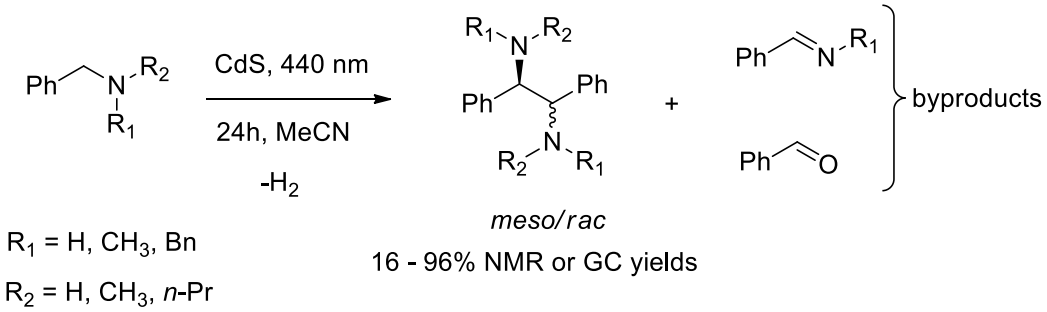

Scheme 21. CdS photocatalyzed conversion of benzylamines.

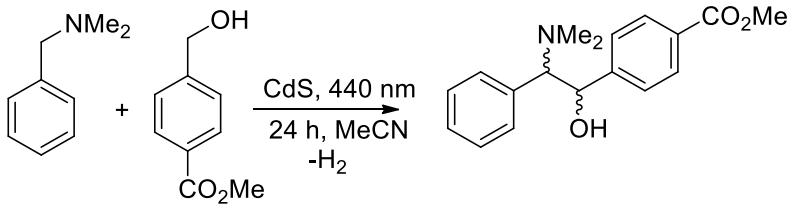

Scheme 22. CdS photocatalyzed cross-coupling of benzylamine and benzyl alcohol derivatives.

As mentioned in section 3.1 tertiary amines are good substrates for one-electron oxidation processes and particularly tetrahydroisoquinolines performed well under TiO_2 photocatalysis (Scheme 6).[19] Almost at the same time, a Mannich type reaction of N-aryltetrahydro-isoquinolines with ketones employing L-proline as the organocatalyst and CdS as a photoredox catalyst upon irradiation with blue light LEDs (460 nm) was investigated (Scheme 23).[34] The product yields range from 76-89% with the neat ketone being used as a solvent. It was possible to reduce its amount to a 2- to 10-fold excess in acetonitrile as a solvent. Switching from TiO_2 to CdS (section 3.1) allowed sensitization by a visible light source (440n nm LEDs) and the desired products could be observed in 85-97% yield (Scheme 24).[32] When no nucleophile is present in the reaction mixture, the radicals undergo homocoupling and form dimers with 52-89% yield along with trace amounts of dehydrodimers, dehydroisoquinoline and N-benzylpyrrol (Scheme 25).[32]

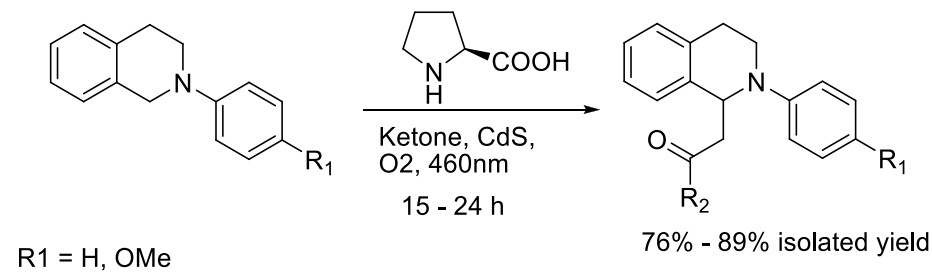

Scheme 23. CdS photocatalyzed and L-proline organocatalyzed Mannich reaction of N-aryltetraisoquinolines and ketones.

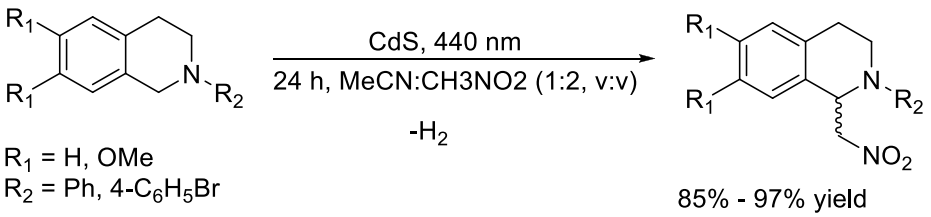

Scheme 24. CdS photocatalyzed Aza-Henry reaction of N-aryltetrahydroisoquinoline and nitromethane.

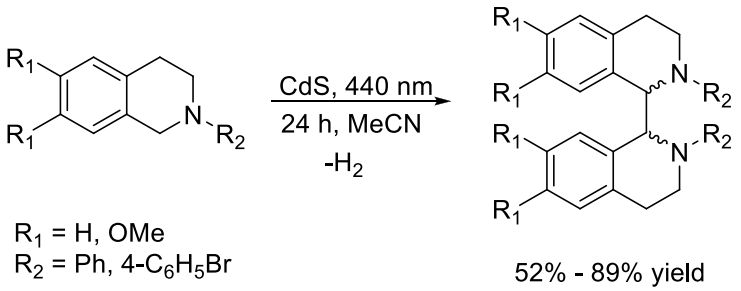

Scheme 25. CdS photocatalyzed dehydrodimerisation of N-aryltetrahydroisoquinolines.

The production of enantiomerically enriched molecules is always an important goal in organic synthesis. Combining photoredox- with organocatalysis provides an elegant way to achieve this and the method can be employed for homogeneous as well as heterogeneous systems. An interesting way of merging the favorable properties of homogeneous dyes with the advantages of heterogeneous systems (easy recovery, etc) is the immobilization of photoredox active dyes on solid supports (e.g. TiO_2, SiO_2). This method allows the use of the redox power of soluble organic dyes known to be effective in photocatalysis (e.g. Eosin Y, Ru(II) and Ir(III) dyes or Cu(I) complexes and etc.) in a heterogeneous manner.

In a recent report this approach was used for a photooxidative Michael addition/oxyamination under visible light irradiation.[35] The photosensitizer N719 immobilized on TiO_2 surface together

with (S)-2-[diphenyl(trimethylsilyloxy)methyl]-pyrrolidine as organocatalyst afforded the α, β-substituted aldehydes in good to excellent yields (30% - 80%) with high diastereo- and enantioselectivities (90% - 99%). It was determined that 0.04 mol% of the immobilized dye in respect to the starting α, β-unsaturated aldehyde is sufficient to provide an excellent 80% yield under optimized conditions (Scheme 26). The optimized conditions involve an adamantane carboxylic acid additive that promotes the formation of the iminium ion from the starting aldehyde and the chiral organocatalyst according to the mechanism given in Scheme 27 where the enantioselectivity of the β-position is determined by the iminium catalysis step and the enantioselectivity of the α-position is directed by the chiral intermediate during the SOMO (single occupied molecular orbital) photocatalysis in the second step. Moreover even if heterogeneous TiO_2 serves only as the solid support to the visible light absorbing N719 dye, the reaction is less efficient when performed with the two photocatalysts separately.

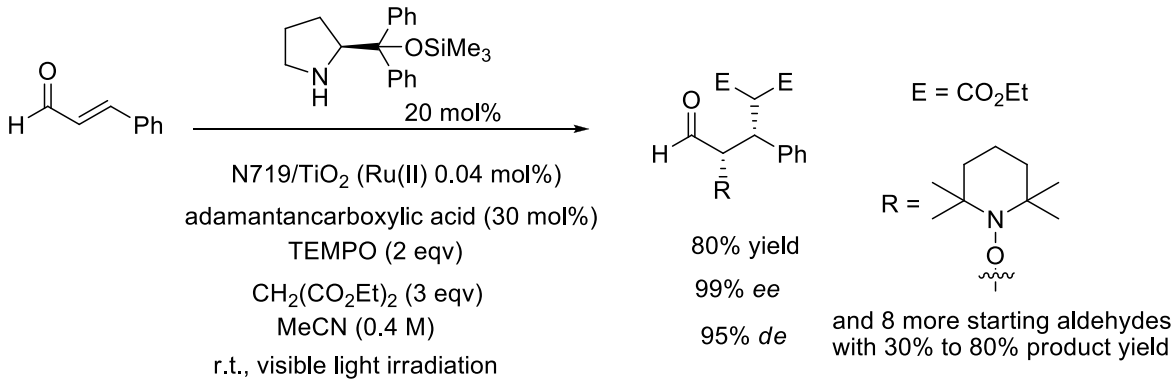

Scheme 26. Photocatalyzed Michael addition/oxyamination to α, β-unsaturated aldehydes.

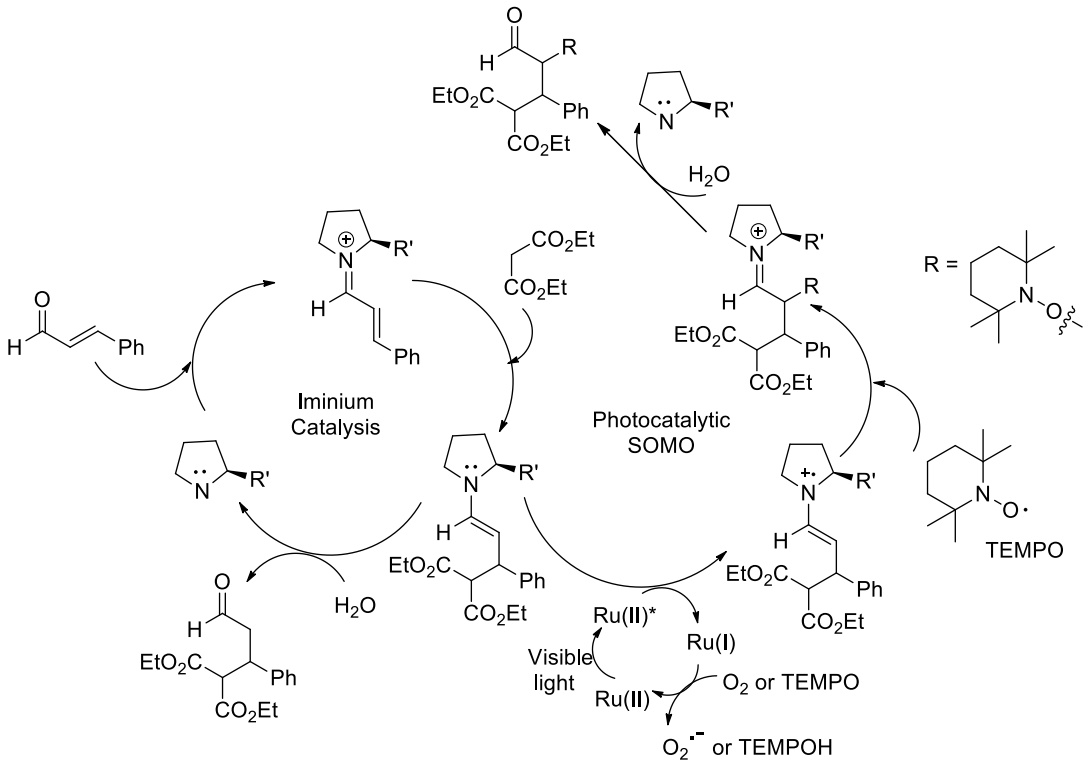

Scheme 27. Mechanism of the photocatalytic Michael addition/oxyamination.

In order to develop photocatalytically more active semiconductors that absorb visible light the group of Huang designed a new layer-structured $PbBiO_2Br$ compound with 2.47 eV band gap energy.[36] The material turned out to be much more active in methyl orange and methylene blue degradation experiments in comparison to already known visible-light absorbing $PbBi_2Nb_2O_9$, $TiO_{2-x}N_x$ and BiOBr semiconductors. These semiconductors are characterized by 2.6, 2.88 and 2.9 eV band gaps, respectively. The material was obtained in two crystal modifications as bulk and nano crystals with 0.17 m^2g^{-1} and 10.8 m^2g^{-1} specific surface areas, respectively, and employed in visible-light-promoted stereoselective alkylation of aldehydes.[34] The enantioselective C–C bond constructions by reduction of halogen precursors, explored earlier in the MacMillan group,[21] was investigated using visible light excited semiconductor-photocatalysts. Several semiconductors were compared in a model α-alkylation of octanal (Scheme 28, a) where the enantioselectivity is induced by a chiral secondary amine (Scheme 28, b). In a row with the promising $PbBiO_2Br$ material in nano and bulk crystal modifications, the well-known TiO_2 as unmodified P25 Degussa and surface-modified were involved in the photocatalysis. The surface-modified TiO_2 was prepared via immobilization of the visible-light responsive redox active Phos-Texas-Red dye (λ_{max} = 578 nm) on the semiconductor surface

(Figure 3). The UV measurements indicate that with respect to the halogen precursor used in the reaction an amount of 1.2 mol% of the dye are surface immobilized.

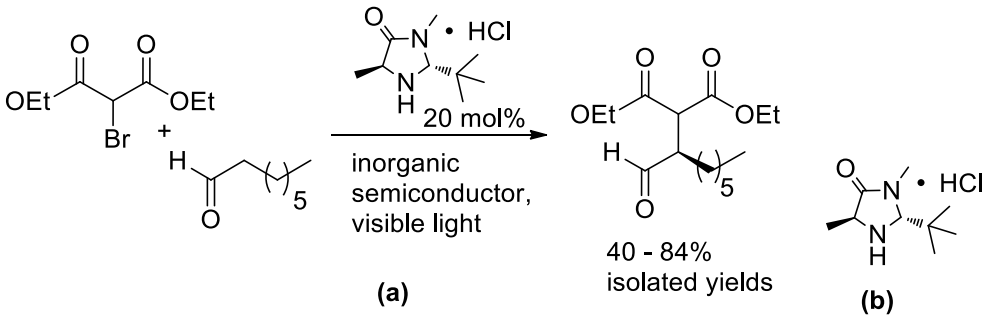

Scheme 28. α-Alkylation of an aldehyde by photocatalysis using inorganic semiconductor.

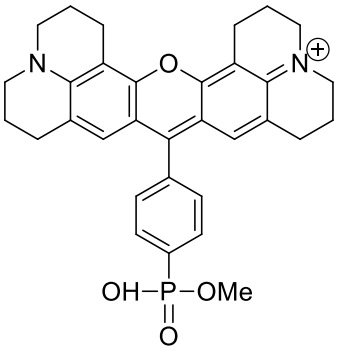

Figure 3. Phos-Texas-Red dye for immobilization on TiO_2 surface.

All used semiconductors have more negative reduction potential than the halogen precursors (Figure 2) thus making a single electron transfer from the conduction band of the excited photocatalyst cleaving the C-Br bond possible. The product yield depends on several parameters, e.g. the specific surface area, the reaction temperature and the visible-light absorption. $PbBiO_2Br$ semiconductors were used in two particle sizes and the smaller nanometer sized ones with larger specific surface area gave a better product yield. Unmodified Degussa P25 TiO_2 with an even larger surface area of 50 m^2g^{-1} gave low yields, due to its weak absorption in the visible-light region. TiO_2 surface modification with a green-light absorbing dye extends the absorption into the visible-light wavelength range of 530 nm high-power LEDs, but the yield remained largely unchanged. By lowering the reaction temperature from room temperature to -10°C the yield for the same reaction time drops by 15-30% in almost all cases, but the enantioselectivity increases slightly. The light penetration path length is crucial: Transferring the heterogeneous reaction mixture from a batch reactor into 1 mm diameter

tubes increases the yields dramatically within even shorter irradiation time. Recycling experiments showed the possibility to use the recovered TiO_2 semiconductor in additional photocatalytical reactions with no loss in product yield. The established method is useful for other halogen precursors such as 2, 4-dinitrobenzylbromide and bromoacetophenone with descent yields of the α-alkylated products of octanal (72% and 65% respectively).

1.4.3 CARBON-HETEROATOM BOND FORMING REACTIONS

1.4.3.1 C-O bond forming reactions

An interesting approach to realize difficult C-H bond transformations was used by Fu et al., who combined several semiconductors with the aim to enhance their photocatalytic properties. To achieve this, they used a surface-chlorinated $BiOBr/TiO_2$ semiconductor-photocatalyst.[37] Visible-light sensitive BiOBr has a narrower band gap of 2.88 eV (TiO2: 3.2 eV) and a lower valence band energy (3.18 eV vs. NHE, pH 7) than TiO_2 (2.91 eV vs. NHE, pH 7). As depicted in Scheme 29 the holes from the valence band (VB) of visible-light excited BiOBr thus can be transferred to the VB of TiO_2 due to the 0.27 eV difference between the oxidation potentials of these two semiconductors. The TiO_2 then acts as the active one-electron oxidizing agent to produce chlorine radicals or hydroxyl radicals from the chlorine or hydroxyl groups that are chemisorbed on the surface. Free chlorine radicals as major participants in the organic layer abstract hydrogen atoms from alkanes to afford alkyl radicals that under aerobic conditions react with O_2 to form ROO almost exclusively (Scheme 29, path I). The peroxy radicals are then reduced with electrons from the conduction band (CB) and protonation leads to the formation of the peroxyacid that in turn forms aldehydes and ketones after dehydration as the major products of this reaction.

The method was applied to aromatic and cyclic aliphatic hydrocarbons including cyclohexane, toluene, ethylbenzene and *p*-xylene yielding cyclohexanone, benzaldehyde, acetophenone or *p*-tolualdehyde, respectively. The generated alkyl radicals could be further applied in C-C bond construction reactions, which would allow the direct functionalization of hydrocarbons without preliminary activation via functional groups (Scheme 29, Path II).[37]

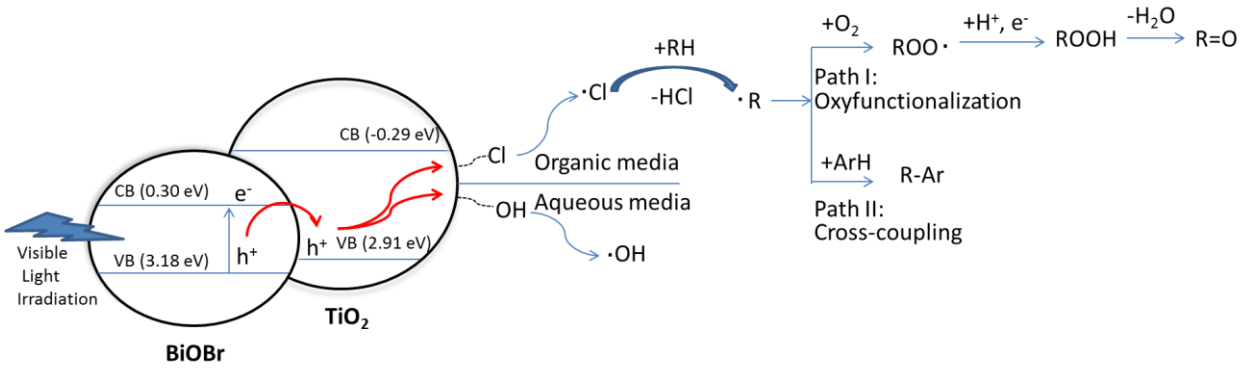

Scheme 29. Mechanistic pathway of hydrocarbon oxyfunctionalyzation under photocatalytic conditions with surface-chlorinated BiOBr/TiO_2 (CBT).

Another case of challenging C-H transformations into C-O bonds was investigated in the group of Y. J. Xu.[38] The activation of the inert C-H bonds can result in poor conversions, selectivity and overoxidation as observed in toluene and saturated hydrocarbon photooxidation experiments using TiO_2 with UV light irradiation.[39,40,41] In order to prevent the formation of undesired products and use mild photocatalytic conditions for C-O bond construction they synthesized photoeffective CdS semiconductors with 1) a specific sheet structure morphology with cubic phase crystallinity (1.9 nm crystals), 2) high surface area (132 m^2g^{-1}) and 3) efficient separation of photogenerated charges upon visible light irradiation. This newly prepared CdS semiconductor has a narrower band gap of *ca*. 2.2 eV and showed 100% selectivity in the catalytic photooxidation of toluene and toluene derivatives to the corresponding aldehydes under visible light irradiation (Scheme 30, b). The yields of the target products after 10 h of irradiation remain moderate (27 – 39%), but could be increased with extended irradiation time. Also the photocatalyst is stable and reusable at least for four photocatalytic cycles in the selective oxidation of toluene with the same 33% yield of benzaldehyde. The proposed mechanism suggests that the photocatalytic oxidation of toluene and its derivatives over CdS is driven by photogenerated positive holes together with O_2 and $O_2^{\cdot-}$ as shown in Scheme 30, a.

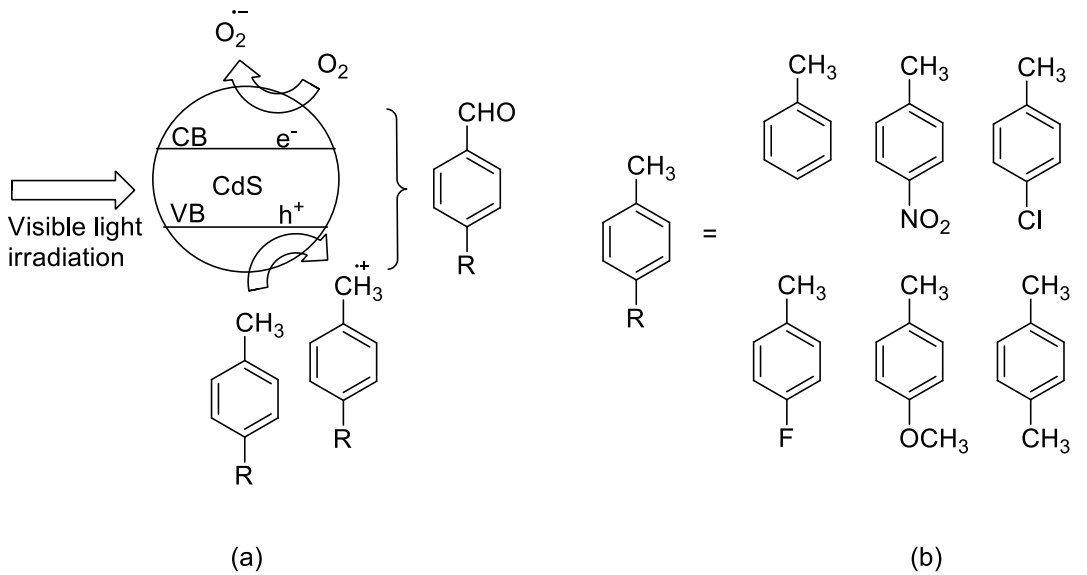

Scheme 30. (a) The mechanism of photocatalytic toluene and toluene derivative oxidation using visible-light irradiated CdS. (b) Scope of toluene derivatives that undergo photocatalytic oxidation.

1.5 CONCLUSIONS

Heterogeneous photocatalysts can be effectively applied for organic synthesis. The reported applications range from simple oxidations and reductions to enantioselective carbon-carbon bond forming reactions. Combining homogeneous organo- or metal catalysis with heterogeneous semiconductor photocatalysis has proven to be particular useful. Advantages of heterogeneous photocatalysts are the wide variety of accessible redox potentials, they are easy to reuse and often very photostable and readily available. However, several aspects in the application of heterogeneous photocatalysts are still challenging and need future improvement to broaden their application in organic synthesis. The number of suitable inorganic semiconductors with well characterized physical properties, including the valence and conducting band energies in different solvents, is still limited. Our understanding of the detailed photocatalytic mechanisms is for many reactions limited, as investigations at the interface between the catalyst surface and the homogeneous reaction medium are difficult. This lack of knowledge hampers a rational design and improvement of heterogeneous photocatalytic processes. Another limitation is the available redox energy of a semiconductor, which is defined by its band gap and therefore correlated to the absorption wavelength. Using visible

light, particular sun light with highest intensities in the blue and green region of the spectrum, but still gaining strongly oxidizing or reducing potentials requires the combination of two or more semiconductors as photocatalysts.

With continuing progress in these different aspects of heterogeneous photoredox catalysis more applications may certainly develop – from lab scale synthetic steps to light mediated medium or larger scale solar production of chemicals.

1.6 REFERENCES

1. a) G Ciamician *Science* **1912**, *36*, 385; b) H. Kisch, *Angew. Chem. Int. Ed.* **2013**, *52*, 812; A. O. Ibhadon, P. Fitzpatrick, *Catalysts* **2013**, *3*, 189

2. A M Roy, G De, N Sasmal, S S Bhattacharryya *Int. J. Hydrogen Energy* **1995**, *8,* 627

3. W Schindler, H Kisch *J. Photochem. Photobiol. A* **2007**, *103***,** 257

4. Suga, Suzuki, Yoshida *J. Am. Chem. Soc.* **2002,** *124,* 30

5. T Shono. *Electrorganic Synthesis, Academic Press, New York* 71 (1991)

6. S Friedman *Tetrahedron* **1961**, *2,* 238

7. T Yoshimitsu, Y Arano, H Nagaoka *J. Am. Chem. Soc.* **2005**, *127***,** 11610

8. A Citterio, A Gentile, F Minisci, M Serravalle, S Ventura *J. Org. Chem.* **1984**, *49*, 3364

9. D Dondi, M Fagnoni, A Molinari, A Maldotti, A Albini *Chem. Eur. J.* **2004***, 10*, 142

10. D Dondi, M Fagnoni, A Albini *Chem. Eur. J.* **2006**, *12***,** 4153

11. S Angioni, D Ravelli, D Emma, D Dondi, M Fagnoni, A Albini *Adv. Synth. Catal.* **2008**, *350*, 2209

12. I Ryu, A Tani, T Fukuyama, D Ravelli, M Fagnoni, A Albini *Angew. Chem. Int. Ed.* **2011**, *50*, 1869

13. S Montanaro, D Ravelli, D Merli, M Fagnoni *Org. Let.* **2012***, 14,* 4218

14. T Caronna, C Gambarotti, L Palmisano, C Punta, F Recupero *Chem. Comm.* **2003**, *18,* 2350

15. Caronna, C Gambarotti, L Palmisano, C Punta, C *J. Photochem.Photobiol. A: Chemistry* **2005**, *171*, 237

16. N Zeug, J Bücheler, H Kisch *J. Am. Chem. Soc.* **1985***, 107***,** 1459

17. L Cermenati, D Dondi, M Fagnoni, A Albini *Tetrahedron* **2003**, *59,* 6409

18. L Cermenati, A Albini, C Richter *Chem Comm.* **1998***,* 805

19. M Rueping, J Zoller, D C Fabry, K Poscharny, R M Koenigs, T E Weirich, L Meyer *Chem. Eur. J.* **2012**, *18,* 3478

20. P Wu, C Cheng, J Wang, X Peng, X Li, Y An, C Duan *J. Am. Chem. Soc.* **2012**, *134*, 14991

21. D A Nicewicz, D W C MacMillan *Science* **2008**, *322,* 77

22. D P Hari, B König *Org. Let.* **2011**, *13,* 3852

23. M Rueping, C Vila, R M Koenigs, K Poscharny, D C Fabry *Chem. Comm.* **2011**, *47*, 2360

24. H Kisch *Advances in Photochemistry* **2001**, *26*, 93

25. Y Shiraishi, K Fujiwara, Y Sugano, S Ichikawa, T Hirai *ACS Catalysis* **2013**, *3,* 312

26. D Stíbal, J Sá, J A Bokhoven *Catalysis Science & Technology* **2013**, *3,* 94

27.O T Ohno, K Nakabeya, M Matsumura *J. Catalysis* **1998***, 176,* 76

28. S Füldner, R Mild, H I Siegmund, J A Schroeder, M Gruber, B König *Green Chem.* **2010**, *12*, 400

29. S Füldner, T Mitkina, T Trottmann, A Frimberger, M Gruber, B König *Photochem. Photobiol. Sci.* ***2011****, 10,* 623

30. S Füldner, P Pohla, H Bartling, S Dankesreiter, R Stadler, M Gruber, A Pfitzner, B König *Green Chem.* **2011**, *13,* 640

31. L H Yum, P Chen, M Grätzel, M K Nazeeruddin *ChemSusChem* **2008**, *1,* 699

32. T Mitkina, C Stanglmair, W Setzer, M Gruber, H Kisch, B König *Org. Biomol. Chem.* **2012**, *10*, 3556

33. Z Jin, Q Li, X Zheng, C Xi, C Wang, H Zhang, L Feng, H Wang, Z Chen, Z Jiang *J. Photochem. Photobiol. A* **1993**, *71*, 85

34. M Cherevatskaya, M Neumann, S Füldner, K Harlander, S Kümmel, S Dankesreiter, A Pfitzner, K Zeitler, B König *Angew. Chem. Int. Ed.* **2012**, *51*, 4062

35. H Yoon, X Ho, J Jang, H Lee, S Kim *Org. Let.* **2012***, 14***,** 3272

36. Z Shan, W Wang, X Lin, H Ding, F Huang *J. Solid State Chem.* **2008**, *181*, 1361

37. R Yuan, S Fan, H Zhou, Z Ding, S Lin, Z Li, Z Zhang, C Xu, L Wu, X Wang, X Fu *Angew. Chem. Int. Ed.* **2013**, *52*, 1035

38. Y Zhang, N Zhang, Z Tang, Y Xu *Chem. Sci.* **2012**, *3*, 2812

39. A Maira, K Yeung, J Soria, J Coronado *Applied Catalysis B: Environmental* **2001**, *29***,** 327

40. V Augugliaro, S Coluccia, V Loddo, L Marchese *Applied Catalysis B: Environmental* **1999***, 20***,** 15

41. M Gonzalez, S Howell, S Sikdar *J. Cat.* **1999**, *183***,** 159

CHAPTER 2

2. VISIBLE LIGHT PROMOTED STEREOSELECTIVE ALKYLATION BY COMBINING HETEROGENEOUS PHOTOCATALYSIS WITH ORGANOCATALYSIS†

† This chapter was published as: Cherevatskaya, M., Neumann, M., Füldner, S., Harlander, C., Kümmel, S., Dankesreiter, S., Pfitzner, A., Zeitler, K., König, B. Visible Light Promoted Stereoselective Alkylation by Combining Heterogeneous Phototcatalysis with Organocatalysis. *Angew. Chem. Int. Ed.* **2012**, *51*, 4062-4066. Dankesreiter, S. performed the synthesis and characterization of $PbBiO_2Br$ semiconductors. Neumann, M. and Kümmel, S. performed the experiments with CdS. Harlander, C. synthesized and performed the experiments with TiO_2 immobilized MacMillan organocatalyst. Cherevatskaya, M. and Füldner, S. performed the alkylation experiments with TiO_2 and $PbBiO_2Br$ semiconductors. Cherevatskaya, M. performed synthesis and immobilization of Phos-Texas Red dye.

2.1 INTRODUCTION

The application of sensitizers to utilize visible light for chemical reactions is known for long.[1] Several recent publications[2] have impressively demonstrated the versatile use of visible light for various transformations, such as the conversion of alcohols to alkyl halides,[3] [2+2],[4] [3+2][5] and [4+2][6]-cycloadditions or carbon-carbon[7] and carbon-heteroatom bond formations.[8] The cooperative merger of organocatalysis with visible light photoredox catalysis using ruthenium- or iridium metal complexes[9] or organic dyes[9d] as photocatalysts allows for an expansion to enantioselective reactions.[10] Although inorganic semiconductors, such as titanium dioxide, have been widely used in the photocatalytic degradation of organic waste,[11] the number of examples in which they photocatalyze bond formation in organic synthesis is still limited.[12] Kisch[13] explored CdS mediated bond formations and oxidative C-C coupling reactions with titanium dioxide[14] are known. However, bond formations on heterogeneous photocatalysts typically proceed without control of the stereochemistry and mixtures of isomers are obtained.[15,16] We demonstrate in this work that the combination of stereoselective organocatalysis with visible light heterogeneous photoredox catalysis allows for the stereoselective formation of carbon-carbon bonds in good selectivity and yield. The approach combines the advantages of heterogeneous catalysis, as robust, simple and easy to separate catalyst material, with the stereoselectivity achieved in homogeneous organocatalysis.[17,18]

2.2 RESULTS AND DISCUSSION

The enantioselective α-alkylation of aldehydes developed by MacMillan et al.9[a] was selected as a test reaction to apply inorganic heterogeneous photocatalysts (Table 1). Five semiconductors were used: commercially available white TiO_2 (**1**),[19] the same material covalently surface modified with a Phos-Texas Red dye increasing the visible light absorption (Phos-Texas-Red-TiO_2, **2**), yellow $PbBiO_2Br$, which absorbs blue light, as *bulk* material (**3**) and in nano-crystalline form (**4**). TiO_2 (**1**) with an average particle size of 21 nm is a stable and inexpensive semiconductor with a band gap of 3.2 eV, but the unmodified powder absorbs only weakly up to 405 nm due to defects and surface deposits.[20] Its absorption range can be extended into the visible range by structure modification[21] or dye surface modification.[22,23] The Texas Red derived

dye **10**,[24], was covalently anchored on TiO_2 yielding **2**, which absorbs at 560 nm (see Supporting Information for the synthesis of **10** and the characterization of **2**). $PbBiO_2Br$ **3** and **4** were prepared by different synthetic routes leading to different particle sizes of the semiconductors: $PbBiO_2Br$ bulk material **3** with 2.47 eV band gap was prepared by high temperature solid phase synthesis,[25] while the nanocrystalline material **4** was obtained from aqueous solution synthesis leading to an average calculated particle size of 28 ± 6 nm and an optical band gap of 2.56 eV. Yellow CdS (**5**) has a band gap of 2.4 eV and was prepared as previously reported.[26]

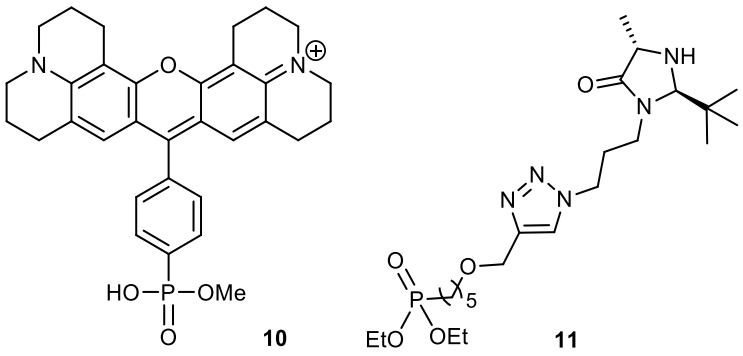

Scheme 1. Compounds for covalent surface immobilization on TiO_2. Left: Phos-Texas-Red (**10**); right: chiral organocatalyst **11.**

The α-alkylation of aldehyde **7** in the presence of 20 mol% of secondary amine **8** as chiral catalyst and unmodified TiO_2 affords product **9** in moderate yield and good enantioselectivity after extended irradiation time (entry 1), as only a small fraction of the visible light at 440 nm is absorbed. TiO_2 can be reused giving similar results (entry 2). With higher light intensity in a microreactor set up (entry 3) the reaction time can be reduced to 3 h. Lowering the reaction temperature to -10 ^oC increases the stereoselectivity of the reaction to 83% *ee*, but slows down the reaction significantly (entry 4). Surface modified TiO_2 **2** allows the reaction to run with green light (530 nm, entries 5 and 6) yielding 65% product in 81% *ee* at -10 ^oC. $PbBiO_2Br$ (**3**) absorbs in the visible range and catalyzes the reaction with blue light (entries 7 and 8). However, its surface area is with only 0.17 m^2/g small compared to TiO_2 (50 m^2/g). This explains the still rather long reaction time. Nanocrystalline $PbBiO_2Br$ (**4**) has a larger surface area of 10.8 m^2/g and at room temperature and 440 nm irradiation the product can be isolated with a yield of 84% and 72% *ee* after 20 h (entry 9). Again, the stereoselectivity increases to 83% *ee* at -10 ^oC, but with lower conversion (entry 10). The microreactor reduces reaction times to 3 or 10 h,

resp. with yields of 69% and *ee´*s of 80% (entries 11 and 12). The reuse of **4** is possible, but black organic surface deposits lead to significantly slower conversions.

The mechanism of the alkylation reaction presumably follows the proposed pathway for photoredox catalysis (see SI for scheme): Electron transfer from the conduction band of the semiconductor to the halogenated carbonyl compound generates *via* the loss of a bromide anion the α-carbonyl radical, which adds to the enamine obtained by condensation of the chiral catalyst with octanal. The α-amino radical is then oxidized by a hole of the valence band yielding the iminium ion that releases catalyst and product.

In an attempt to create a completely heterogeneous catalyst system we prepared the chiral amine phosphonate ester **11** (see Supporting Information for the synthesis) and immobilized it on TiO_2. However, the catalyst system is inactive and no product formation could be observed under identical conditions as used before. The close proximity of the secondary amine organocatalyst to the semiconductor surface may lead to its rapid oxidative photo-decomposition. The non-immobilized catalyst, mostly present in solution as enamine, will only very rarely encounter the surface as the free amine and is thereby protected from oxidative decomposition.

Table 1. Enantioselective alkylations using MacMillan´s chiral secondary amine and inorganic semiconductors as photocatalysts.

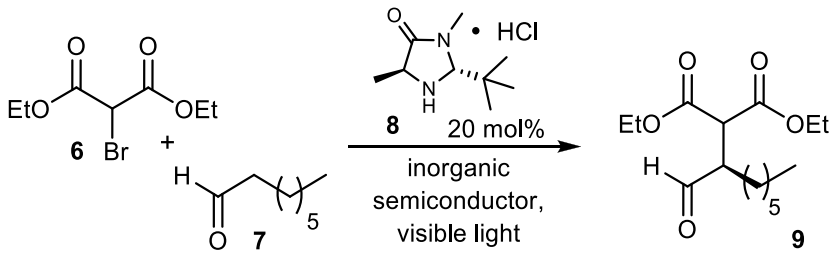

Entry	Photo-catalyst[a]	Wave-length[b] [nm]	Reaction time [h]	Reaction temp. [°C]	Yield **9** [%][c]	*ee* [%][d]
1	**1**	440	20	20	55	71
2	**1**[e]	440	20	20	60	72
3	**1**[f]	440	3	20	76	74
4	**1**	440	20	-10	40	83
5	**2**	530	20	20	55	72
6	**2**	530	20	-10	65	81
7	**3**	440	20	20	69	71
8	**3**	440	20	-10	40	84
9	**4**	440	20	20	84	72
10	**4**	440	20	-10	49	83
11	**4**[f]	455	3	20	41	71
12	**4**[f]	455	10	-10	69	80

[a] 64 mg photocatalyst/1 mmol of **6** in 2.5 mL of degassed CH_3CN. [b] high power LED (440, 455 or 530 nm ± 10 nm, 3 W, LUXEON as indicated). [c] isolated yield. [d] determined by chiral HPLC or by NMR using a chiral diol.[27] [e] photocatalyst reused. [f] irradiation in microreactor in 1.5 mL of CH_3CN.

Our attempts to use CdS (**5**) for this transformation were not successful. A comparison of the relevant potentials of the widely employed photocatalyst $Ru(bpy)_3Cl_2$ and the investigated semi-conductors explains the observation. $Ru(bpy)_3^+$ is proposed as the electron donor with a potential of -1.33 V (SCE). The conduction band potential of TiO_2 at -2.0 V (SCE) in acetonitrile is sufficient

for this step, while the respective reported potential for CdS in acetonitrile of -1.05 V may be too low (Figure 1).[28,29] On the other hand, the reductive quenching step potential of excited $Ru(bpy)_3^{2+*}$ leading to the oxidation of the α-aminoradical intermediate is estimated to be +0.84 V (SCE), which is matched by the hole potentials (all *vs.* SCE in acetonitrile) of TiO_2 (+1.0 V)[29, 30] and CdS (+1.6 V).

The combination of heterogeneous inorganic and homogeneous organic catalysts is applicable to other substrates, such as bromoacetophenone (**12a**). For the conversion of the more difficult to reduce dinitro benzylbromide (**12b**) iridium complexes are required in the case of homogeneous photocatalysis.[9c] However, the estimated conduction band potentials of TiO_2 and $PbBiO_2Br$ in acetonitrile (Figure 1) should be still sufficient and we indeed could observe the clean conversion to the expected products in good yield and high stereoselectivity (Scheme 2).

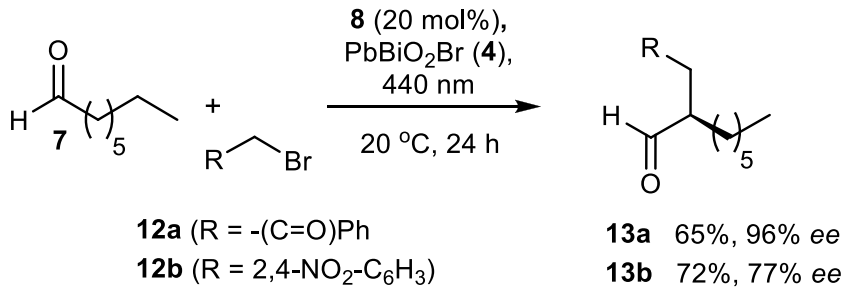

Scheme 2. Alkylations using bromoacetophenone (**12a**) in CH_3CN or 2,4-dinitrobenzylbromide (**12b**) in DMSO, chiral amine **7**, $PbBiO_2Br$ (**4**) and blue light.

Recently, several cross-dehydrogenative couplings[31] on tetrahydroisoquinolines by homogeneous photocatalysis using Ir- or Ru-based transition metal complexes5[b,]5[c,]7[d,]8[b,]8[d,15,32] or organic dyes,[33] such as Eosin Y[8a] have been reported. Here the photocatalytic key step is the reductive quenching of the excited chromophore leading to an amine radical cation, which subsequently can transform to an electrophilic iminium species. Considering the use of inorganic semiconductors for this reaction, the potential of the photogenerated holes in the valence band is now of importance. Based on the band gap and its redox potential (see Figure 1) CdS should be a suitable heterogeneous visible light photocatalysts for oxidations to generate the desired amine radical cation. The combination of proline as organocatalysts with CdS, as inorganic photocatalyst, indeed allows for a clean conversion of *N*-aryltetrahydroiso-quinolines **14** in a photooxidative Mannich type reaction[32b,33a] with ketones **15** upon irradiation

with blue light of 460 nm. The products **16a-d** arising from the reaction with acyclic or cyclic ketones can be obtained in good yields of 76-89% (Table 2).[34] While the reaction can also successfully be performed in CH_3CN with a significantly reduced amount of ketone (see Table 2, entry 1a-c), the reaction is most conveniently run in neat ketone if inexpensive (liquid) ketones are employed.

The flat band potentials of some common inorganic (and organic) semiconductors are summarized in Figure 1.[35] Importantly, with changing pH or upon exposure to different organic solvents these values shift significantly and the currently available data for organic solvents are limited. However, comparing the semiconductor flat band potentials with the potentials required for catalytic key steps from known photoredox catalysts (e. g. Ru-, Ir-complexes, xanthene dyes etc.) allows the prediction of suitable combinations of (inorganic) semiconductors with organocatalysts.

Table 2. Photocatalytic Mannich reaction of N-aryltetrahydroisoquinolines 14 with ketones 15 and L-proline on CdS (5)[a]

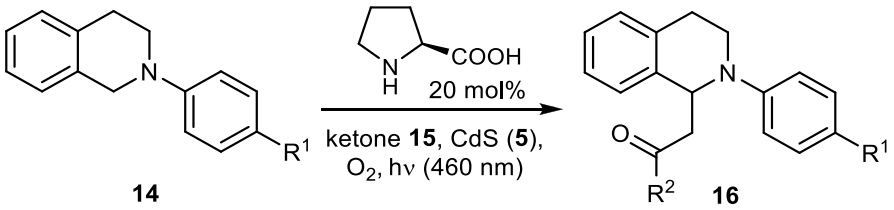

entry	R^1	Ketone	product	reaction time [h]	yield [%][b]
1a	H	 15a	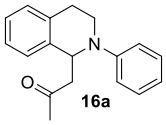 16a	24	86[c]
1b				24	90[d]
1c				24	100[e]
1d				24	87
2	OMe	 15a	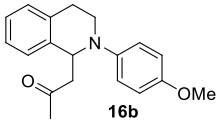 16b	18	89
3	H	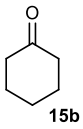 15b	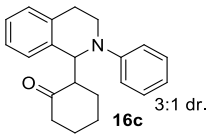 16c 3:1 dr.	24	79
4	H	 15c	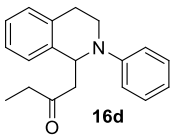 16d	15	76

[a] Unless otherwise noted all experiments were performed with amine (1 eq) and L-proline (0.2 eq) in a 5 mg/ml mixture of CdS in neat ketone (c_{amine}=0.25 mol/l). Reactions were run in schlenk tubes with an attached oxygen balloon and irradiated with high power LEDs (460 nm) for the time indicated. [b] Given yields correspond to isolated product. [c] Reaction performed in CH_3CN with 2 equiv. of acetone; the conversion was determined by GC analysis. [d] Reaction performed in CH_3CN with 5 equiv. of acetone; the conversion was determined by GC anaylsis. [e] Reaction performed in CH_3CN with 10 equiv. of acetone; the conversion was determined by GC analysis.

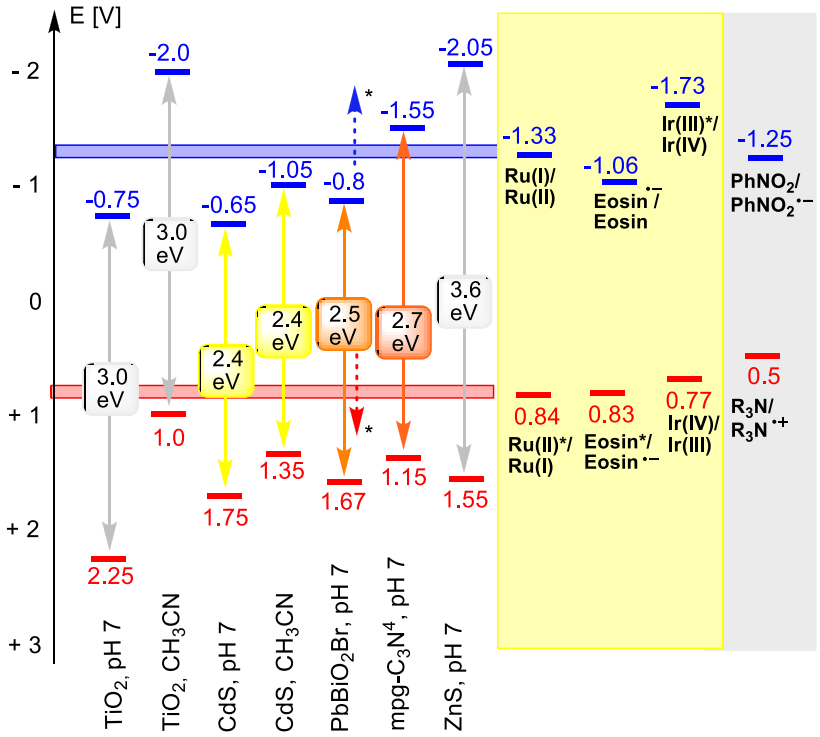

Figure 1. Band gaps (in eV) and redox potentials (in V *vs*. SCE) of common inorganic semiconductors in comparison with molecular photocatalysts and redox potentials of some photocatalytic key steps. *Estimated change of $PbBiO_2Br$ flat band potential in acetonitrile. Given values for Ru relate to $Ru(bpy)_3^{2+}$; values for Ir are related to *fac*-$Ir(ppy)_3$.

2.3 CONCLUSION

We have demonstrated that the well-directed combination of heterogeneous semiconductor photocatalysts with chiral organocatalysts allows for different types of stereoselective bond formation by visible light photocatalysis. Yields and stereoselectivity are comparable to previously reported homogeneous reactions using transition metal complexes or organic dyes. Electrons are exchanged in the course of the reaction between the chiral reaction intermediates in solution and the semiconductor surface, if the redox potentials of substrates and band gaps match. The covalent immobilization of the organocatalyst on the semiconductor surface leads to its oxidative decomposition and must be avoided.

The good availability of inorganic semiconductors with different band gaps and redox potentials, their simple removal and recycling make them the perfect partners for chiral organocatalysts in stereoselective photocatalysis.

2.4 EXPERIMENTAL PART

2.4.1 GENERAL INFORMATION

For irradiation high power LEDs (440 nm, 455 nm or 530 nm±10 nm) with 3 W electrical power STAR LB BL ZXHL-LBBC LUXEON were used.

Commercial reagents and starting materials were purchased from Aldrich, Fluka, VWR or Acros and used without further purification. Solvents were used as p.a. grade or dried and distilled as described in common procedures.

For NMR-spectroscopy a Bruker Avance 300 (1H: 300 MHz, 13C: 75 MHz, T = 295 K), a Bruker Avance 400 (1H: 400 MHz, 13C: 100 MHz, T = 295 K) and Bruker Avance 600 (1H: 600MHz, 13C: 150 MHz, 31P: 243 MHz, T = 295 K) were used. The chemical shifts are reported in δ [ppm] relative to internal standards (solvent residual peak). The spectra were analyzed by first order, the coupling constants J are given in Hertz [Hz].

Absorption spectra were recorded on a Varian Cary BIO 50 UV/VIS/NIR spectrometer, 1 cm quartz cuvette (Hellma) was used.

Specific optical rotation was measured on Kruess (A. Kruess Optonics).

Preparative HPLC was performed on Agilent 1100 Series.

2.4.2 HETEROGENEOUS PHOTOCATALYSTS

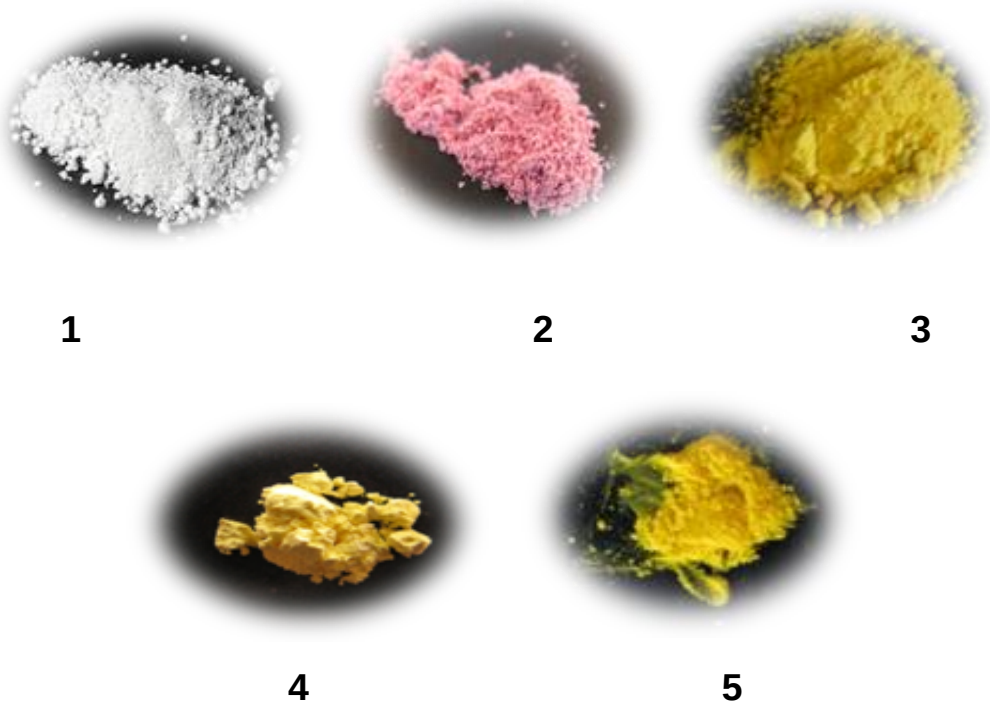

Figure 2. Heterogeneous photocatalysts used in this study: TiO_2 (**1**), Phos-TexasRed-TiO_2 (**2**), $PbBiO_2Br$ (**3**) and nanocrystalline $PbBiO_2Br$ (**4**), CdS (**5**).

2.4.3 GENERAL PROCEDURES

General procedure 1 (aldehyde α-alkylation): Bromo-alkyl (1 equiv.), octanal (2.5 equiv.), (2*R*,5*S*)-2-*tert*-butyl-3,5-dimethylimidazolidin-4-one hydrochloride **8** (0.2 equiv.), 2,6-lutidine (2 equiv.) and the semiconductor (64mg/$mol_{Br\text{-}alkyl}$) in the indicated solvent were degassed by repeated freeze-pump-thaw cycles. The vial was irradiated with high power LEDs wavelength temperature and time as given in Table 1. For work up the reaction mixture was filtered with the aid of Acetonitrile (3×2ml) and EtOAc (2×2ml). The filtrates were washed with aqueous sat. solutions of $NaHCO_3$, NH_4Cl, NaCl. The aqueous layers were extracted with EtOAc (2×10 ml), the combined organic layers were evaporated to dryness, and the crude products were purified by column chromatography.

General procedure 2 (Aza-Henry reactions): 1,2,3,4-Tetrahydroisoquinoline derivative (1 equiv.), L-proline (0.2 equiv.) and ketone (c_{THIQ} = 0.25 mol/l) were mixed in a schlenk tube. CdS (5 mg/ml_{Ketone}) was added and an oxygen atmosphere was applied by balloon. The vial was irradiated with high power LEDs (460 nm) in a distance of approximately 5 cm for the indicated time. After full conversion of the Starting material (as judged by TLC) the crude mixture was purified by column chromatography (hexanes:ethyl acetate 9:1).

2.4.4 PROPOSED MECHANISM OF THE PHOTOCATALYSIS

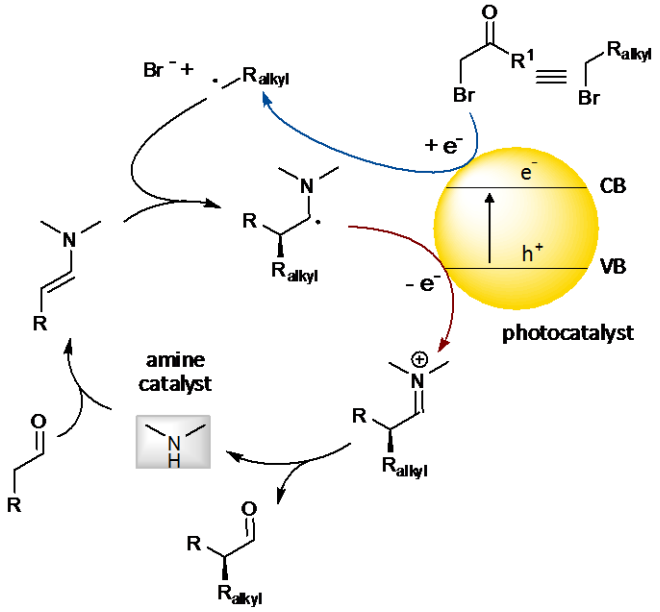

Scheme 3. Proposed mechanism of the semiconductor photoredox catalysis of enamines and bromo malonate

2.4.5 EXPERIMENTAL DATA FOR ALDEHYDE α-ALKYLATIONS

(*R*)-Diethyl 2-(1-oxohexan-2-yl)propanedioate (9)

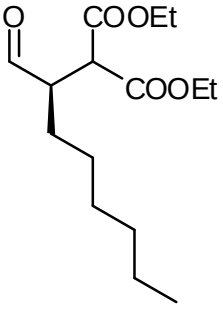

286,36 g/mol

According to **general procedure 1**: Bromo-diethylmalonate **6** (133 µL, 0.78 mmol) catalyst **8** (33 mg, 156 µmol), octanal (305 µL, 195 µmol), 2,6-lutidine (182 µL, 156 µmol) and the semiconductor (50 mg, **table 1**) in acetonitrile (2.5 mL). Column chromatography (hexanes:diethylether, 6:1; R_f = 0.3) afforded **9** as

a colorless oil. ^{1}H NMR (300 MHz, CD3CN): δ 9.67 (d, *J* = 1.1 Hz, 1H), 4.30 – 4.10 (m, 4H), 3.71 (dd, *J* = 8.6, 4.4 Hz, 1H), 3.04 – 2.96 (m, 1H), 1.71 – 1.51 (m, 2H), 1.28 – 1.16 (m, 14H), 0.87 (t, *J* = 6.7 Hz, 3H). For determination of the enantiomeric excess 20 mg of the product was dissolved in 5 ml of dichloromethane, 2S,4S-(+)-pentanediol (10 mg) and TsOH (3 mg) were added, the reaction mixture was stirred under nitrogen atmosphere for 5 h, the solvent was removed and the *ee* was determined by the integration of the NMR signals (400 MHz, CD_3CN) at 3.54 ppm (major) and 3.57 ppm (minor)[1]. Alternatively, the enantiomeric excess was determined by chiral HPLC using Phenomenex Lux Cellulose-1 column, 4.6×250 mm, 5 µm, *n*-heptane/*i*-propanol 1.0 ml/min.

(*R*)-2-(2-Oxo-2-phenylethyl)hexanal (13a)

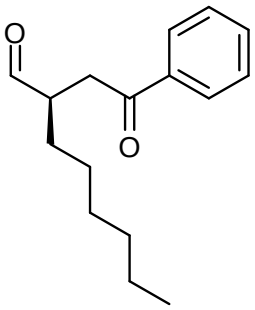

246,34 g/mol

According to **general procedure 1**: 2-Bromacetophenone **12a** (100 mg, 0.5 mmol), catalyst **8** (21 mg, 0.1 mmol), octanal (195 µl, 1.25 mmol), 2,6-lutidine (116 µl, 1 mmol), PbBiO2Br *nano* (**4**, 32 mg) in acetonitrile (2 ml). Column chromatography (hexanes:diethylether; 10:1; *R*f = 0.3) afforded **13a** (76.2 mg, 62 % yield, 96% ee) as a colorless oil. 1H NMR (300 MHz, CD3CN): δ 9.70 (d, *J* = 1.4 Hz, 1H), 8.01 – 7.94 (m, 2H), 7.65 – 7.59 (m, 1H), 7.53 – 7.48 (m, 2H), 3.44 (dd, *J* = 18.1, 8.4 Hz, 1H), 3.13 (dd, *J* = 18.1, 4.4 Hz, 1H), 2.99 – 2.89 (m, 1H), 1.79-1.70 (m, 1H), 1.55-1.46 (m, 1H), 1.41 – 1.24 (m, 8H), 0.88 (t, *J* = 6.8 Hz, 3H). The enantiomeric excess was determined by optical rotation $[\alpha]_D^{23}$ = +69.1 (c = 1.3, CHCl3, 96% ee)[36].

(*R*)-2-(2,4-Dinitrobenzyl)octanal (13b)

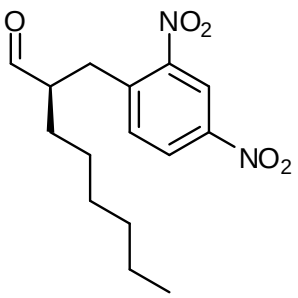

308,33 g/mol

According to **general procedure 1:** 2,4-dinitrobenzyl bromide **12b** (100 mg, 0.38 mmol), catalyst **8** (16 mg, 0.076 mmol), octanal (149 µL, 0.95 mmol), 2,6-lutidine (89 µL, 0.76 mmol) and $PbBiO_2Br$ *nano* (**4**, 25 mg) in DMSO (2 mL). Column chromatography (hexanes:diethyl ether; 7:1; R_f = 0.23) afforded **13b** (85.5 mg (72 % yield, 77 % ee) as a yellowish oil.

^{1}H NMR (300 MHz, CD_3CN): δ 9.58 (d, *J* = 2.0 Hz, 1H), 8.68 (d, *J* = 2.4 Hz, 1H), 8.37 (dd, *J* = 8.6, 2.4 Hz, 1H), 7.70 (d, *J* = 8.6 Hz, 1H), 3.34 (dd, *J* = 14.1, 8.5 Hz, 1H), 3.04 (dd, *J* = 14.1, 5.7 Hz, 1H), 2.82 – 2.70 (m, 1H), 1.79 – 1.65 (m, 1H), 1.60 – 1.47 (m, 1H), 1.37 – 1.22 (m, 8H), 0.88 (t, *J* = 6.8 Hz, 3H). For determination of the enantiomeric excess 20 mg of the product was dissolved in 5 ml of dichloromethane, 2S,4S-(+)-pentanediol (10 mg) and TsOH (3 mg) were added, the reaction mixture was stirred under dinitrogen atmosphere for 5 h, the solvent was removed and the *ee* was determined by the integration of the NMR resonance signals (400 MHz, CD_3CN) at 8.55 ppm (major) and 8.53 ppm (minor).

For microreactor reactions the reaction mixture was injected by syringe into a glass microreactor (1.5 mL acetonitrile) (LTF factory, 11 x 5.7 cm, 1.7 mL internal volume) previously flushed with nitrogen. For pictures see topic (9).

2.4.6 SYNTHESIS AND IMMOBILIZATION OF COMPOUND 10

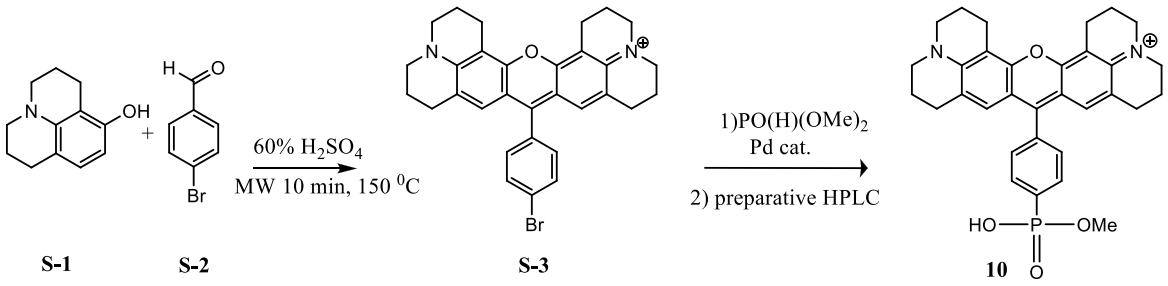

Scheme 4. Synthesis of Phos-Texas Red (**10**) for surface modification of TiO_2.

Phos-TexasRed dye **10** was synthesized *via* Pd-catalyzed reaction of compound **S-3** with diethyl phosphate.[37] Compound **S-3** was obtained from the condensation of 8-hydroxyjuloidine (**S-1**) and 4-bromobenzaldehyde (**S-2**).[38] The synthetic procedure is simpler compared to the reported syntheses of other dyes of this type for surface immobilization[39] and the phosphonate group has excellent anchoring properties to the TiO_2 surface.[40] The absorption maximum of dye **10** in methanol solution is λ_{max} = 578 nm(c = 4.7×10^{-5} M) with an extinction coefficient of ε = 83000 $cm^{-1}M^{-1}$. TiO_2 was surface modified with Phos-Texas Red dye **10**. After

immobilization the absorption maximum shifted slightly to 560 nm. The amount of immobilized dye was estimated from the UV-Vis spectra to be 9.3×10^{-3} mmol/50mg TiO_2. This corresponds to 1.2 mol% in respect to diethyl 2-bromomalonate used in the catalysis reaction.

Texas Red dye S-3.[41] *p*-Bromobenzaldehyde (90 mg, 0.5 mmol) and 8-hydroxyjulolidine (200 mg, 1.05 mmol) were dissolved in 10 ml of $CHCl_3$ and the solvent was removed *in vacuo* to give a homogenous mixture. The mixture was then suspended in 10 ml of 60% H_2SO_4, heated in the microwave reactor for 10 min to 150 ^{0}C with vigorous stirring. Chloranil (185 mg, 0.75 mmol) was added and the mixture was allowed to cool to room temperature. The reaction mixture was adjusted with 10 M NaOH to neutral pH and filtered. The filtered mixture was then extracted with dichloromethane (3×200 ml) and the combined organic layers were washed with brine and water, dried over $MgSO_4$ and the solvent was removed under reduced pressure. The residue was further purified by chromatography on silicagel (EtOAc/MeOH 4/1) to give the compound **S-3** as violet solid. ^{1}H NMR (300 MHz, MeOD) δ 7.76 (d, *J* = 8.4 Hz, 2H), 7.28 (d, *J* = 8.4 Hz, 2H), 6.79 (s, 2H), 3.56 (t, *J*=5.5 Hz, 4H), 3.53 (t, *J*=5.5 Hz, 4H), 3.02 (t, *J* = 6.4 Hz, 3H), 2.68 (t, *J* = 6.4 Hz, 3H), 2.10 – 2.00 (m, 4H), 1.98 – 1.86 (m, 4H). MS (ESI) m/z 526/528 (M^+).

Phos-Texas Red dye 10. Texas Red dye (**S-3**, 50 mg, 0.11 mmol), $Pd_2(dba)_3CHCl_3$ (11.4 mg, 0.011 mmol) and xantphos (12.7 mg, 0.022 mmol) were dissolved in 30 ml of dry dichloro-methane under exclusion of air. The reaction mixture was refluxed in nitrogen atmosphere and diisopropylethyl amine (20 µl, 0.11 mmol) and dimethylphosphite (10.1 µl, 0.11 mmol) were added at once. The reaction mixture was allowed to reflux for 10 h, it was filtered and the solvent was removed under reduced pressure. The residue was further purified on Al_2O_3 (EtOAc/MeOH 4/1) and by preparative HPLC (Phenomenex Luna 250×21.2 mm, MeCN/H_2O) to give compound **10** as dark violet solid (20 mg, 33% yield). The compound dissolves in water, methanol, DMSO and is partially soluble in EtOAc. ^{1}H NMR (600 MHz, MeOD): δ 8.00 (dd, *J* = 12.2, 7.9 Hz, 2H), 7.45 (dd, *J* = 7.8, 2.7 Hz, 2H), 6.82 (s, 2H), 3.65 (s, 3H), 3.55 (m, 4H), 3.51 (m, 4H), 3.07 (t, *J* = 6.3 Hz, 4H), 2.70 (t, *J*=6.3 Hz, 4H), 2.12 – 2.07 (m, 4H), 1.98 – 1.92 (m, 4H), 1.40 (t, *J* = 7.15, 7,15 Hz, 6H). ^{13}C NMR (150 MHz, MeOD): δ 19.46, 19.56, 20.38, 21.60, 27.11, 50.04, 50.50, 51.06, 106.35, 112.33, 126.15, 129.00, 131.33. ^{31}P NMR (243 MHz, MeOD) δ 14.43. HRMS (ESI) m/z 541/543 (M^+).

Immobilization of dye 10 on TiO_2. TiO_2 particles (400 mg) were added to a solution of the Phos-Texas Red dye **10** (18.1 mg, 33.8 µmol) in 15 ml of methanol. The mixture was stirred for 2 days in nitrogen atmosphere. Then solvent was removed *in vacuo* and the solid particles were washed several times with methanol and dried in high vacuum.

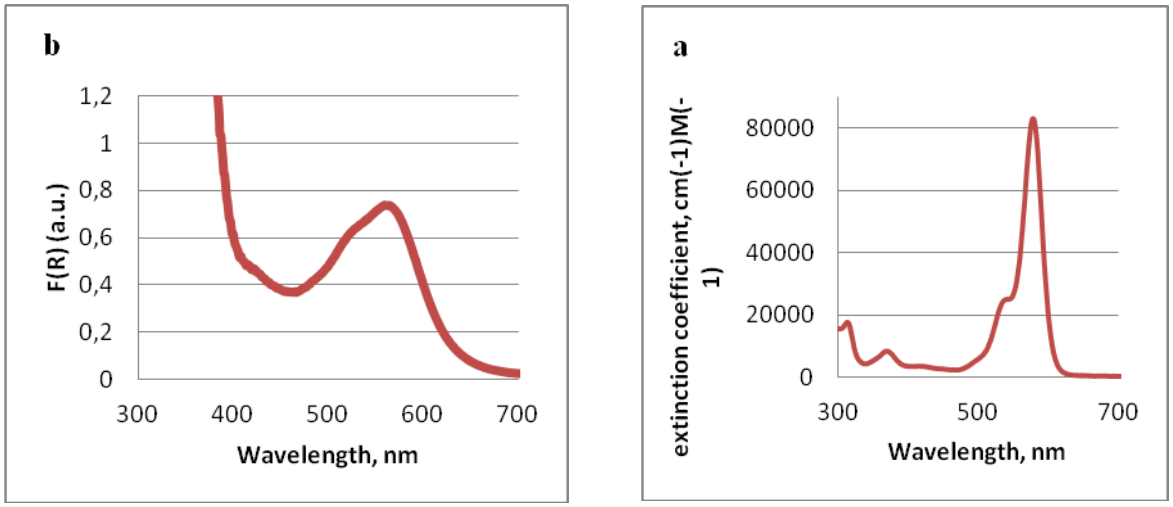

Figure 3. UV/Vis absorption spectra of **10** in methanol solution (a, left). Diffuse UV/Vis reflectance spectra of Phos-Texas Red surface modified TiO_2 (**2**) plotted as the Kubelka-Munk function on the reflectance (R) (b, right).

2.4.7 SYNTHESIS OF COMPOUND 11

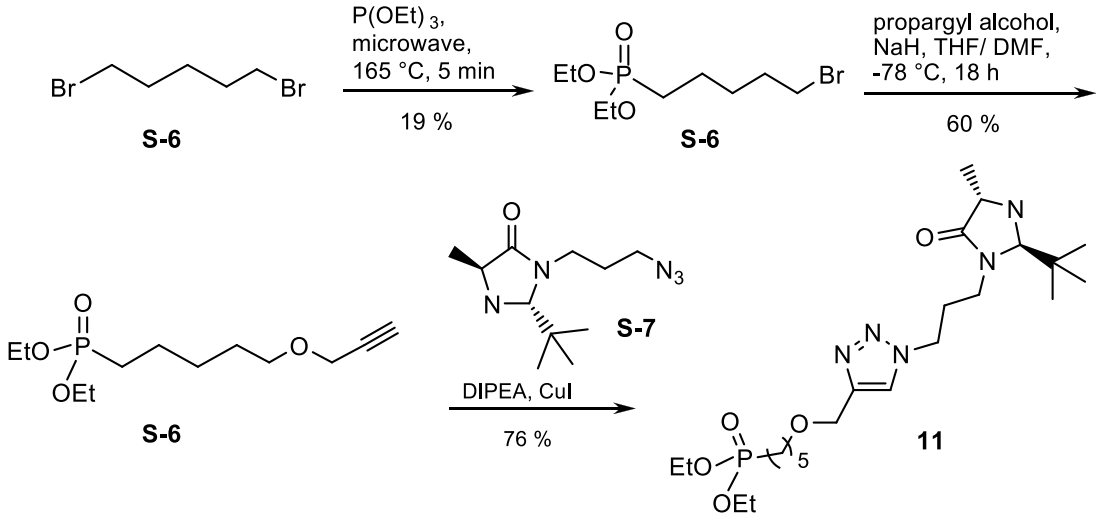

Scheme 5. Synthesis of diethyl 5-((1-(3-((2*R*,4*S*)-2-*tert*-butyl-4-methyl-5-oxoimidazolidin-1-yl) propyl)-1*H*-1,2,3-triazol-4-yl)methoxy)pentylphosphonate (**11**) for surface modification

Diethyl 5-bromopentylphosphonate (S-5)[42]

Distilled 1,5-dibromopentane (**S-4,** 5.45 mL, 40 mmol) and triethylphosphite (1.72 mL, 10 mmol) were placed in a quartz tube. Before the reaction vessel was closed it was saturated with argon. The solution was irradiated in the microwave (max. power: 150 Watt, temperature: 165 °C, pressure: 1 bar, time: 5 min). The excess dibromopentane was removed at 2 mbar and 130 °C. The crude product was purified by flash chromatography (silica gel, dichloromethane/ MeOH 30:1; R_f = 0.46, dichloromethane/ MeOH 20:1) to give 545 mg (yield: 19 %, literature:[6] 94 %) of the pure product as a colorless liquid and 1.18 g of a mixed fraction.

^{1}H NMR (300 MHz, $CDCl_3$, 22 °C, TMS): δ = 1.31 (t, *J* = 7.1 Hz, 6 H, 1/1'-H), 1.46-1.78 (m, 6 H, 3/4/5-H), 1.86 (tt, *J* = 7.2 Hz, 6.8 Hz, 2 H, 6-H), 3.39 (t, *J* = 6.8 Hz, 2 H, 7-H), 3.99-4.16 (m, 4 H, 2/2'-H).

^{31}P NMR (121 MHz, $CDCl_3$): δ = 32.52.

^{13}C NMR (75 MHz, $CDCl_3$): δ = 16.6 (d, *J* = 6.0 Hz, C-1/1'), 21.9 (d, *J* = 5.1 Hz, C-5), 25.7 (d, *J* = 141.1 Hz, C-3), 29.2 (d, *J* = 16.9 Hz, C-4), 32.3 (d, *J* = 1.1 Hz, C-6), 33.5 (C-7), 61.6 (d, *J* = 6.6 Hz, C-2/2').

Diethyl 5-(prop-2-ynyloxy)pentylphosphonate (S-6)[43]

In a 100 mL-Schlenk-flask sodium hydride (752 mg, 18.81 mmol, 60 wt% in oil) was washed with dry Et_2O (5 x 5 mL). The sodium hydride was dried under vacuum and freshly distilled THF (11 mL) was added. The suspension was cooled to -78 °C. A solution of propargyl alcohol (732 µL, 12.54 mmol) in THF (2.7 mL) was added drop wise. The mixture was stirred for 30 min at -78 °C. A solution of diethyl 5-bromopentylphosphonate **S-5** (1.8 g, 6.27 mmol) in abs. DMF (11 mL) was added drop wise by syringe injection over a period of 25 min. The mixture was allowed to warm up to room temperature over night. The solution was evaporated to dryness *in vacuo*. Saturated NH_4Cl solution (20 mL) was added and the solution was extracted with dichloromethane (4 x 30 mL). The organic layer was dried over $MgSO_4$, filtered and concentrated. The crude product was purified by kugelrohr distillation (174 °C/ 0.017 mbar) to give 988 mg (yield: 60 %, literature:[7] 79 %) of a colorless liquid.

R_f = 0.32 (DCM/ MeOH 30:1).

^{1}H NMR (300 MHz, $CDCl_3$, 22 °C, TMS): δ = 1.31 (t, *J* = 7.1 Hz, 6 H, 1/1'-H), 1.42-1.78 (m, 8 H, 3/4/5/6-H), 2.41 (t, *J* = 2.4 Hz, 1 H, 10-H), 3.50 (t, *J* = 6.4 Hz, 2 H, 7-H), 4.01-4.14 (m, 6 H, 2/2'/8-H).

^{31}P NMR (121 MHz, $CDCl_3$): δ = 32.91.

^{13}C NMR (75 MHz, $CDCl_3$): δ = 16.6 (d, *J* = 6.0 Hz, C-1/1'), 22.4 (d, *J* = 5.1 Hz, C-5), 25.8 (d, *J* = 140.6 Hz, C-3), 27.3 (d, *J* = 17.4 Hz, C-4), 29.2 (d, *J* = 1.1 Hz, C-6), 58.2 (C-8), 61.5 (d, *J* = 6.4 Hz, C-2/2'), 69.9 (C-7), 74.3 (C-10), 80.0 (C-9).

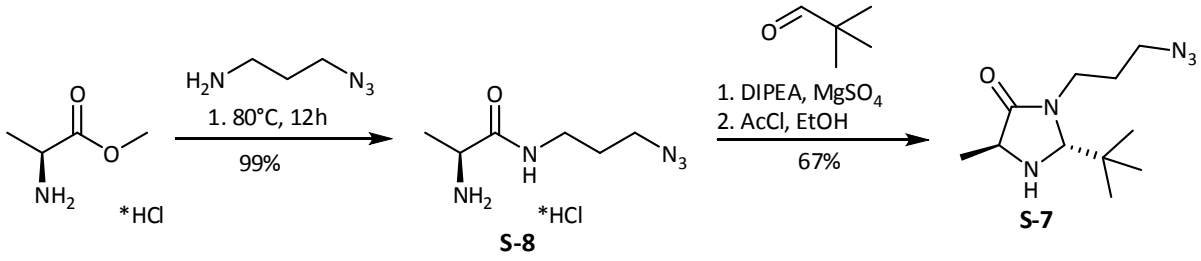

Scheme 6. Synthesis of azido-modified MacMillan Imidazolidinone catalyst (**S-7**).

(*S*)-2-Amino-N-(3-azidopropyl)propanamide hydrochloride (S-8)

L-Alanine methyl ester hydrochloride (1 equiv.) and 3-aminopropane-1-azide[44] (1.2 equiv.) were dissolved in methanol (c_{Ala}= 7.5 mol/l) in a sealed tube. The mixture was heated to 80°C for 12h. After full conversion (as judged by IR spectra 1738 cm^{-1} (ester); 1655 cm^{-1} (amide)) the solvent and excess azide were removed in vacuum yielding quantitatively the pure product as a brown oil.

^{1}H NMR (300 MHz, $CDCl_3$) δ: 3.70 (q, *J* = 6.9 Hz, 1H), 3.47 (t, *J* = 6.4 Hz, 2H), 3.39 – 3.20 (m, 4H), 3.02 (t, *J* = 7.3 Hz, 2H), 2.07 – 1.88 (m, 2H), 1.85 – 1.66 (m, 2H), 1.37 (d, *J* = 7.0 Hz, 3H).

(2*R*,5*S*)-3-(3-Azidopropyl)-2-tert-butyl-5-methylimidazolidin-4-one (S-7)

(*S*)-2-Amino-N-(3-azidopropyl)propanamide hydrochloride (**S-8**, 1 equiv.), magnesium sulfate (2 equiv.), DIPEA (1 equiv.) and pivalaldehyde (70% in propanol, 2 equiv.) were mixed in dichloromethane $c_{S\text{-}8}$ = 0.5 mol/l. The flask was argon flushed and closed by an argon filled balloon, stirred at room temperature for 18h, as the reaction was completed (monitored by TLC) the magnesium sulfate was filtered off and the solution was concentrated in vacuum. The residue was redissolved in dry ethanol (c = 0.8 mol/l) and cooled to -10°C. Acetylchlorid (1.5 equiv.) was added drop wise via syringe over a period of 1.5h, the cooling bath was allowed to melt and stirring was continued for additional 12h. The reaction mixture was diluted with dichloromethane, neutralized by saturated $NaHCO_3$ solution; organic phase was separated, dried over magnesium sulfate and concentrated in vacuum. The crude product was purified by column chromatography (SiO_2, hexanes/ethyl acetate 1:1) yielding **S-7** as yellow brown oil in 67% yield and 96 %de.

^{1}H NMR (400 MHz, $CDCl_3$) δ 4.14 (brs, 1H), 3.85 – 3.74 (m, 1H), 3.56 (q, *J* = 6.8 Hz, 1H), 3.38 – 3.25 (m, 2H), 3.19 (m, 1H), 2.04 – 1.91 (m, 1H), 1.89 – 1.69 (m, 2H), 1.26 (d, *J* = 6.8 Hz, 3H), 0.94 (s, 9H). ^{13}C NMR (75 MHz, $CDCl_3$) δ 177.2, 80.6, 54.3, 49.2, 41.0, 38.4, 26.4, 25.9, 25.6, 18.8.

Diethyl 5-((1-(3-((2*R*,4*S*)-2-*tert*-butyl-4-methyl-5-oxoimidazolidin-1-yl)propyl) -1*H*-1,2,3-triazol-4-yl)methoxy)pentylphosphonate (11)

In a 25 mL-round-bottom-flask (2*R*,5*S*)-3-(3-azidopropyl)-2-*tert*-butyl-5-methylimidazolidin-4-one (**S-7**, 130 mg, 0.54 mmol), diethyl 5-(prop-2-ynyloxy)pentylphosphonate **S-6** (130 mg, 0.49 mmol) and copper(I) iodide (9.40 mg, 0.05 mmol) were dissolved in dichloromethane (5 mL) to give a colorless suspension. DIPEA (172 µL, 0.99 mmol) was added and the cooled mixture was degassed by argon purge for 5 min. The solution was stirred for 18 h under an argon atmosphere. The solution was diluted with dichloromethane (20 mL) and washed with saturated NH_4Cl solution (3 x 15 mL). The aqueous layer was extracted with dichloromethane (2 x 20 mL), the combined organic layers were washed with brine (1 x 30 mL), dried over $MgSO_4$

and evaporated to dryness. The crude product was purified by flash chromatography (silicagel, dichloromethane/ MeOH 15:1; R_f = 0.29) to give 188 mg (76 %, 10:1 dr (82 % *de*)) of a pale yellow oil. The diastereomeric excess was determined from integration of ^{1}H-NMR signals ($CDCl_3$) at 0.92 ppm (major) and 0.96 ppm (minor).

^{1}H NMR (300 MHz, $CDCl_3$, 22 °C, TMS): δ = 0.92 (s, 9 H, 20/20'/20''-H), 1.27 (d, *J* = 6.8 Hz, 3 H, 16-H), 1.31 (t, *J* = 7.1 Hz, 6 H, 1/1'-H), 1.38-1.76 (m, 8 H, 3/4/5-H), 2.09-2.42 (m, 3 H, 12/17-H), 3.17 (dt, *J* = 14.3, 6.9 Hz, 1 H, 13-H), 3.50 (t, *J* = 6.4 Hz, 2 H, 7-H), 3.58 (q, *J* = 6.8 Hz, 1 H, 15-H), 3.77 (dt, *J* = 14.3, 6.9 Hz, 1 H, 13-H), 4.00-4.13 (m, 4 H, 2/2'-H), 4.15 (d, *J* = 1.3 Hz, 1 H, 18-H), 4.25-4.43 (m, 2 H, 11-H), 4.59 (s, 2 H, 8-H), 7.65 (s, 1 H, 10-H).

^{31}P NMR (121 MHz, $CDCl_3$): δ = 32.95.

^{13}C NMR (75 MHz, $CDCl_3$): δ = 16.6 (d, *J* = 6.0 Hz, C-1/1'), 18.8 (C-16), 22.4 (d, *J* = 5.2 Hz, C-5), 25.7 (d, *J* = 140.7 Hz, C-3), 26.0 (C-20/20'/20''), 27.3 (d, *J* = 17.3 Hz, C-4), 27.9 (C-12), 29.3 (C-6), 38.5 (C-19), 40.8 (C-13), 47.9 (C-11), 54.5 (C-15), 61.6 (C-2/2'), 64.4 (C-8), 70.6 (C-7), 80.7 (C-18), 122.9 (C-9), 145.6 (C-10), 177.6 (C-14).

UV-VIS (MeCN): λ_{max} (nm)/ ε($L \cdot M^{-1} \cdot cm^{-1}$) = 217/ 4475.

IR: $\tilde{\nu}$ [cm^{-1}] = 3451, 2980, 2944, 2914, 2869, 1682, 1222, 1097, 1024, 960.

ESI-MS: m/z = 502.3 (MH^+).

Immobilization of diethyl 5-((1-(3-((2*R*,4*S*)-2-*tert*-butyl-4-methyl-5-oxoimidazolidin-1-yl) propyl)-1*H*-1,2,3-triazol-4-yl)methoxy) pentyl phosphonate (11) on TiO_2

TiO_2 (485 mg, 6.07 mmol), compound **11** (20.5 mg, 41 µmol) and MeCN (3 mL) were placed in a 5 mL snap cap vial equipped with a magnetic stirring bar. The vial was closed with a septum and the suspension was stirred at 40 °C. After 24 h the solvent was removed and the TiO_2 was dried for 1.5 h at 65 °C. The TiO_2 was suspended in MeCN (2 mL), centrifuged and the solvent was removed. The procedure was repeated three times, the modified TiO_2 was dried at 65 °C and under high vacuum over night. 79 % of the initial amount of compound **11** was immobilized as determined by UV spectroscopy.

2.4.8 EXPERIMENTAL DATA FOR AZA-HENRY REACTIONS[45]

Screening of different ketone equivalents for Aza-Henry reactions:

2-Phenyl-1,2,3,4-tetrahydroisoquinoline **14a** (1 equiv., 52 mg; 0.25 mmol), L-proline (0.2 equiv., 6 mg; 0.05 mmol) and 2, 5 or 10 equiv. of ketone were mixed in a schlenk tube together with CH_3CN as solvent (total volume: 1 ml; c_{THIQ} = 0.25 mol/l)). CdS (5 mg/$ml_{solvent}$) was added and an oxygen atmosphere was applied by balloon. The vial was irradiated with high power LEDs (460 nm) in a distance of approximately 5 cm for 24h. Analysis by TLC and determination of conversion by gas chromatography.

Overview:

2 equiv. of ketone using 37 µl of acetone in 960 µl of CH_3CN
5 equiv. of ketone using 91 µl of acetone in 910 µl of CH_3CN
10 equiv. of ketone using 182 µl of acetone in 820 µl of CH_3CN

1-(2-phenyl-1,2,3,4-tetrahydroisoquinolin-1-yl)propan-2-one (**16**a)

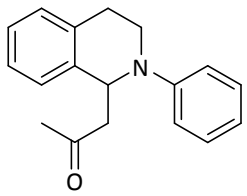

265,35 g/mol

According to **general procedure 2**: 2-phenyl-1,2,3,4-tetrahydroisoquinoline **14a** (97 mg, 463 µmol), L-proline (10.5 mg, 91 µmol) and CdS (10mg, 69 µmol) in acetone **15a** (1.8 ml) afforded 107 mg (87 %) of **16a** after 24 h irradiation as a colorless solid. R_f (hexanes:ethyl acetate 3:1) = 0.51. ^{1}H NMR (300 MHz, $CDCl_3$) δ 7.31 – 7.21 (m, 2H), 7.17 (t, *J* = 2.9 Hz, 4H), 6.95 (d, *J* = 8.0 Hz, 2H), 6.79 (t, *J* = 7.3 Hz, 1H), 5.41 (t, *J* = 6.3 Hz, 1H), 3.72 – 3.60 (m, 1H), 3.60 – 3.46 (m, 1H), 3.14 – 2.97 (m, 2H), 2.90 – 2.75 (m, 2H), 2.08 (s, 3H). ^{13}C NMR (75 MHz, $CDCl_3$) δ 207.3, 148.9, 138.3, 134.5, 129.4, 128.7, 126.9, 126.8, 126.3, 118.3, 114.8, 54.8, 50.2, 42.1, 31.1, 27.2.

1-(2-(4-methoxyphenyl)-1,2,3,4-tetrahydroisoquinolin-1-yl)propan-2-one (16b)

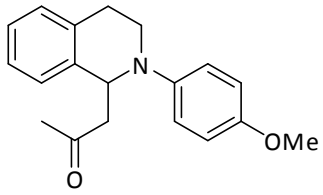

295,38 g/mol

According to **general procedure 2**: 2-(4-methoxyphenyl)-1,2,3,4-tetrahydroisoquinoline **14b** (42 mg, 176 µmol), L-proline (4 mg, 35 µmol), and CdS (3.5 mg, 24 µmol) in acetone **15a** (0.7 ml) afforded 46 mg (89 %) of **16b** after 18 h irradiation as a colorless solid. R_f (hexanes:ethyl acetate 3:1) = 0.53. ^{1}H NMR (300 MHz, $CDCl_3$) δ 7.20 – 7.05 (m, 4H), 6.95 – 6.87 (m, 2H), 6.86 – 6.76 (m, 2H), 5.24 (t, *J* = 6.4 Hz, 1H), 3.75 (s, 3H), 3.61 – 3.38 (m, 2H), 3.08 – 2.92 (m, 2H), 2.82 – 2.67 (m, 2H), 2.06 (s, 3H). ^{13}C NMR (75 MHz, $CDCl_3$) δ 207.4, 153.3, 143.7, 138.3, 134.3, 129.0, 126.8, 126.7, 126.2, 118.4, 114.6, 56.0, 55.6, 50.0, 42.9, 30.9, 26.7.

2-(2-phenyl-1,2,3,4-tetrahydroisoquinolin-1-yl)cyclohexanone (**16c**)

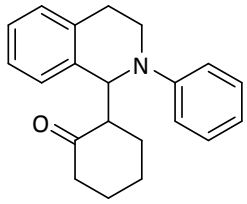

305,41 g/mol

According to **general procedure 2**: 2-phenyl-1,2,3,4-tetrahydroisoquinoline **14a** (94 mg, 449 µmol), L-proline (10.3mg, 90 µmol) and CdS (10mg, 69 µmol) in cyclohexanone **15b** (1.8 ml) afforded 108mg (79 %) **16c** after 24 h irradiation as colorless oil after 24 h irradiation. R_f (hexanes:ethyl acetate 3:1) = 0.55. ^{1}H NMR (400 MHz, $CDCl_3$, *major diastereomer) δ 7.27 – 7.18 (m, 3H), 7.18 – 7.09 (m, 3H), 6.92*, 6.82 (d, 8.1 Hz, 2H), 6.76*, 6.68 (t, 7.2 Hz, 1H), 5.67, 5.63* (d, 6.6 Hz, 1H), 3.77 – 3.48 (m, 2H), 3.09 – 2.67 (m, 3H), 2.53 – 2.43 (m, 1H), 2.37 – 2.32 (m, 2H), 1.96 – 1.79 (m, 3H), 1.78 – 1.54 (m, 2H). ^{13}C NMR (101 MHz, $CDCl_3$) δ 211.9, 149.3, 136.0, 135.1, 129.4, 128.7, 128.0, 126.7, 125.8, 118.1, 114.9, 112.3, 56.5, 55.0, 42.6, 42.0, 41.4, 30.2, 27.3, 25.03, 23.8.

1-(2-phenyl-1,2,3,4-tetrahydroisoquinolin-1-yl)butan-2-one (16d)

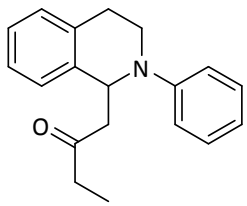

279,38 g/mol

According to **general procedure 2**: 2-phenyl-1,2,3,4-tetrahydroisoquinoline **14a** (108 mg, 516 µmol), L-proline (11.9mg, 103 µmol) and CdS (10mg, 69 µmol) in 2-butanone **15c** (1.8 ml) afforded 109mg (76 %) **16d** after 15 h irradiation as brownish solid. R_f (hexanes:ethyl acetate 3:1) = 0.55. ^{1}H NMR (400 MHz, $CDCl_3$) δ 7.30 (m, 2H), 7.19 (m, 4H), 7.00 (d, *J* = 8.0 Hz, 2H), 6.82 (t, *J* = 7.3 Hz, 1H), 5.48 (t, *J* = 6.4 Hz, 1H), 3.73 – 3.63 (m, 1H), 3.62 – 3.52 (m, 1H), 3.10 (m, 2H),

2.92 – 2.78 (m, 2H), 2.34 (m, 2H), 1.03 (t, *J* = 7.3 Hz, 3H). ^{13}C NMR (101 MHz, $CDCl_3$) δ 210.0, 148.9, 138.5, 134.5, 129.4, 128.7, 126.9, 126.9, 126.3, 118.2, 114.7, 55.2, 49.0, 42.0, 37.3, 27.4, 7.6.

2.4.9 SYNTHESIS AND CHARACTERIZATION OF $PBBIO_2Br$ SEMICONDUCTORS

The **$PbBiO_2Br$ bulk semiconductor** was synthesized according to a literature procedure.[46]

$PbBiO_2Br$ *nano* semiconductor. For the synthesis of $PbBiO_2Br$ *nano* all chemicals were of analytical grade and were used as received.

$Bi_5O(OH)_9(NO_3)_4$ (2 mmol) were mixed with $Pb(CH_3COO)_2{\times}3H_2O$ (10 mmol) and NaBr (10 mmol). Subsequently, 200 ml of H_2O were added. The mixture was stirred for 24 h yielding a white suspension. About 100 ml of the suspension were heated under stirring for 72 h at 80°C in a round bottom flask with stopper. The suspension turned yellow. Then it was centrifuged at 6000 rpm for 30 min, the solid precipitate was dispersed in deionized water and centrifuged again. The procedure was repeated once and the yellow product was washed once with ethanol (99%) and again centrifuged at 6000rpm for 30 min. Ethanol was removed and the solid was dried at 50 °C for 3 days.

Characterization

X-ray powder diffraction (XRD) patterns of the products were measured by using a STOE STADI P (STOE & Cie GmbH, Darmstadt, Germany) at 40 kV and 40 mA(Cu $K\alpha_1$ radiation, Ge monochromator) equipped with a PSD unit. The diffractograms were measured at room temperature from 8° ≤ 2θ ≤ 90° with a step size of Δθ = 0.02°. Diffuse UV/Vis reflectance spectra were recorded by using a Bruins Instruments Omega 20 spectrometer. Data were transferred to absorption spectra by the Kubelka-Munk method.[47]

2.4.10 GLASS MICROREACTOR AND IRRADIATION SET UP USED FOR PHOTOCATALYSIS

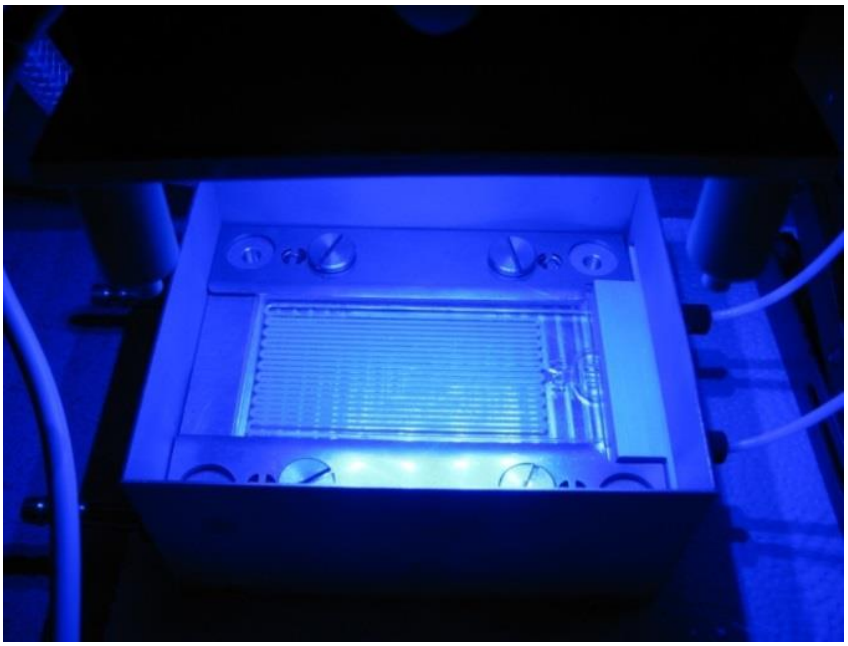

Figure 4. Glass microreactor with suspension of reaction mixture and heterogeneous semiconductor catalyst (no-flow mode)

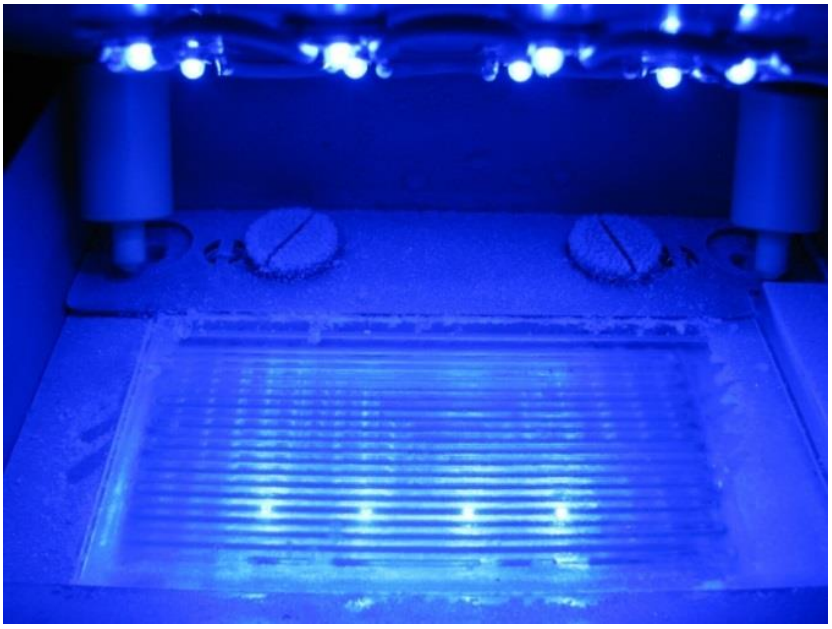

Figure 5**.** Irradiation set-up for the reaction in the microreactor.

2.5 SUPPORTING INFORMATION

2.5.1 SPECTRA OF COMPOUNDS 10, 11 AND 13

Phos-TexasRed dye (10).

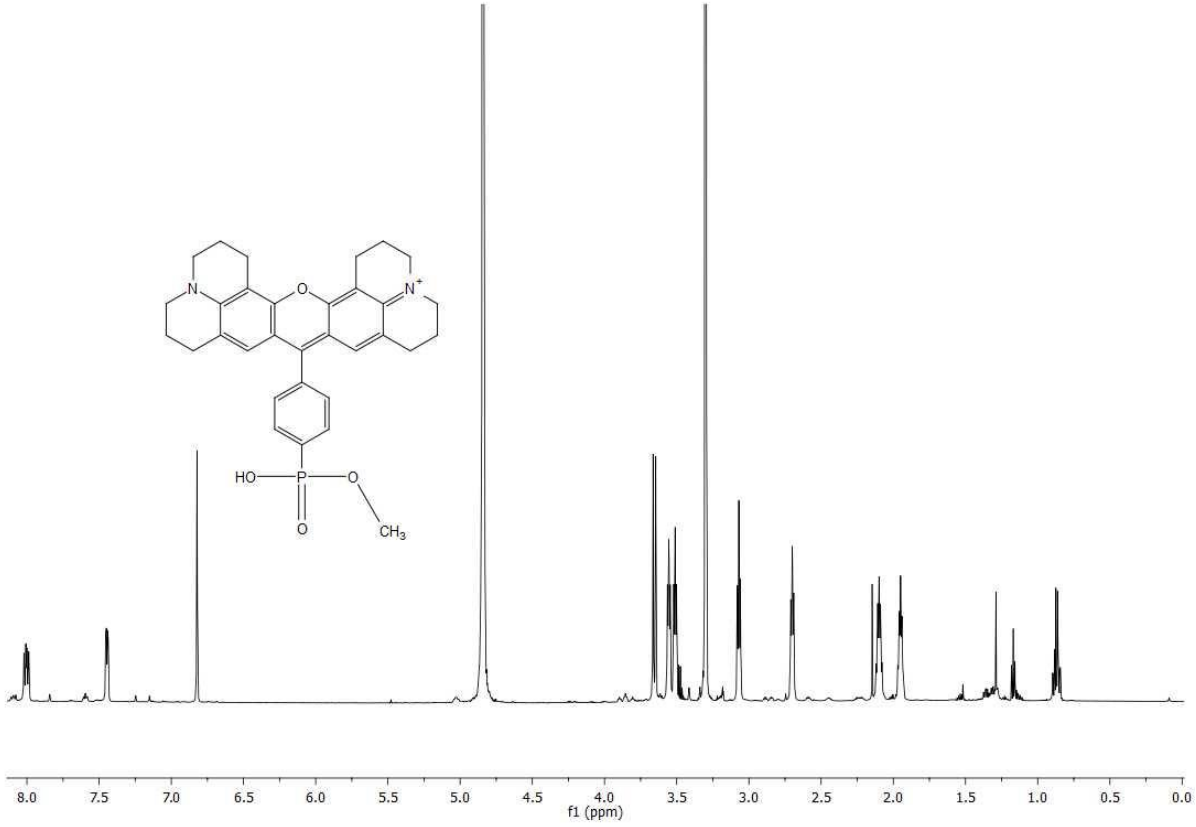

Figure 6**.** ^{1}H NMR (600 MHz, MeOD): Phos-TexasRed dye (**10**).

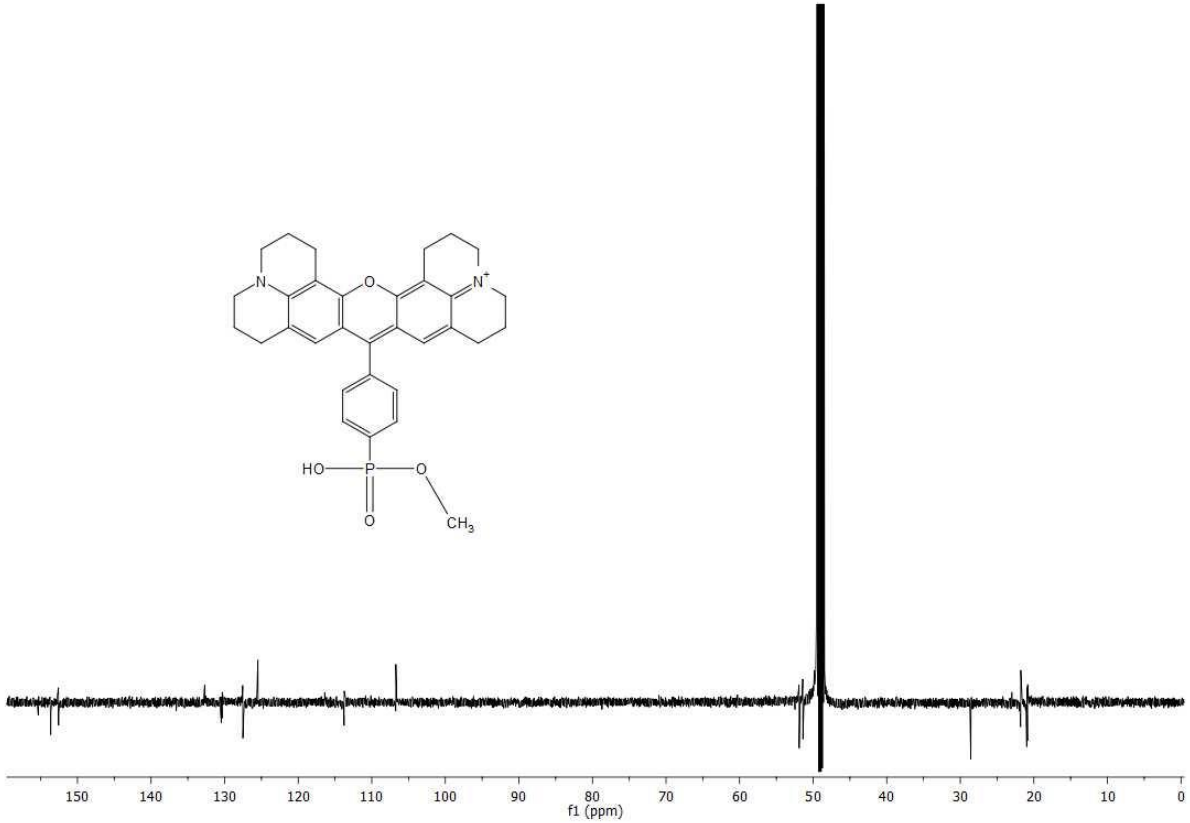

Figure 7**.** ^{13}C NMR (150 MHz, MeOD): Phos-TexasRed dye (**10**).

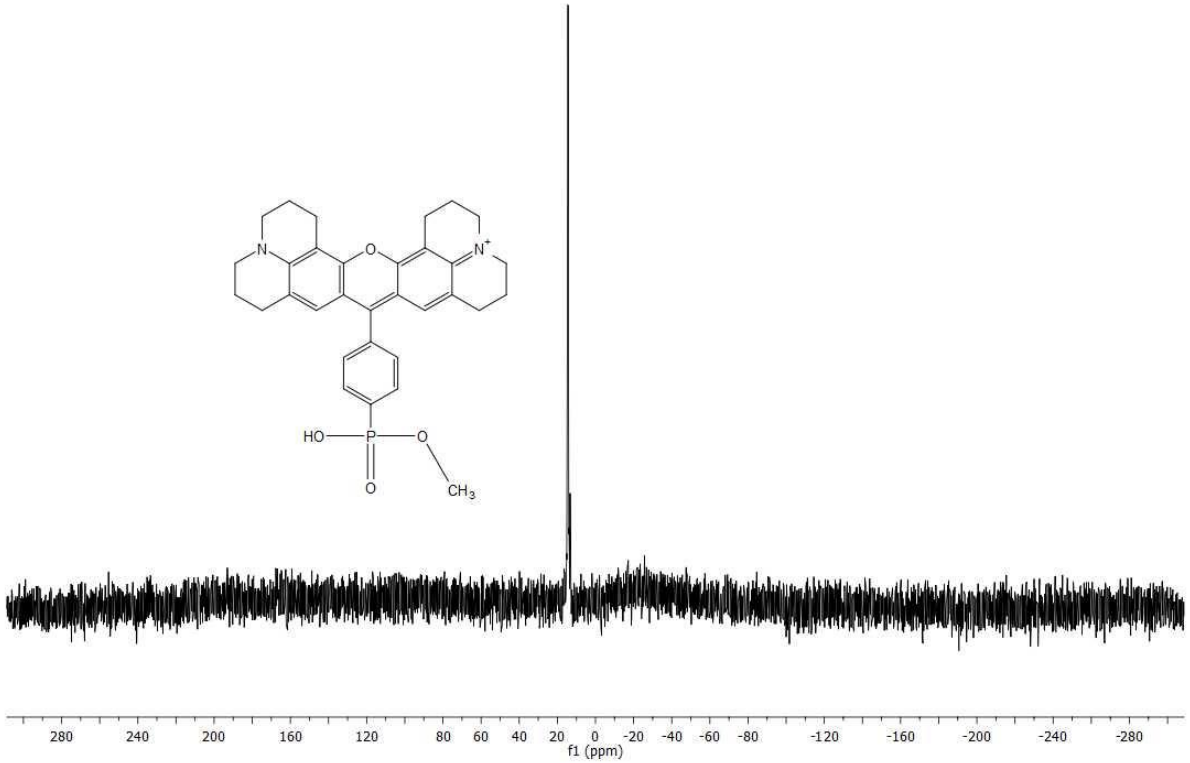

Figure 8**.** ^{31}P NMR (243 MHz, MeOD): Phos-TexasRed dye (**10**).

Diethyl 5-((1-(3-((2*R*,4*S*)-2-*tert*-butyl-4-methyl-5-oxoimidazolidin-1-yl)propyl) -1*H*-1,2,3-triazol-4-yl)methoxy)pentylphosphonate (**11**)

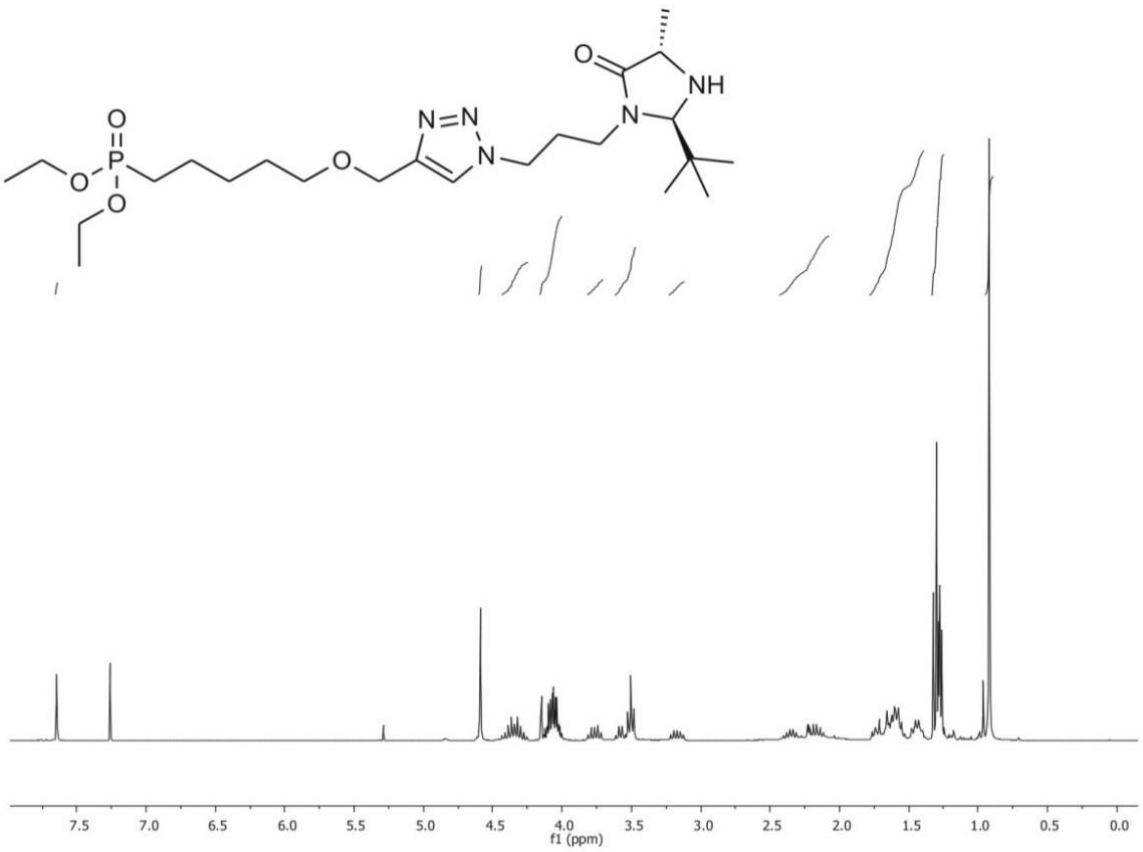

Figure 9. ^{1}H NMR (300 MHz, $CDCl_3$): Diethyl 5-((1-(3-((2*R*,4*S*)-2-*tert*-butyl-4-methyl-5-oxoimidazolidin-1-yl) propyl)-1*H*-1,2,3-triazol-4-yl)methoxy)pentylphosphonate **(11).**

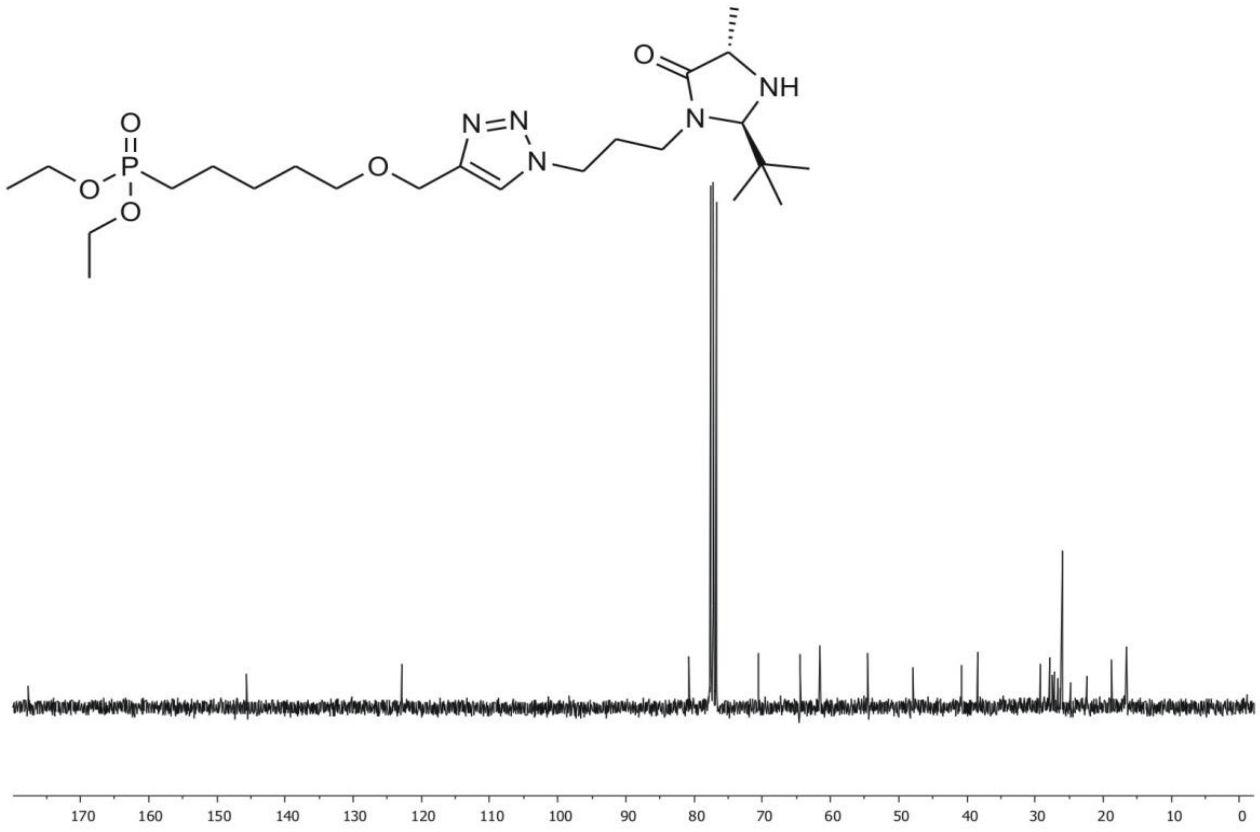

Figure 10**:** ^{13}C NMR (75 MHz, $CDCl_3$): Diethyl 5-((1-(3-((2*R*,4*S*)-2-*tert*-butyl-4-methyl-5-oxoimidazolidin-1-yl) propyl)-1*H*-1,2,3-triazol-4-yl)methoxy)pentylphosphonate **11**.

2.6 REFERENCES

1. a) A. J. Bard, *Science* **1980**, *207*, 139–144. b) F. Teply, *Coll. Czech. Chem. Commun.* **2011**, *76*, 859–917. c) G. Pandey, M. K. Ghorai, S. Hazra, *Pure Appl. Chem.* **1996**, *68*, 653.
2. For recent reviews, see: a) J. M. R. Narayanam, C. R. J. Stephenson. *Chem. Soc. Rev.* **2011**, *40*, 102–113. b) ref. 1b. c) T. P. Yoon; M. .A. Ischay; J. Du, *Nature Chem.* **2010**, *2*, 527–532. d) K. Zeitler, *Angew. Chem. Int. Ed.* **2009**, *48*, 9785–9789.
3. C. Dai, J. M. R. Narayanam, C. R. J. Stephenson, *Nat. Chem*. **2011**, *3*, 140-145.
4. a) M. A. Ischay, M. E. Anzovino, J. Du, T. P. Yoon, *J. Am. Chem. Soc*. **2008**, *130*, 12886–12887. b) J. Du, T. P. Yoon, *J. Am. Chem. Soc*. **2009**, *131*, 14604-14605. c) M. A. Ischay, Z. Lu, T. P. Yoon, *J. Am. Chem. Soc*. **2010**, *132*, 8572–8574. d) J. Du, L. Ruiz. Espelt, I. A. Guzei, T. P. Yoon, *Chem. Sci.* **2011**, *2*, 2115-2119.
5. a) Z. Lu, M. Shen, T. P. Yoon, *J. Am. Chem. Soc*. **2011**, *133*, 1162–1164. b) Y.-Q. Zou, L.-Q. Lu, L. Fu, N.-J. Chang, J. Rong, J.-R. Chen, W.-J. Xiao, *Angew. Chem. Int. Ed.* **2011**, *50*, 7171–7175. c) M. Rueping, D. Leonori, T. Poisson, *Chem. Commun*. **2011**, *47*, 9615–9617. d) S. Maity, M. Zhu, R. S. Shinabery, N. Zheng, *Angew. Chem. Int. Ed.* **2012**, DOI: 10.1002/anie.201106162.
6. a) A. E. Hurtley, M. A. Cismesia, Mi. A. Ischay, T. P. Yoon, *Tetrahedron* **2011**, *67*, 4442–4448. b) S. Lin, M. A. Ischay, C. G. Fry, T. P. Yoon, *J. Am. Chem. Soc*. 2**011**, *133*, 19350–19353.
7. For selected recent examples: a) L. Furst, B. S. Matsuura, J. M. R. Narayanam, J. W. Tucker, C. R. J. Stephenson, *Org. Lett*. **2010**, *12*, 3104–3107. b) P. V. Pham, D. A. Nagib, D. W. C. MacMillan, *Angew. Chem. Int. Ed.* **2011**, *50*, 6119–6122. c) J. D. Nguyen, J. W. Tucker, M. D. Konieczynska, C. R. J. Stephenson, *J. Am. Chem. Soc.* **2011**, *133*, 4160-4163. d) M. Rueping, S. Zhu, R. M. Koenigs, *Chem. Commun*. **2011**, *47*, 12709–12711. e) A. McNally, C. K. Prier, D. W. C. MacMillan, *Science*, **2011**, *334*, 114–117. f) D. Kalyani, K. B. McMurtrey, S. R. Neufeldt, M. S. Sanford, *J. Am. Chem. Soc.* **2011**, *133*, 18566. g) D. A. Nagib, D. W. C. MacMillan, *Nature* **2011**, *480*, 224–228.
8. For the formation of C-P bonds, see: a) D. P. Hari, B. König, *Org. Lett.* **2011**, *13*, 3852–3855. b) M. Rueping, S. Zhu, R. M. Koenigs, *Chem. Commun.* **2011**, *47*, 8679 - 8681. For

the formation of C-S bonds, see: Y. Cheng, J. Yang, Y. Qu, P. Li, *Org. Lett.* **2011**, DOI: 10.1021/ol2028866. For the formation of C-N bonds, see: J. Xuan, Y. Cheng, J. An, L.-Q. Lu, X.-X. Zhang, W.-J. Xiao, *Chem. Commun.* **2011**, *47*, 8337–8339.

9. a) D. A. Nicewicz, D. W. C. MacMillan, *Science* **2008**, *322*, 77–80. b) D. A. Nagib, M. E. Scott, D. W. C. MacMillan, *J. Am. Chem. Soc*. **2009**, *131*, 10875-10877. c) H.-W. Shih, M. N. Vander Wal, R. L. Grange, D. W. C. MacMillan, *J. Am. Chem. Soc*. **2010**, *132*, 13600–13603. d) M. Neumann, S. Füldner, B. König, K. Zeitler, *Angew. Chem. Int. Ed.* **2011**, *50,* 951-954.

10. For seminal and recent examples of UV light promoted enantioselective photocatalytic reaction, see: a) A. Bauer, F. Westkämper, S. Grimme, T. Bach, *Nature* **2005**, *436*, 1139–1140. b) Ch. Müller, A. Bauer, M. M. Maturi, M. C. Cuquerella, M. A. Miranda, T. Bach, *J. Am. Chem. Soc.* **2011**, *133*, 16689–16697. For a review on enantioselective photocatalysis using hydrogen-bonding templates, see: c) C. Müller, T. Bach, *Aust. J. Chem.* **2008**, *61*, 557-564.
11. a) A. Atyaoui, L. Bousselmi, H. Cachet, Peng Pu, E. M. M. Sutter, *J. Photochem. Photobiol. A* **2011**, *224*, 71–79; b) F. Spadavecchia G. Cappelletti, S. Ardizzone, C. L. Bianchi, S. Cappelli, C. Oliva, P. Scardi, M. Leoni, P. Fermo, *Appl. Cat. B* **2010**, *96*, 314–322; c) M. K. Seery, R. George, P. Floris, S. C. Pillai, *J. Photochem. Photobiol. A* **2007**, *189*, 258–263; d) J. Tang, J. Ye, *Angew. Chem. Int. Ed.* **2004**, *43*, 4463–4466.
12. An active area of current research is the use of inorganic semiconductors as photocatalysts for water splitting and hydrogen generation. For a recent review, see: a) X. Chen, S. S. Mao, *Chem. Rev*. **2007**, *107*, 2891−2959; b) R. M. Navarro, M. C. Álvarez-Galván, F. del Valle, J. A. Villoria de la Mano, J. L. G. Fierro*, ChemSusChem* **2009**, *2*, 471–485; c) H. Xu, R. Q. Zhang, A. N. C. Ng, A. B. Djurišić, H. T. Chan, W. K. Chan, S. Y. Tong, *J. Phys. Chem. C* **2011**, *115*, 19710-19715**;** d) M. Antoniadou, P. Lianos, *Appl. Cat. B* **2011**, *107*, 188–196; e) M. Antoniadou, V. M. Daskalaki, N. Balis, D. I. Kondarides, C. Kordulis, P. Lianos. *Appl. Cat. B* **2011**, *107*, 188–196.
13. a) H. Kisch, W. Schindler, *J. Photochem. Photobiol. A* **1993**, *103,* 257–264; b) H. Kisch, W. Linder, *Chem. Unserer Zeit* **2001**, *35*, 250–257; c) M. Gartner, H. Kisch, *Photochem. Photobiol Sci.* **2007**, *6*, 159–164; d) N. Zeug, J. Bücheler, H. Kisch, *J. Am. Chem Soc.* **1985**, *107*, 1459–1465; e) W. Hetterich, H. Kisch, *Chem. Ber.*1987, **121**, 15-20.

14. L. Cermenati, C. Richter, A. Albini, *Chem. Commun*, **1998**, *7*, 805–806.

15. For selective examples using metal-organic frameworks and polymers, see: a) Z. Xie, C. Wang, K. E. deKrafft, W. Lin, *J. Am. Chem. Soc.* **2011**, *133*, 2056–2059. b) C. Wang, Z. Xie, K. E. deKrafft, W. Lin, *J. Am. Chem. Soc.* **2011**, *133*, 13445–13454.

16. For selective examples using organic semiconducting material, see: a) F: Su, S: C. M:, L: Möhlmann, M. Antonietti, X. Wang, S. Blechert, *Angew. Chem. Int. Ed.* **2010**, *49,* 657–660. b) F. Su, S. C. Mathew, G. Lipner, X. Fu, M. Antonietti, S. Blechert, X. Wang, *J. Am. Chem. Soc.* **2010**, *132*, 16299–16301.

17. For selected recent reviews on organocatalysis, see: a) S. Bertelsen, K. A. Jørgensen, K. A. *Chem. Soc. Rev*. **2009**, *38*, 2178–2189. b) B. List, (Ed.) *Top. Curr. Chem*. **2010**, *291*, 1–456 (Asymmetric Organocatalysis). c) *Chem. Rev.* **2007**, *107* (12), 5413–5883 (special issue on organocatalysis).

18. For a recent example combining organocatalysis and UV light TiO_2 photocatalyis, see: X.-H. Ho, M.-J. Kang, S.-J. Kim, E. D. Park, H.-Y. Jang, *Catal. Sci. Technol*. **2011**, ***1***, 923–926.

19. P25 Degussa with an anatase: rutile ratio of 80:20 was used.

20. a) P. Roy, S. Berger, P. Schmuki, *Angew. Chem. Int. Ed*. **2011**, *50*, 2904–2939; b) S. Higashimoto, N. Kitao, N. Yoshida, T. Sakura, M. Azuma, H. Ohue, Y. Sakata, *J. Catal.* **2009**, *266*, 279–285. c) The visible light absorption was attributed to surface deposits of organic material on TiO_2.

21. a) S. U. M. Khan, M. Al-Shahry, W. B. Ingler Jr., *Science* **2002**, *297*, 2243-2245; b) X. Chen, L. Liu, P. Y. Yu, S. S. Maol, *Science* **2011**, *331*, 746–750.

22. S. Füldner, R. Mild, H. I. Siegmund, J. A. Schroeder, M. Gruber, B. König, *Green Chem.* **2010**, *12*, 400–406.

23. L. Xiong, F. Yang, L. Yan, N. Yan, X. Yang, M. Qiu, Y. Yu, *J. Phys. Chem. Solids* **2011** *72* , 1104–1109.

24. D. Chatterjee, V. R. Patnama, A. Sikdar, P. Joshi, R. Misra, N. N. Rao. *J. Hazard. Mat*. **2008**, *156*, 435–441.

25. A. Pfitzner, P. Pohla, *Z. Anorg. Allg. Chem.* **2009**, *635*, 1157–1159.

26. M. Hopfner, H. Weiss, D. Meissner, F. W. Heinemann, H. Kisch, *Photochem. Photobiol. Sci.*, **2002**, *1*, 696–703.

27. Procedure according to ref. 9a; for details please see the supporting information of this article.

28. H. Kisch, *Adv. Photochem*. **2001**, *26*, 93–143.

29. The flat band potential of $PbBiO_2Br$ in acetonitrile has not been determined. The expected shift of the potential is + 0.5 to + 1.0 V in acetonitrile compared to water, pH 7. This would be sufficient for the observed transformations. The potentials of $PbBiO_2Br$ in water were determined to 1.67 V for the valence band and -0.80 V for the conduction band.

30. For the redox potential of Texas-Red, see: M. Torimura, S. Kurata, K. Yamada, T. Yokumaku, Y. Kamagata, T. Kanagawa, R. Kurane, *Analyt. Sci*. **2001**, *17*, 155–160.

31. For recent reviews on dehydrogenative coupling using oxidation reagents: a) C.-J. Li, *Acc. Chem. Res.* **2009**, *42*, 335–344; b) C. J. Scheuermann , *Chem. Asian J***. 2010**, *5*, 436 – 451; c) C. S. Yeung, V. M. Dong, *Chem. Rev*. 2011, **111**, 1215–1292.

32. a) A. G. Condie, J.-C. González-Gómez C. R. J. Stephenson, *J. Am. Chem. Soc.* **2010**, *132*, 1464. b) M. Rueping, C. Vila, R. M. Koenigs, K. Poscharny, D. C. Fabry, *Chem. Commun.* **2011**, *47*, 2360–2362.

33. a) Y. Pan, C. W. Kee, L. Chen, C.-H. Tan, *Green Chem.*, **2011**, *13*, 2682-2685. b) Y. Pan, S. Wang, C. W. Kee, E. Dubuisson, Y. Yang, K. P. Loh, C.-H, Tan, *Green Chem***.**, **2011**, *13*, 3341–3344.

34. Klussmann et al. reported slow racemization of the products under their oxidative reaction conditions: A. Sud, D. Sureshkumarz, M. Klussmann *Chem. Commun*., **2009**, 3169–3171. Our stereochemical analysis also reveals only low *ee* values as similarly noted in previous reports by Rueping (see ref. 32b) and Tan (see ref. 33a).

35. For a recent paper on the calculation of flat band potentials of semiconductor oxides, see: M. C. Toroker, D. K. Kanan, N. Alidoust, L. Y. Isseroff, P. Liaob, E. A. Carter, *Phys. Chem. Chem. Phys*., **2011**, *13*, 16644–16654.

36. D. A. Nicewicz, D. W. C. MacMillan, *Science* **2008**, *322*, 77-80.

37. G. Laven, M. Kalek, M. Jezowska, J. Stawinski, *New J. Chem*., **2010**, *34*, 967–975.

38. G.-S. Jiao, J. C. Castro, L. H. Thoresen, K. Burgess.*Org. Lett.* **2003**, *5*, 3675-3677.

39. Y. Yang, J. O. Escobedo, A. Wong, C. M. Schowalter, M. C. Touchy, L. Jiao, W. E. Crowe, F. R. Fronczek, R. M. Strongin, *J. Org. Chem*. **2005**, *70*, 6907-6912.

40. P. Hubert Mutin, Gilles Guerrero and Andre´ Vioux, J. Mater. Chem., **2005**, *15*, 3761-3768.

41. G. Jiao, J. C. Castro, L. H. Thoresen, K. Burgess, *Org. Lett.* **2003**, *5*, 3675-3677.

42. D. Villemina, F. Simeona, H. Decreusa, P.-A. Jaffres, *Phosphorus, Sulfur and Silicon* **1998**, *133*, 209-213.

43. L. Delain-Bioton, D. Villemin, P.-A. Jaffrès*, Eur. J. Org. Chem.* **2007**, 1274-1286.

44. J. Hannant, J. H. Hedley, J. Pate, A Walli, Said A. Farha Al-Said, M. A. Galindo, B. A. Connolly, B. R. Horrocks, A. Houlton and A. R. Pike, *Chem. Commun.*, **2010**, ***46***, 5870.

45. a) M. Rueping, C. Vila, R. M. Koenigs, K. Poscharny, D. Fabry, *Chem. Commun.* **2011**, *47*, 2360 - 2362. b) A. Sud, D. Sureshkumar, M. Klussmann, *Chem. Commun.* **2009**, 3169–3171

46. A. Pfitzner, P. Pohla. *Z. Anorg. Allg. Chem*., **2009**, *635*, 1157-1159.

47. P. Kubelka, F. Munk, *Z. Tech. Phys.* **1931**, *12*, 593–601.

CHAPTER 3

3. PHOTOCATALYTIC [4 + 2] CYCLOADDITIONS ‡

‡ $PbBiO_2Br$ semiconductor was synthesized and characterized by S. Dankesreiter.

3.1 INTRODUCTION

The Diels-Alder reaction is one of the best reactions in organic chemistry for the synthesis of six-membered rings. The reaction depends on the electronic structure of the dienophile and diene and is thermally initiated as predicted by the Woodward-Hoffmann rules. However, photocatalytic methods have been developed to extend the substrate scope of the reaction. Particularly, Jones[1] and Bauld[2,3] found that photoinduced electron transfer initiated by sensitizers facilitates the formation of the corresponding radical cation from an electron-rich dienophile that than reacts with an electron-rich diene to form the [4+2] cycloaddition product (Scheme 1). The conversion of an electron rich and therefore unreactive alkene, into its corresponding radical cation, which is highly electron deficient and therefore extremely reactive, is a mechanistic alternative to the classic Diels-Alder procedure. The radical cation concept turned out to be particularly useful for typically unreactive electron-rich π-systems as Diels-Alder dienophiles that are readily converted into radical cations under photoinduced electron transfer (PET).

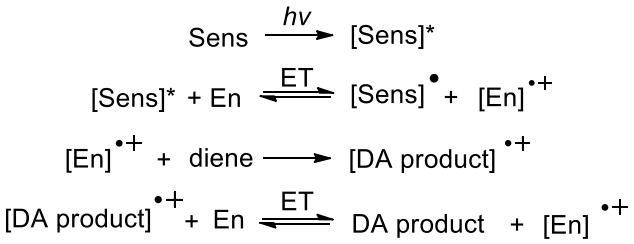

Scheme 1. Photosensitized radical cation Diels-Alder cycloaddition. Sens = sensitizer, EN = dienophile, ET = electron transfer.

Using this concept the Bauld group extended the scope of electron-rich alkenes as dienophiles to hydrocarbon dienes (1,3-pentadiene, 1,1'-dicyclopentenyl, 1-methoxy-1,3-cyclohexadiene, for examples) using 1,4-dicyanobenzene (DCB) as sensitizer as shown as example in Scheme 2.[2,3] However, for some hydrocarbon dienes (1-acetoxy-1,3-cyclohexadiene or 2,5-dimethyl-2,4-hexadiene) a fast back electron transfer made the overall photoinduced electron transfer unsuccessfully. The situation could be improved if 2,4,6-triphenylpyrylium tetrafluoroborate (TPP^+) is used (Scheme 3).[4] Recently, the Yoon group reported intramolecular[5] and intermolecular[6] versions of Diels-Alder reaction using visible light photoredox catalysis based on same radical cation concept. A variety of sterically bulky, aryl- and heteroatom-substituted,

cyclic dienes reacted successfully in intermolecular Diels-Alder cycloadditions when the electron transfer was initiated by a Ru(II) photocatalyst.[7] The Ru(II) photocatalyst was also effective in intramolecular radical cation Diels-Alder reactions with substrates bearing three-carbon tethers (as example on Scheme 4).[5]

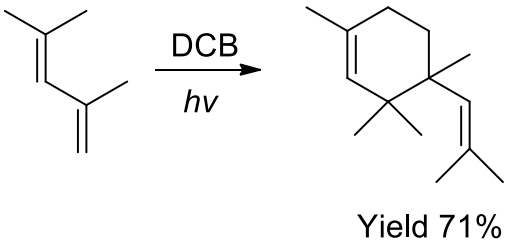

Scheme 2. Diels-Alder cycloaddition under PET conditions utilizing DCB as sensitizer.

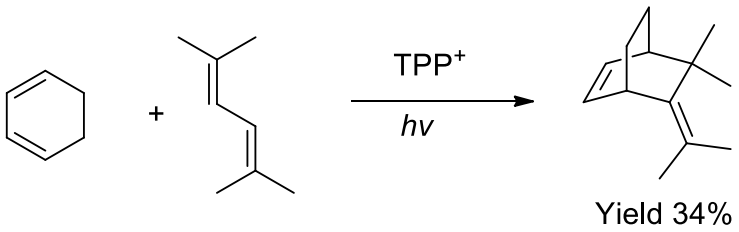

Scheme 3. Diels-Alder cycloaddition under PET utilizing TPP^+ as sensitizer.

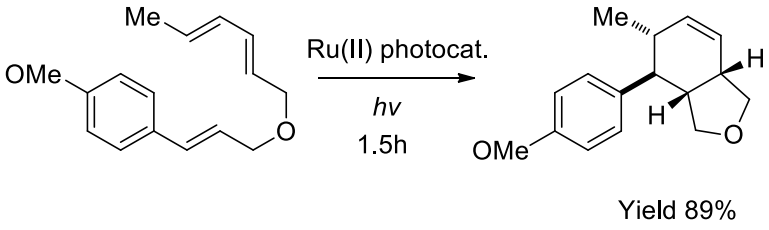

Scheme 4. Diels-Alder cycloaddition under PET utilizing Ru(II) as sensitizer.

3.2 RESULTS AND DISCUSSION

Following promising achievements of heterogeneous semiconductor photocatalysts in organic synthesis (see Chapter 2) we decided to extend their use further into cycloaddition reactions. The model process we selected is the radical cation intermolecular Diels-Alder reaction described earlier by the Yoon group (Scheme 5).[7] The [4+2] cycloaddition between an electron-rich dienophile and an electron-rich diene is unfavorable, and thermally this process cannot be realized due to the electronic mismatch, which was proven by the control experiment without the photocatalyst. The typical situation for this kind of reaction is when an electron-rich component (usually the diene) meets an electron-deficient component (usually the dienophile). Photocatalysis facilitates the process between two electron-rich components if one of them undergoes a single electron oxidation thus transforming the electron-rich reaction partner into an electron-deficient one. Moreover the electron-rich substrate is an easy precursor for the photocatalytic oxidation process. Essential for the investigated model process by the Yoon group was that the Ru(II) complex has a sufficiently high oxidation potential in the exited state to initiate the electron transfer. We substituted the photosensitizer by an inorganic semiconductor. Heterogeneous photocatalysts can be easily separated from the reactants and therefore recycled. In addition, the redox properties of semiconductors can be tuned as they are dependent on the reaction media. Generally, the redox potential shifts anodically when moving from an organic media to an aqueous solution. Examples of this phenomenon are known for TiO_2 and CdS photocatalysts. As illustrated in Figure 2 in Chapter 1 of this thesis the anodic shift in the oxidation potential of TiO_2 is with 1.25 V large increasing the oxidation potential to 2.25 V in aqueous media (pH = 7). The anodic shift for CdS is smaller with 0.4 V leading to an oxidation potential in water of 1.75 V (pH 7).[8] The designed $PbBiO_2Br$ semiconductor is a quite strong photocatalytic one-electron oxidant in water with a valence band at 1.67 V at pH 7.

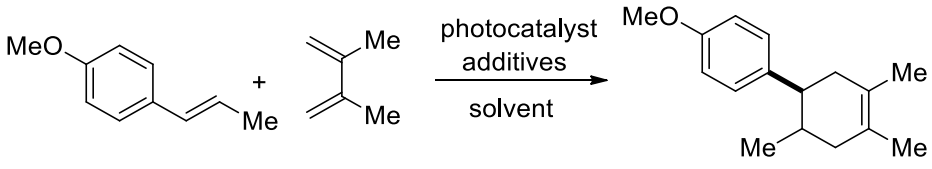

Scheme 5. Photocatalytic Diels-Alder cycloaddition.

The first step in the mechanism (Scheme 6) is a one electron oxidation of the dienophile anethole (**1**) with E_{ox} = 1.1 V, SCE, CH_3CN) that requires a quite strong oxidation power of the applied photocatalyst. This requirement for inorganic semiconductors could be achieved by using them in aqueous media. TiO_2 and $PbBiO_2Br$[9] (Figure 1, **6** and **7** respectively), which performed well in the α-alkylation of aldehydes where we utilized the reductive power of the excited state of the semiconductors,[10] should be suitable. They are recyclable and stable in the reaction media. For the [4+2] cycloaddition discussed here, the valence band potential of TiO_2 and $PbBiO_2Br$ should be sufficient for the oxidation of the precursor **1 (**Scheme 6) when water is used as the reaction medium. To provide a better solubility of the organic components that are not soluble in water we used mixtures of water and organic solvents (1/1).

The mechanism of the reaction starts with one electron oxidation of the substrate by the excited state photocatalyst to give the radical cation of **1** , which is further reacts with the electron rich olefin **2** to afford the [4+2] cycloaddition intermediate **3.** Finally, the intermediate **3** is reduced to **4** by taking up an electron from another molecule of anethole in a chain transfer mechanism.

Noteworthy when designing the conditions for the investigated Diels-Alder cycloaddition is the conduction band of the excited semiconductor that hosts the recombined electron. To facilitate a radical chain mechanism it was considered to add an electron scavenger that prevents back electron/hole recombination of the excited semiconductor and facilitates the electron withdrawing path from the oxidizable precursor to the valence band of the semiconductor.[11] Among known and often used electron scavengers are oxygen, methyl viologen (**5**) and sodium persulfate (Scheme 6).

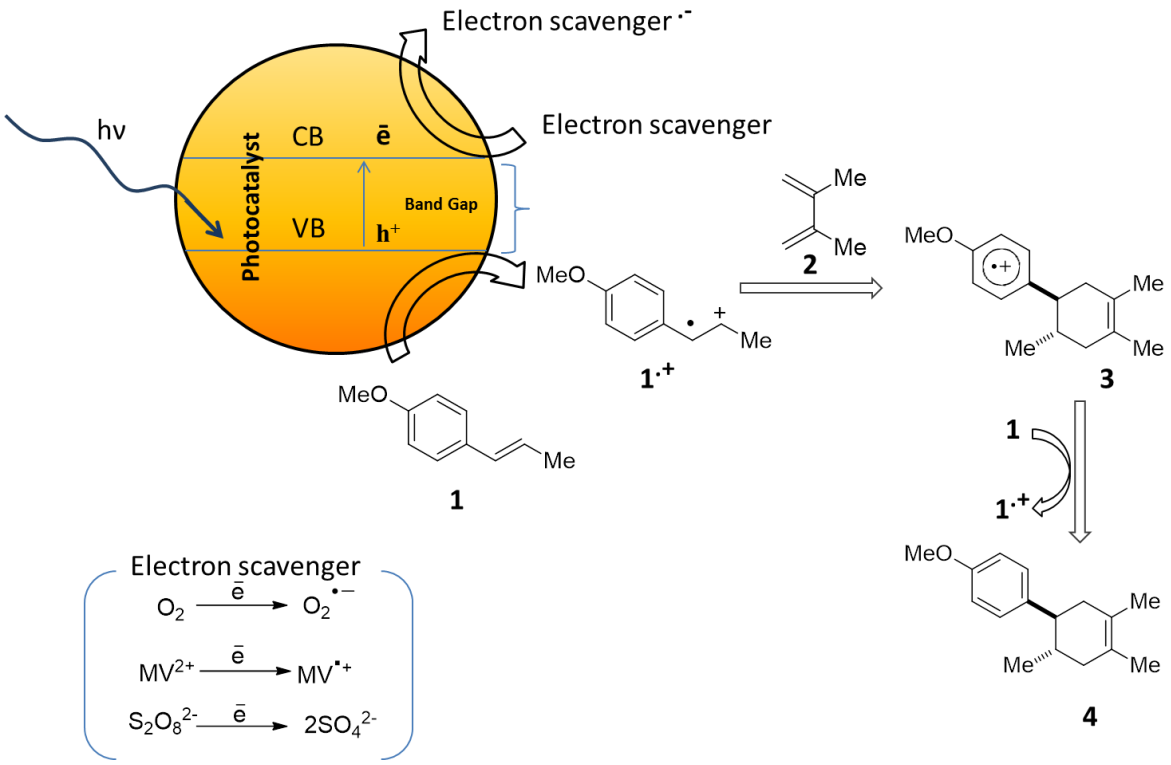

Scheme 6. Mechanism of the photocatalytic [4+2] cycloaddition driven with semiconductor photocatalyst.

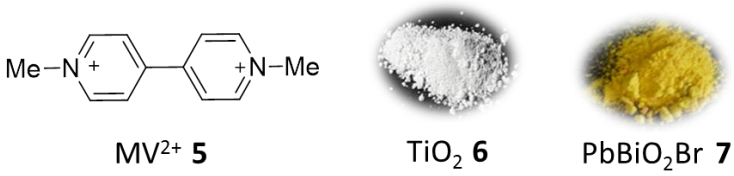

MV^{2+} **5** TiO_2 **6** $PbBiO_2Br$ **7**

Figure 1. Photocatalysts applied in [4+2] cycloddition and methyl viologen as electron scavenger (**5**).

When screening the conditions for the model process on Scheme 7 we started from TiO_2 as photocatalyst (Figure 1, **6**) in oxygen atmosphere which was irradiated with 455 nm LEDs in a 1/1 water mixtures with acetone, ethanol or acetonitrile for 48 hours (Table 1, entry 1). As known from previous experiments we expected the excitation of TiO_2 with such a long wavelength due to some defects in the band structure.[12] The exclusively forming product was p-anisaldehyde (p-methoxybenzladehyde) as a result of anethole oxidation with oxygen. This observation leads to the conclusion that the oxidation process with oxygen is much faster than the target photocycloaddition. Moreover, ethanol and acetone are found to be easily oxidized on the photoexcited semiconductor surface thus competing with the main oxidizing process of anethole.[11] When we changed the electron scavenger to methyl viologen or sodium persulfate

excluding the oxygen atmosphere and irradiated with the same wavelength (455 nm) for 48 hours to obtain the target product in traces with anisaldehyde as still the main reaction product in the water/acetonitrile mixtures (Table 1, entry 2). To increase the number of excitation events the TiO_2 irradiation wavelength was lowered to 400 nm in water/acetonitrile with methyl viologen or sodium persulfate as electron scavengers. However, this did not improve the yield of product **4**. The main side product in this case (Table 1, entry 3) was still p-anisaldehyde indicating that the competing addition reaction of the anethole radical cation with hydroxyl anions from water and further oxidation to the aldehyde is a faster process. The reaction is known from the photocatalytic oxidation of p-methoxybenzyl alcohol over TiO_2.[13,14]

More positive results were obtained when $PbBiO_2Br$ bulk (Figure 1, **7**) semiconductor was employed in the investigated Diels-Alder process (Table 1, entry 4). We applied light of 455 nm wavelength from LEDs as the semiconductor absorbs in the visible part of the spectrum due to its 2.5 eV band gap. The target product **4** was obtained in 50% yield when the H_2O/CH_3CN 1/1 mixture of the reaction components was irradiated for 48 hours in an oxygen-free atmosphere with the $PbBiO_2Br$ bulk semiconductor. The side product p-anisaldehyde was observed this time in trace amounts, but the long irradiation time caused also semiconductor degradation which irreversibly destroyed turning grey.

The control experiments with TiO_2 and $PbBiO_2Br$ semiconductors (Table 1, entries 5 and 6 respectively) in oxygen-free conditions with methyl viologen as electron scavenger and in pure acetonitrile media gave only starting material after 48 hours of irradiation. This observation proves that the aqueous media is essential for achieving the sufficient oxidation potential of the semiconductors.

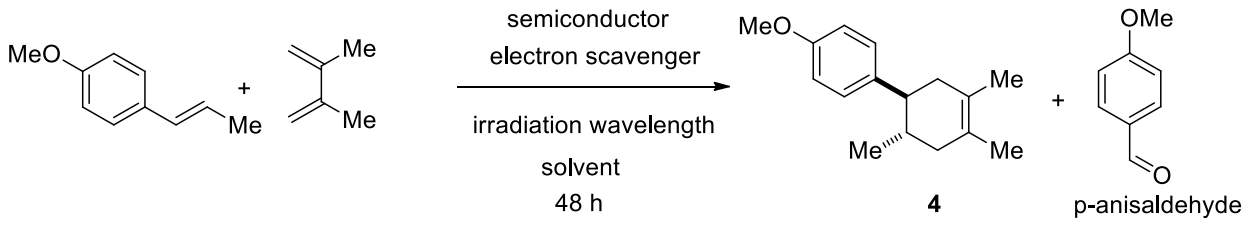

Scheme 7. Photocatalytic [4+2] cycloaddition of an electron-rich dienophile with an electron-rich diene.

Table 1. Screening of the reaction conditions for photocatalytic [4+2] cycloaddition with semiconductor photocatalysts.

Entry	**Semicon -ductor**	**Irradiation wavelength [nm]**	**Electron scavenger**	**Yield of4 [%]**	**Solvent**	**Note**
1	TiO_2	455	O_2	0	H_2O/CH_3CN (CH_3OH, $(CH_3)_2CO$) 1/1	Anis aldehyde as the only product
2	TiO_2	455	MV^{2+} or $Na_2S_2O_8$	traces	H_2O/CH_3CN 1/1	Anis aldehyde as the main product
3	TiO_2	400	MV^{2+} or $Na_2S_2O_8$	traces	H_2O/CH_3CN 1/1	Anis aldehyde as the main product
4	$PbBiO_2Br$	455	MV^{2+} or $Na_2S_2O_8$	50%	H_2O/CH_3CN 1/1	traces of anis aldehyde
5	TiO_2	400	MV^{2+}	0	CH_3CN	only starting anethole
6	$PbBiO_2Br$	455	MV^{2+}	0	CH_3CN	only starting anethole

3.3 CONCLUSION

The investigated heterogeneously photocatalyzed Diels-Alder cycloaddition requires long reaction times of 48 h of irradiation, while the homogeneous reaction is much faster. Benefits of the heterogeneous photocatalysts are their possible recyclability and their easy separation from the reactants. The competing fast anisaldehyde formation in the heterogeneously catalyzed process in aqueous solution gives only traces amounts of the target cycloaddition product in case of TiO_2. With $PbBiO_2Br$ as heterogeneous photocatalyst a maximal yield of 50% is obtained, but the photocatalyst degrades under the experimental conditions.

3.4 EXPERIMENTAL PART

3.4.1 GENERAL INFORMATION

All NMR spectra were recorded on a Bruker Avance 300 MHz spectrometer at 300 K. Chemical shifts are reported in δ [ppm] relative to an internal standard (solvent residual peak). Coupling constants are reported in Hertz [Hz]. Characterization of the signals: s = singulet, d = dublet, t = triplet, q = quartet, m = multiplet, bs = broad singulet, dd = dublet of dublet. Integration is directly proportional to the number of the protons. The used solvents are indicated for each spectrum.

Mass spectra were recorded using ESI ionistaion techniques.

All reagents were obtained from commercial suppliers and used without further purification unless otherwise specified. If necessary, solvents were dried accordingly to standard techniques.

Standard Schlenk techniques were applied to guarantee inert N_2 or Ar atmosphere if needed. Reaction monitoring via TLC was performed using silica gel coated aluminium plates (Merck $60F^{254}$ Silicagel, 0,2 mm). The visualization was done by UV light at 254 nm or 366 nm.

For preparative column chromatography Merck Geduran SI 60 (70- 230 grain diameter) and Macherey-Nagel 60M (0,04 - 0,063 mm, 230 - 400 grain diameter) silica gel was used.

High-power LED arrays CREE XP Serie 455 nm or 400 nm; max 700 mA; 1.12 W; max 3.9 V.

3.4.2 PHOTOCATALYTIC EXPERIMENTS

General procedure for [4+2] cycloaddition. In a 25ml Schlenk flask were placed *trans*-anethole (100 mg, 0.675 mmol, 1 eqv.), semiconductor (50 mg), freshly distilled 2,3-dimethylbutadiene (229 µL, 3 eqv.) and $Na_2S_2O_8$ (1g/100 mg *trans*-anethole) in 8 mL solvent. The reaction mixture was degassed with three freeze-pump-thaw cycles and charged with nitrogen. The reaction mixture was then irradiated for 48 hours with high-power LEDs of the respective wavelength. After irradiation of the reaction mixture it was filtered and the filter was washed with 3×5 mL ethyl acetate and the organic phase was washed with *sat.* NaCl solution. The aqueous layer was extracted with ethyl acetate (3×10 mL), the combined organic layers were evaporated and the crude cycloaddition product **4** purified on SiO_2 with PE/EtOAc 9/1, R_f=0.9.

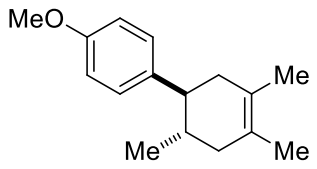

4

^{1}H NMR: (300 MHz, $CDCl_3$) δ 7.07 (d, J=8.6 Hz, 2H), 6.83 (d, J=8.6 Hz, 2H), 3.77 (s, 3H), 2.33 (m, 1H), 2.16 (m, 1H), 2.08 (m, 2H), 1.84 (m, 2H), 1.64 (s, 3H), 1.61 (s, 3H), 0.70 (d, J=6.1 Hz, 3H). HRMS (EI) calculated for $[C_{16}H_{22}O]^+$ requires *m/z* 230.16, found *m/z* 230.20.

3.5 REFERENCES

1. C. R. Jones, B. J. Allman, A. Mooring, B. Spahic. *J. Am. Chem. Soc.* **1983**, *105***,** 652

2. R. Pabon, D. Bellville, N. L. Bauld. *J. Am. Chem. Soc.* **1983***, 105,* 5158

3. N. L. Bauld. *Tetrahedron* **1989**, *45,* 5307

4. J. Mlcoch, E. Steckhan. *Angew. Chem. Int. Ed.* **1985**, *24,* 412

5. S. Lin, C. E. Padilla, M. A. Ischay, T.P. Yoon. *Tetrahedron Let.* **2012**, *53,* 3073

6. S. Lin, M. Ischay, C. Fry, T. P. Yoon. *J. Am. Chem. Soc.* **2011**, *133*, 19350

7. S. Lin, M. Ischay, C. Fry, T. P. Yoon. *J. Am. Chem. Soc.* **2011**, *133*, 19350

8. M. A. Fox. *Top. Curr. Chem.* **1987**, *142***,** 71

9.S. Füldner, P. Pohla, H. Bartling, S. Dankesreiter, R. Stadler, M. Gruber, A. Pfitzner, B. König. *Green Chem.* **2011**, *13***,** 640

10. M. Cherevatskaya, M. Neumann, S. Füldner, C. Harlander, S. Kümmel, S. Dankesreiter, A. Pfitzner, K. Zeitler, B. König. *Angew. Chem. Int. Ed.* **2012**, *51,* 4062

11. R. Solarska, I. Rutkowska, R. Morand, Augustynski, J. *Electrochimica Acta* 2006, **51,** 2230

12. M. Cherevatskaya, M. Neumann, S. Füldner, C. Harlander, S. Kümmel, S. Dankesreiter, A. Pfitzner, K. Zeitler, B. König. *Angew. Chem. Int. Ed.* **2012**, *51,* 4062

13. S. Yurdakal, V. Augugliaro, V. Loddo, G. Palmisano, L. Palmisano. *New Journal of Chemistry* **2012***, 36***,** 1762

14. G. Palmisano, S. Yurdakal, V. Augugliaro, V. Loddo, L. Palmisano. *Adv. Synth Catal* **2007**, *349,* 964

CHAPTER 4

4. Ir(III) COMPLEXES AS PHOTOCATALYSTS IN CATALYTIC DEHALOGENATION REACTIONS of BENZYL HALIDES §

§ Theoretical calculations of the Ir(DMA-py-^{t}Bu-Ph)$_3$ complex were done by Christian Ehrenreich (Merck KGaA Darmstadt). Excitited state lifetime and photoluminescence quantum yield for compound Ir(DMA-py-^{t}Bu-Ph)$_3$ was measured by Markus Leitl (group of Prof. Dr. Hartmut Yersin, University of Regensburg). Synthesis of the Ir(DMA-py-^{t}Bu-Ph)$_3$ complex as well as cyclic voltammetry, UV-Vis and fluorescence spectroscopy, Stern-Volmer quenching experiments were performed by Andreas Hohenleutner. Cyclic voltammetry data of the benzyl bromide derivatives and other reaction components except of Ir(III) complexes were obtained by Maria Cherevatskaya, photocatalytic experiments and results interpretation were performed by Maria Cherevatskaya.

4.1 INTRODUCTION

Although photocatalytic methods have been rapidly developed and widely applied to organic synthesis over the last decade the activation of inert, less reactive substrates and their use in photocatalytic synthesis remains a challenge. The photosensitizer or photocatalysts is of central importance to achieve photoinduced electron transfer from or to the substrate. The employed photosensitizers can be organic dyes,[1,2] organo-transition metal complexes[3,4,5,6] and even inorganic or organic semiconductors.[7] This chapter discusses an attempt to develop new transition metal complexes that may allow the visible light induced transformation of challenging substrates.

The Ir (III) complexes studied here are commercially available or were synthesized by Andreas Hohenleutner (University of Regensburg). Most of the Ir(III) complexes absorb visible light in the near UV region around 400 nm and readily donate or accept an electron in their excited states thus enabling the activation of a broad range of substrates for synthetic transformations. Upon absorption of light of the appropriate wavelength, the photocatalyst in its excited state can either accept an electron from another molecule (reductive quenching) to give the reduced form of the sensitizer or transfer an electron to another molecule (oxidative quenching) yielding the oxidized sensitizer (see Figure 1).

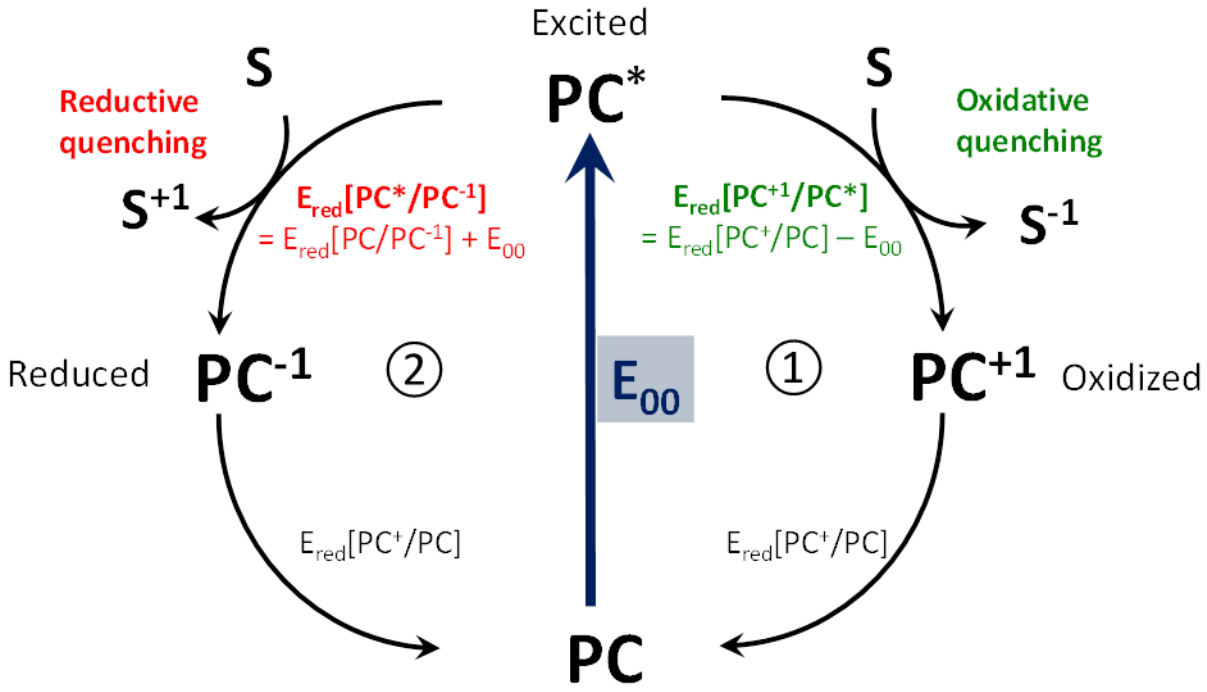

Figure 1. Schematic representation of oxidative and reductive quenching cycles of a photocatalyst. The arrow directions do not represent the direction of the corresponding potentials but rather the progression of the reaction.

The reductive and the oxidative power of Ir(III) complexes in their excited state is determined by the energy difference between the photocatalytically active excited state and the reduced/oxidized form of the sensitizer. The excited state reduction and oxidation potentials can thus be estimated using the oxidation or reduction potentials in the ground state and the $E_{0.0}$ energy according to:[8]

$$\mathbf{E_{red}[PC^*/PC^{-1}] = E_{red}[PC/PC^{-1}] + E_{0,0}\ (reductive\ quenching)}$$

$$\mathbf{E_{ox}[PC^{+1}/PC^*] = E_{ox}[PC^{+1}/PC] - E_{0,0}\ (oxidative\ quenching)}$$

$E_{0.0}$ is the zero-zero transition energy and can be estimated by using the maximum emission energy of the compound. It should be noted however, that the emission occurs from the singlet excited state while the electron transfer typically occurs via the triplet state, which can be significantly lower in energy.

Transition metal complexes as photoredox catalysts offer several advantages: first and foremost, the photophysical properties of these compounds have been extensively studied,[9,10,11] allowing for a better understanding of their behavior in photochemical transformations. Another desired property is their absorption at higher energies compared to the most commonly employed organic dyes. The reductive or oxidative power of the excited photocatalyst scales directly with the energy of the $E_{0,0}$ transition and the activation of challenging substrates is thus only possible with sufficiently high excitation energies. In addition, since electron transfer occurs from the triplet state, for a high performance photocatalyst a high triplet yield is imperative. Transition metal complexes exhibit a large spin orbit coupling leading to a very efficient inter system crossing, thus increasing the fraction of excitation events that lead to the formation of the desired triplet states.[10]

Iridium complexes in particular exhibit very high reductive power in their excited state. Furthermore by careful modification of the ligand structure, it is possible to tune the HOMO/LUMO and emission energies in this class of compounds. Figure 2 shows calculated HOMO and LUMO orbitals for $Ir(ppy)_3$, a OLED emitter that has recently also found applications as a highly reductive photocatalyst.[3,12] It is to the best of our knowledge the transition metal complex with the highest reductive power that has been applied as a sensitizer in photoredox catalysis to date.

Figure 2 shows that the HOMO is mainly located on the metal ion and the phenyl ring of the cyclometalating ligand, the LUMO is located on the ligand and particularly on the pyridine ring. Substitution of the phenyl part of the ligand, especially para to the Ir-C bond changes the electron donation to the metal via the metal-carbon bond. This affects mainly the metal centered HOMO of the complex. Alterations on the pyridine ring on the other hand have a stronger impact on the energy of the LUMO since the LUMO is ligand centered and mostly located on the pyridine. The orbital distribution illustrates the strong MLCT character with contributions from ligand centered (LC) transitions.

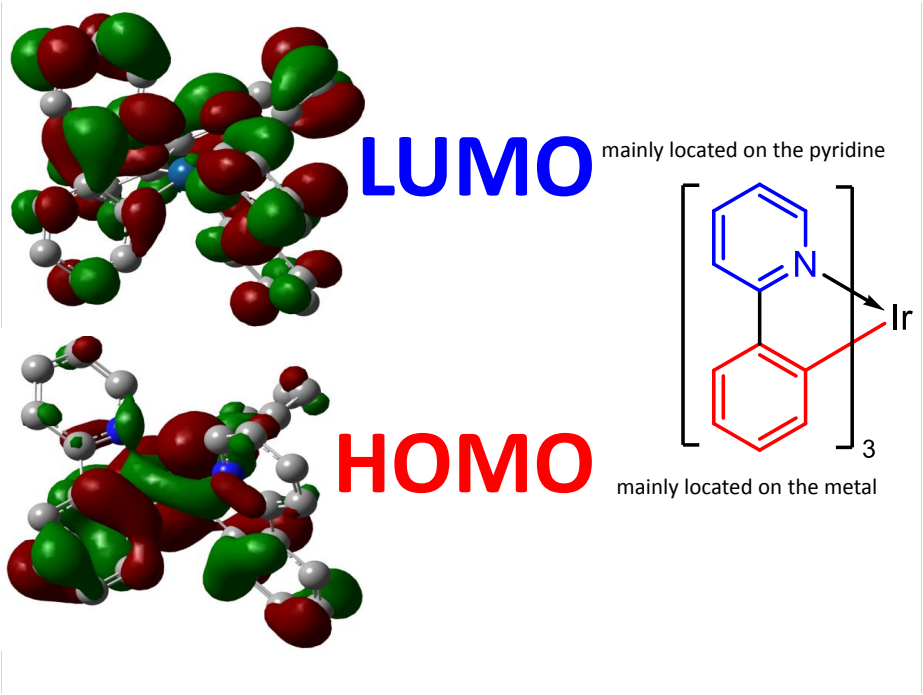

Figure 1: Calculated HOMO (top) and LUMO (bottom) orbitals of $Ir(ppy)_3$.

Non acceptor substituted benzyl bromides are difficult to reduce. The redox properties of the substrates are dependent on the substituents of the aromatic ring as well as on the halides. In the series benzyl chloride, benzyl bromide and benzyl iodide the redox potentials change from -2.21 V, -1.71 V to -1.4 V vs. SCE in DMF, respectively;[13,14] this tendency demonstrates the influence of the halide. Electron-withdrawing groups as substituents in the aromatic ring shift the reduction potential anodic, electron-donating groups shift the reduction potential cathodic and simultaneously destabilize a radical anion.

4.2 RESULTS AND DISCUSSIONS

The photocatalytic one electron reduction of benzyl bromide derivatives was already investigated by MacMillan et al. in the photocatalytic α-benzylation of aldehydes.[3] The one electron reduction step of benzyl halides can be described as:

$$PhCH_2Hal + e^- \longrightarrow PhCH_2^{\bullet} + Hal^-$$

According to the mechanistic scheme (Figure 1) an oxidative quenching of the photocatalyst by a direct one electron transfer from the excited photocatalyst to the radical precursor takes

place. The reduction potentials of the benzyl bromides are essential for this step and the values for the selected compounds are E_{red} = -1.07 V for p-nitrobenzyl bromide, -1.70 V for p-cyanobenzyl bromide and -2.05 V for the parent benzyl bromide, all vs. SCE in DMF.[5] Stronger electron withdrawing groups lead to an anodic shift of the reduction potential. Hence, p-nitrobenzyl bromide undergoes a one electron reduction easier than benzyl bromide. Moreover, the p-nitro substituent group stabilizes the resulting radical anion.

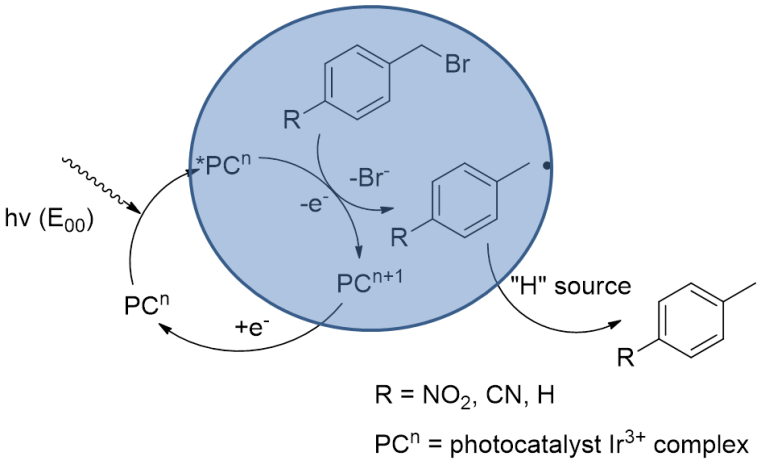

Scheme 1. Photocatalytic dehalogenation mechanism of benzyl bromide derivatives upon excitation of Ir^{3+} complexes.

Three selected Ir^{3+} complexes (Scheme 2) with different redox potentials were used in the photocatalytic dehalogenation process in order to correlate electronic properties of the photocatalysts (Table 1) with electronic properties of the benzyl halides (Scheme 1, highlighted part). For our investigations we used the commercially available $Ir(ppy)_3$ and $Ir(piq)_3$ complexes as well as the newly designed $Ir(DMA\text{-}py\text{-}^{t}Bu\text{-}Ph)_3$ complex. The latter complex has an improved reduction potential in the excited state, because of the introduction of an electron-donating dimethylamino group that enhances the reduction potential in the exited state by raising the HOMO and LUMO energy keeping the complex absorbing at 400 nm.

[5] See experimental part for details and plots of the voltammograms.

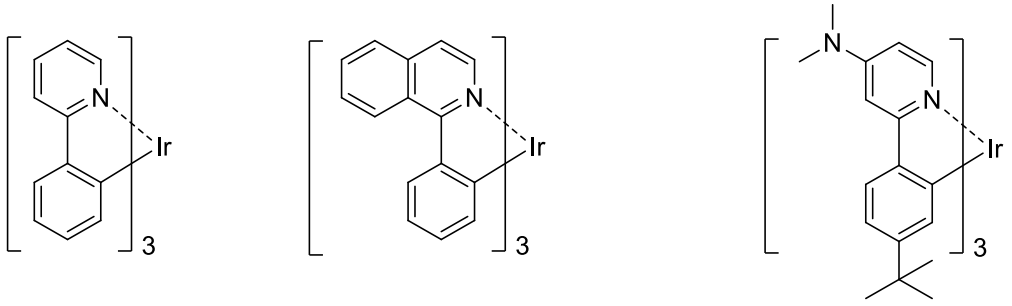

$Ir(ppy)_3$ $Ir(piq)_3$ $Ir(DMA\text{-}py\text{-}^{t}Bu\text{-}Ph)_3$

Scheme 2. Ir(III) complexes used as photocatalysts in the dehalogenation of benzyl bromide derivatives under irradiation.

Table 1: Comparison of the redox potentials, energy levels, estimated reductive power in the excited and ground states and decay times of $Ir(DMA\text{-}py\text{-}^{t}Bu\text{-}Ph)_3$ with $Ir(ppy)_3$ and $Ir(piq)_3$.

	$E_{1/2}$ (Ox) (vs SCE)[a]	*$E_{1/2}$ (Red) (vs SCE)*[a]	*E (HOMO)*[b]	*E (LUMO)*[b]	*Emission*	*$E_{1/2}(C^*/C^+)$ (vs SCE* [c]	*decay time*[d]
Ir(ppy)3	***0.77 V***	***-2.19 V***	***-5.17 eV***	***-2.21 eV***	***2.42 eV***	***-1.65 V***	***1.6 (1.4)[1]µs***
Ir(DMA-py-^{t}Bu-Ph)$_3$	***0.42 V***	***-2.56 V***	***-4.82 eV***	***-1.84 eV***	***2.43 eV***	***-2.01 V***	***0.76 (0.82)µs***
Ir(piq)3	***0.59 V***	***-1.5 V***	***-4.99 eV***	***-2.905 eV***	***2.00 eV***	***-1.41 V***	***1.3(1.25)[1]µs***

[a] determined by cyclic voltammetry. [b]calculated as: E(HOMO/LUMO) = -(4.4 + $E_{1/2\ ox/red}$). [c]calculated as $E_{1/2}(C^*/C^+) = E_{1/2\ ox} - \Delta E$ (Emission).[d] $Ir(DMA\text{-}py\text{-}^{t}Bu\text{-}Ph)_3$ and $Ir(ppy)_3$ were measured in 2-Me-THF, $Ir(piq)_3$ in CH_2Cl_2 – the values in brackets were measured in a spin coated PMMA polymer matrix thin film.

Stern-Volmer quenching studies can indicate if there is any electron transfer between the excited state of the photocatalyst and the electron acceptor. The quenching experiments were performed using p-NO_2-benzyl bromide, *p*-CN-benzyl bromide, benzyl bromide and the Ir(III) photocatalysts. This bimolecular electron transfer process deactivates the excited state and thus leads to a quenching of luminescence intensity, which is proportional to the concentration of the electron acceptor (quencher) present. This is described by the Stern-Volmer equation (Eq. 1) where **I** and $\mathbf{I_0}$ are the emission intensities before and after addition of the quencher, $\mathbf{k_q}$ is the quenching constant and **[Q]** the concentration of the quenching species. The quenching constant $\mathbf{k_Q}$ can be expressed as $\boldsymbol{\tau k_2}$ – the product of the mean lifetime of the photo-excited state (decay time) and the rate constant for the bimolecular quenching process (the rate constant of electron transfer from the catalyst to the substrate).

$$I_0/I = 1 + k_Q[Q] = 1 + \tau k_2[Q] \qquad \text{Equation 1}$$

The results depicted in Scheme 4.1 and 4.2 with benzyl bromide and p-CN-benzyl bromide as quenchers show that the rate constant for the bimolecular quenching process is significantly higher for Ir(DMA-py-^{t}Bu-Ph)$_3$ than for Ir(ppy)$_3$, whereas there is no quenching response for Ir(piq)3 with benzyl bromide and p-CN-benzyl bromide. p-NO_2-Benzyl bromide accepts an electron most easiest among the selected quenchers (Scheme 4.3) quenching the emission of all three Ir(III) complexes in a diffusion controlled manner. The quenching rate for Ir(ppy)$_3$ is comparable with the one observed with Ir(DMA-py-^{t}Bu-Ph)$_3$. A rational for this observation may be the somewhat shorter excited state lifetime of Ir(DMA-py-^{t}Bu-Ph)$_3$ of 0.76 µs compared to Ir(ppy)$_3$ 1.6 µs (Table 1), which leads to lower overall quenching rates.

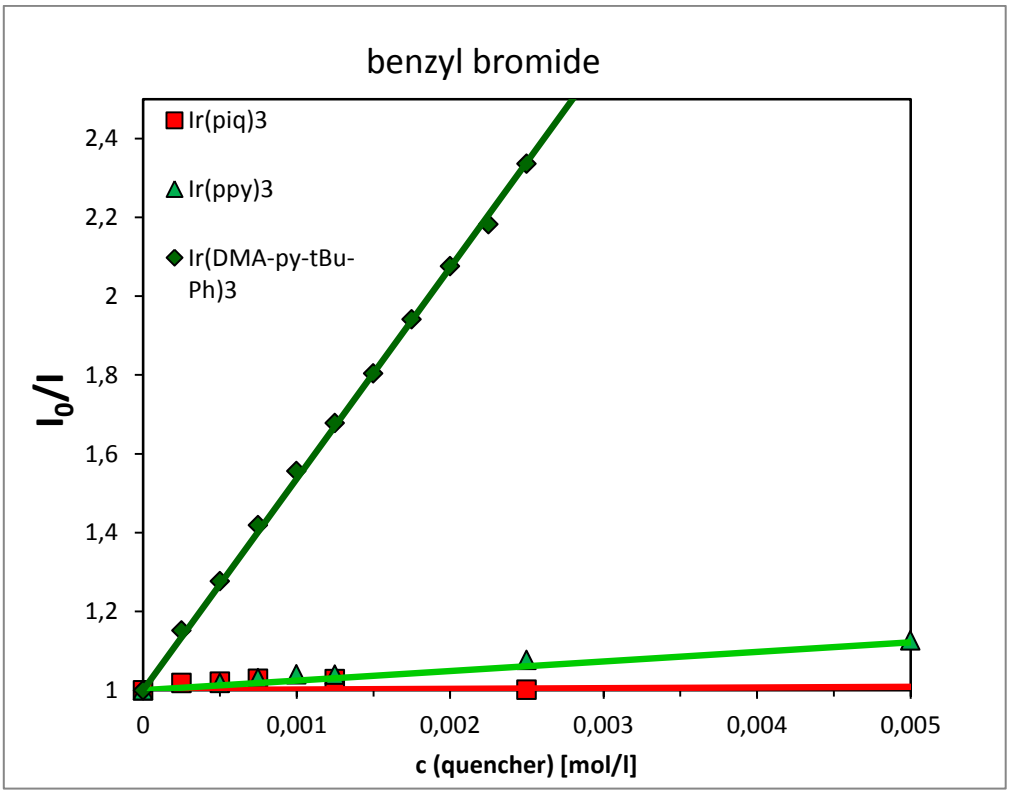

Scheme 4.1 Stern-Volmer quenching plot for the luminescence quenching of Ir(ppy)$_3$, Ir(piq)$_3$, and Ir(DMA-py-^{t}Bu-Ph)$_3$ with benzyl bromide.

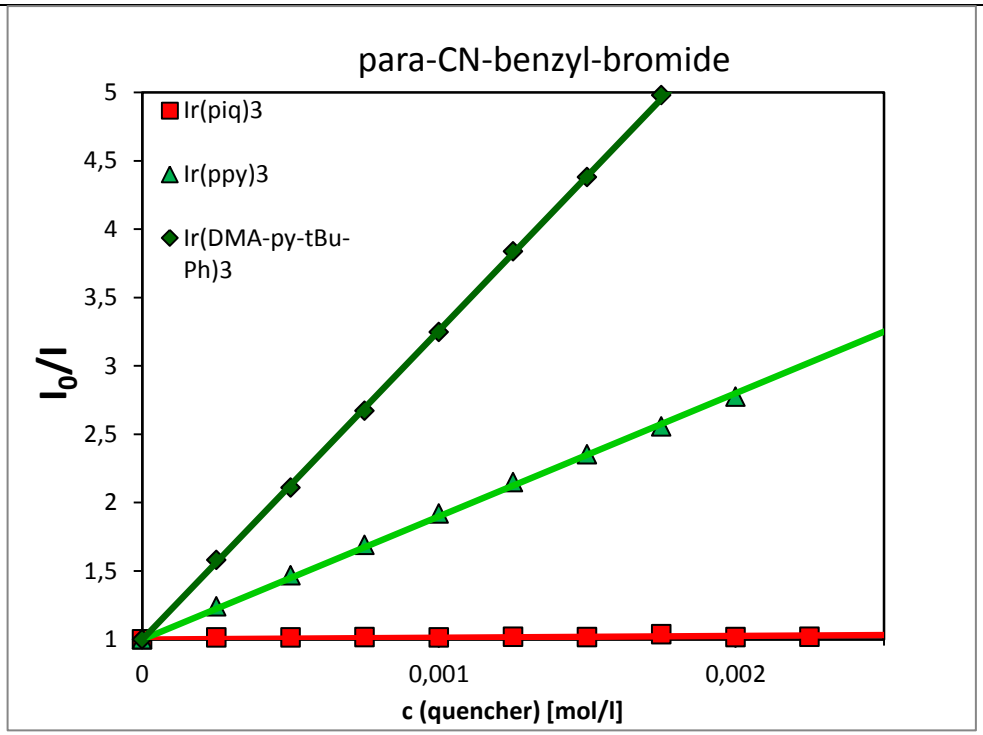

Scheme 4.2 Stern-Volmer quenching plot for the lumineswcence quenching of $Ir(ppy)_3$, $Ir(piq)_3$, and $Ir(DMA\text{-}py\text{-}^tBu\text{-}Ph)_3$ with p-CN-benzyl bromide.

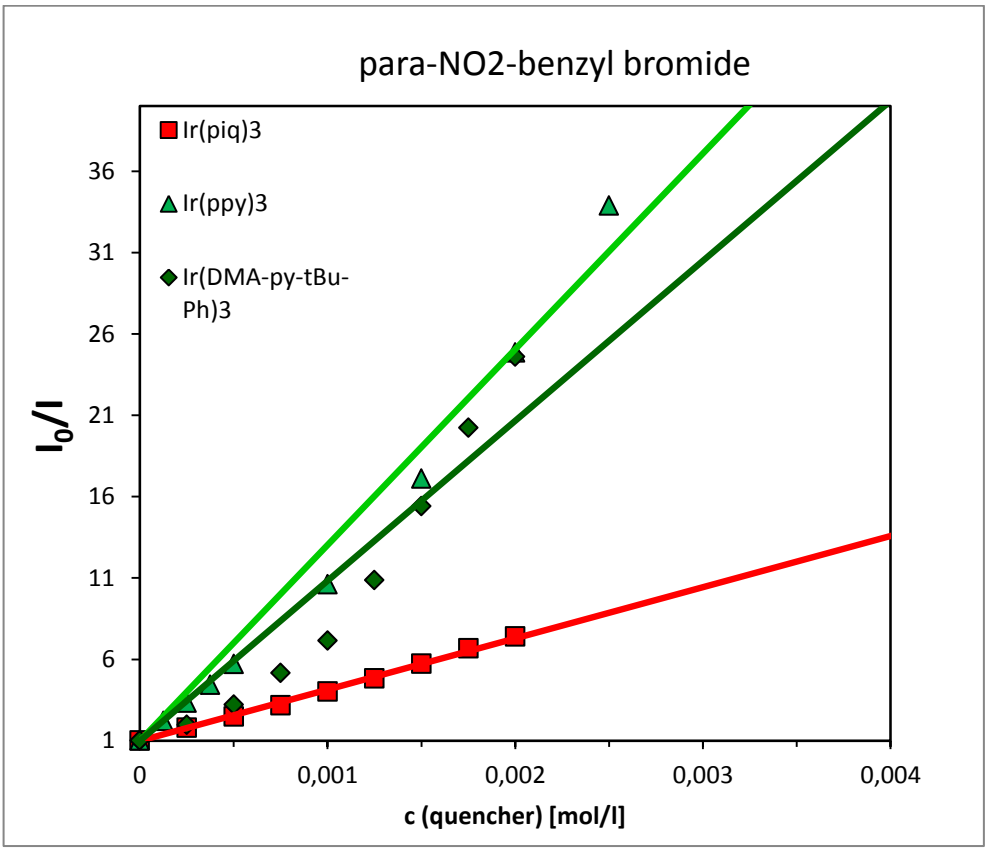

Scheme 4.3 Stern-Volmer quenching plot for the luminescence quenching of $Ir(ppy)_3$, $Ir(piq)_3$, and $Ir(DMA\text{-}py\text{-}^tBu\text{-}Ph)_3$ with p-NO_2-benzyl bromide.

From the Stern-Volmer quenching experiments we can conclude that only the excited state of Ir(DMA-py-^{t}Bu-Ph)$_3$ is quenched by unsubstituted benzyl bromide indicating suitable energy levels for an electron or energy transfer. The experiment shown in Scheme 5 was performed in order to determine if the emission quenching of Ir(DMA-py-^{t}Bu-Ph)$_3$ by benzyl bromide leads to photocatalytic conversion according to the mechanism of Scheme 1; the solvent DMF serves simultaneously as hydrogen donor. No consumption of the starting material benzyl bromide and consequently no product formation was observed in the experiment upon irradiation for 30 hours with a 400 nm LED. A rational for this observation may be a quick back electron transfer consuming the charge separated state before a subsequent reaction.

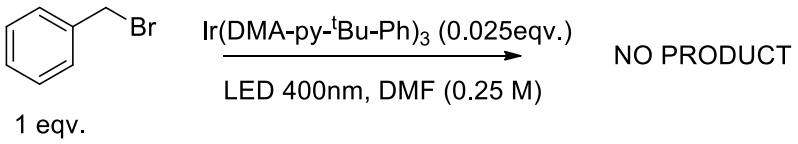

Scheme 5. Attempted photocatalytic dehalogenation of benzyl bromide using Ir(DMA-py-^{t}Bu-Ph)$_3$

However, the mechanism of the photocatalytic process depicted in Figure 1 suggests an alternative pathway in the presence of an electron donor yielding the photocatalyst in its reduced ground state. Upon reduction to formally Ir(II) the photocatalyst gains reductive power. This will be less compared to potentials in the excited state, but the infinite lifetime of the reduced complex facilitates the electron transfer process and allows even endothermic reactions.

To prove this mechanistic hypothesis the Ir(III) complexes and benzyl bromides were used in the conditions of dehalogenation reaction originally described by the Stephenson group on examples involving alkyl bromides and chlorides (Scheme 6).[15] The electron donor in this case is $^{i}Pr_2NEt$ (E_{ox} = 0.73 V *vs.* SCE in DMF[5]) and under this conditions the mechanism changes as shown in Scheme 7. The changed parts of the mechanism are highlighted.

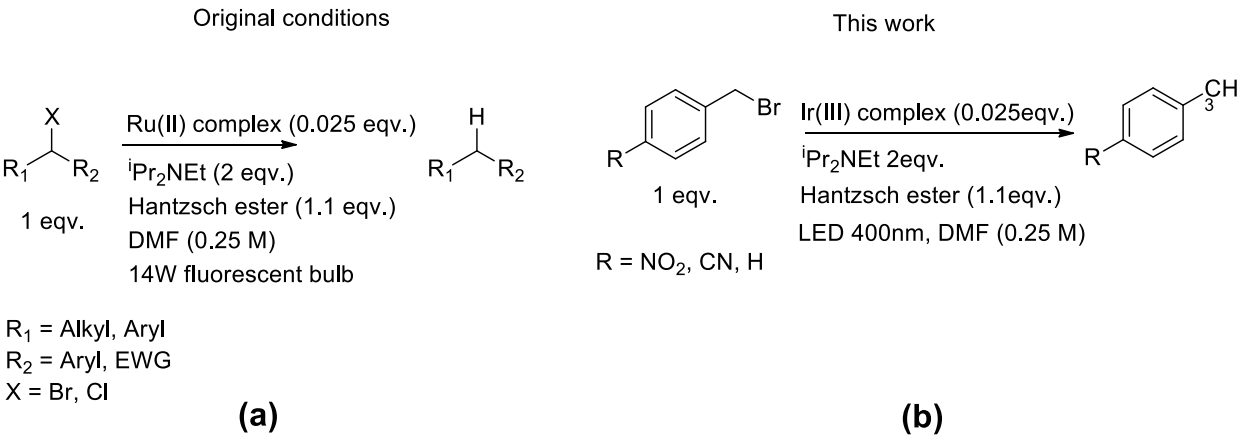

Scheme 6. (a) Photocatalytic dehalogenation described by the Stephenson group. (b) Photocatalytic dehalogenation of benzyl bromide derivatives with Ir(III) complexes as photocatalysts.

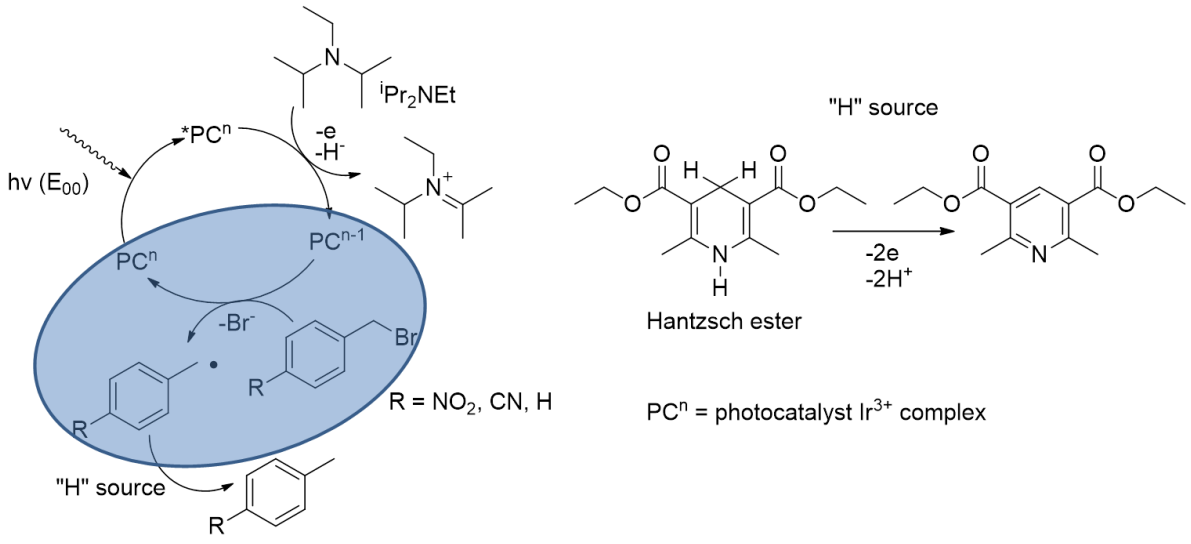

Scheme 7. Photocatalytic dehalogenation mechanism of benzyl bromide derivatives mediated by Ir^{3+} complexes.

The difference between $E_{1/2red}$ of the photocatalyst and E_{red} of the benzyl bromide precursor should facilitate one-electron reduction of the latter if its reduction potential in the reduced ground state is more anodic (Scheme 7, highlighted part). The Gibbs free energy for electron transfer from the reduced ground state photocatalyst to the benzyl halide can be estimated by the equation 2[16] (Table 2):

$$\Delta G_{ET}\ (eV) = E_{ox} - E_{red}, \qquad \text{Equation 2}$$

The value of the Gibbs free energy for electron transfer from $^{i}Pr_2NEt$ to the photocatalyst in the excited state (Scheme 7) can be estimated by the Rehm-Weller equation 3 (Table 2):

$$\Delta G\ (eV) = (E_{ox} - E_{red} - e_0^2/a\varepsilon - E_{00}), \qquad \text{Equation 3}$$

E_{ox} is the potential of the substrate that undergoes one electron oxidation and E_{red} is the potential of the substrate that undergoes one electron reduction. The Coulombic term $e_0^2/a\varepsilon$ is 0.06 kcal/mol (0.0026 eV).[17] The Coulumbic term represents the electrostatic energy gained when the two product ions are brought from "infinite separation" to the actual encounter distance in electron transfer and in our case the value is negligible.[18]

Table 2. Estimated Gibbs free energy (eV) between Ir(III) complexes and cooperating substrates.

	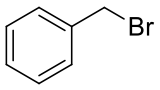	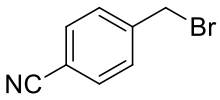	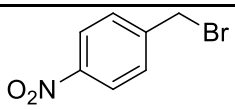	$^{i}Pr_2NEt$
Ir(ppy)$_3$	***-0.14 eV***	***-0.49 eV***	***-1.12 eV***	***-2.46 eV***
Ir(DMA-py-^{t}Bu-Ph)$_3$	***-0.51 eV***	***-0.86 eV***	***-1.49 eV***	***-2.12 eV***
Ir(piq)$_3$	***0.55 eV***	***0.20 eV***	***-0.43 eV***	***-1.86 eV***

Negative values of the estimated Gibbs free energy indicates that the process is thermodynamically allowed and we can expect a successful reaction. There are two positive values of the Gibbs free energy in Table 2 that point out the thermodynamically forbidden process. But as the positive values are rather small, a photocatalytic reaction may still proceed. The energetically uphill process can still occur if the difference between the reduction potentials of the substrate and the photocatalyst does not exceed 0.5 V and the subsequent step (protonation here) is rather fast shifting the process towards the product formation. We found support for this argument in earlier and current investigations of the Little group in electrochemical reactions where they showed that slightly endothermic reactions are still able to proceed.[19,20]

Photocatalytic experiments with p-NO_2-benzyl bromide, p-CN-benzyl bromide and benzyl bromide dehalogenation were successful using Ir(ppy)$_3$, Ir(DMA-py-^{t}Bu-Ph)$_3$ and Ir(piq)$_3$ as

photocatalysts with the same product distribution (Scheme 8). The reaction progress using Ir(DMA-py-^{t}Bu-Ph)$_3$ is similar in comparison to Ir(ppy)$_3$: p-NO$_2$-benzyl bromide and p-CN-benzyl bromide precursors were fully consumed after 3 hours of irradiation (Scheme 9). In the case of unsubstituted benzyl bromide there was a slow consumption of the starting material yielding the dimerization product dibenzyl and toluene in 12 hours using Ir(ppy)$_3$ and Ir(DMA-py-^{t}Bu-Ph)$_3$ as photocatalysts (Scheme 9). With Ir(piq)$_3$ as photocatalyst the full consumption of p-CN-benzyl bromide and benzyl bromide took 24 hours, and the reaction rate is therefore slower compared to Ir(ppy)$_3$ and Ir(DMA-py-^{t}Bu-Ph)$_3$. The weaker reductive power of the reduced photocatalyst may explain the different behavior.

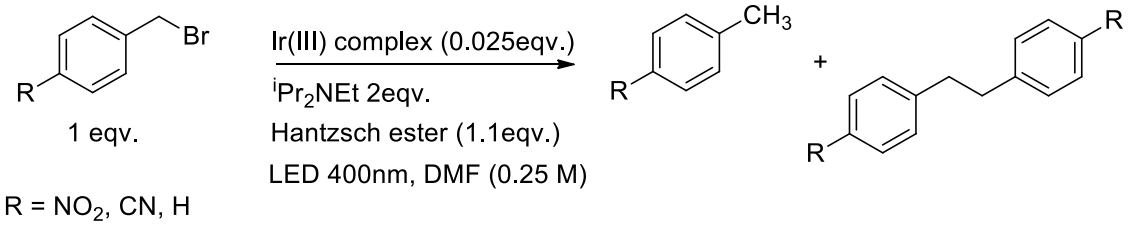

	Ir(DMA-py-^{t}Bu-Ph)$_3$	Ir(ppy)$_3$	Ir(piq)$_3$
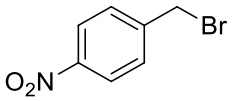	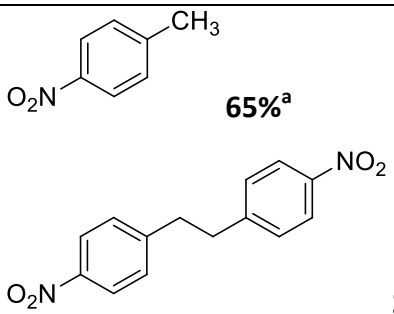 **65%**[a] **35%**[a]		The reaction was not performed.
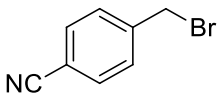	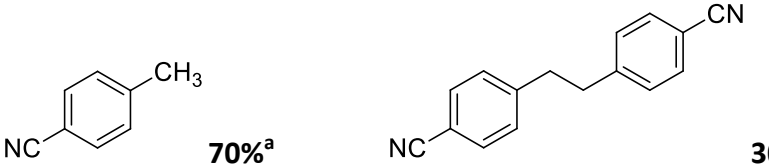 **70%**[a] **30%**[a]		
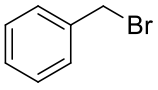	 **50%**[a] **50%**[a]		

Scheme 8. Photocatalytic dehalogenation of benzyl bromides. [a]The product yields are derived from gas chromatographic analyses of the reaction mixtures.

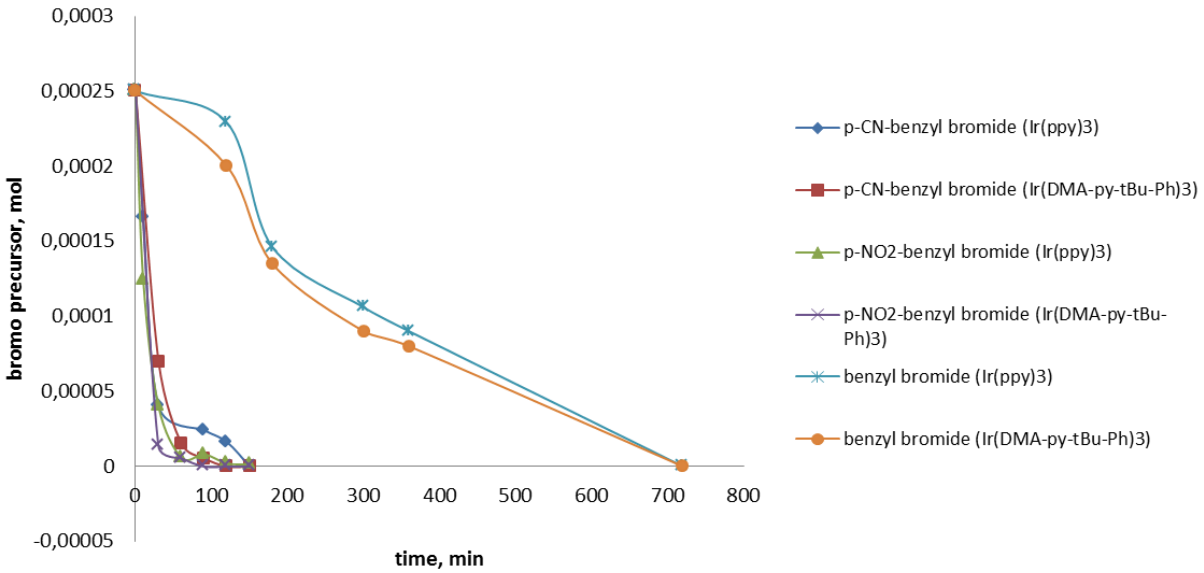

Scheme 9. Benzyl bromide consumption in photocatalytic reactions with $Ir(ppy)_3$ and $Ir(DMA\text{-}py\text{-}^tBu\text{-}Ph)_3$. The moles of the bromo precursors are calculated via calibrated GC data.

The photocatalytic experiment using $Ir(ppy)_3$ with benzyl bromide and Hantzsch ester (E_{ox} = 0.67 V *vs.* SCE in DMF[5]) as the only electron and hydrogen donor lead to full consumption of the latter in 10 hours of irradiation (Scheme 10) with the same set of products as given in Scheme 8.

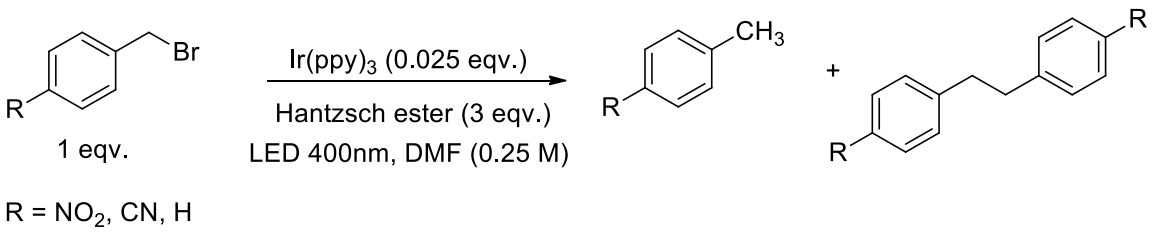

R = NO_2, CN, H

Scheme 10. . Photocatalytic dehalogenation of benzyl bromide derivatives with Ir(III) complexes as photocatalysts and products of the reaction.

4.3 CONCLUSIONS

In conclusion, we examined the photocatalytic behavior of three Ir^{3+} complexes on several benzyl bromide derivatives with different redox properties.

There are two ways the photocatalyst can reduce the benzyl bromides leading to the same products. Either the electron transfer occurs from the photocatalyst exited state to the benzyl bromide. For this process the free enthalphy must be negative or electroneutral. The experimental results indicate that beside the redox potential of the photocatalyst the excited state life time is of importance for their performance as photocatalyst, as the electron transfer occurs from the excited state.

The other pathway of photocatalytic dehalogenation is by the reduction of the excited photocatalyst by a sacrificial electron donor. The stable metal complex in its reduced form may act as reducing reagent. Both reaction pathways may be utilized in synthetic transformations.

4.4 EXPERIMENTAL PART

4.4.1 GENERAL INFORMATION

All reagents were obtained from commercial suppliers and used without further purification unless otherwise specified. If necessary, solvents were dried accordingly to standard techniques. Standard crimp-cap vials were applied to guarantee inert N_2 or Ar atmosphere in photocatalytic reactions. All photocatalytic reaction vials were irradiated in a custom made irradiation unit (SIM GmbH, picture see supporting information). It consists of an aluminum printed circuit board with 30 400 nm LEDs, connected to a cooling unit, that ensures a constant temperature of 20 °C of the board during the irradiation. Each of the sample vials is centered over one LED (d = 1 cm).

4.4.2 GC MEASUREMENTS

GC spectra were measured carried out at the GC 6890 Series Agilent equipped with a J+W Scientific – DB-5MS (30 m x 0.25 µm) capillary column (T(i) = 250 °C, T(d) = 300 °C (FID)) using split injection (40:1 split). Data acquisition and evaluation was done by using the software Agilent ChemStation Rev.A.06.03.(509). The GC oven temperature program adjustment was as follows: The initial temperature was 40 °C, which was kept for 3 min, and then increased constantly at a rate of 15 °C/min for 16 min and the final temperature of 280 °C was kept for 5 min.

4.4.3 QUENCHING EXPERIMENTS

A solution of the respective sensitizer in 1 mL of DMSO in a quartz cuvette equipped with a silicone/PTFE septum was thoroughly degassed via rigorous bubbling with argon for 10 min. After measuring the phosphorescence intensity (integration of the emission peak) of the sample, a 0.25 M solution of the respective quencher in DMSO was added stepwise via a Hamilton syringe (typically in 1 µL amounts) the relative high concentration and low addition volumes were to make sure that dilution effects could be ignored. After each addition, the cuvette was shaken for a few seconds to ensure proper mixing and the phosphorescence intensity determined again. The values for k_q were obtained as the slope of a linear regression fit for I_0/I as a function of the quenchers concentration with a fixed intercept of 1.

4.4.4 CYCLIC VOLTAMMETRY EXPERIMENTS

Measurements were carried out with a glassy carbon working electrode, a platinum counter electrode and a silver or platinum wire pseudo reference electrode. All compounds were measured in DMF with tetrabutyl ammonium tetrafluoroborate as the supporting electrolyte and the solvent was degassed by vigorous argon bubbling prior to the measurements. All experiments were performed under argon atmosphere. Ferrocene was used as an internal reference for determining the reduction and oxidation potentials ($E_{1/2}(Fc/Fc^+)$ = 0.72 V in DMF).

4.4.5 PHOTOCATALYTIC EXPERIMENTS

The bromo-precursor (0.25 mmol, 1 eqv.), DIPEA (0.5 mmol, 2 eqv.) in 1 ml DMF (0.25 M) were added to mixture of solids Hantzsch ester (0.275 mmol, 1.1 eqv.) with Ir^{3+} complex (0.00625 mmol, 0.025 eqv) in a crimp-cap vial that was degassed immediately with 3 freeze-pump thaw cycles and backfilled with nitrogen afterwards. The reaction mixture was irradiated with a 400 nm LED for a definite time. The reaction completion was determined by GC analysis. The peaks that were not assigned by pure reference compounds in GC were determined by GC-MS.

For GC analysis, 5 μL of the reaction mixture were taken out directly by a Hamilton syringe and mixed with 5 μL of a standard (chlorobenzene). 1 μL of this solution was injected in the GC.

4.5 SUPPORTING INFORMATION

4.5.1 CYCLYC VOLTAMMETRY SPECTRA

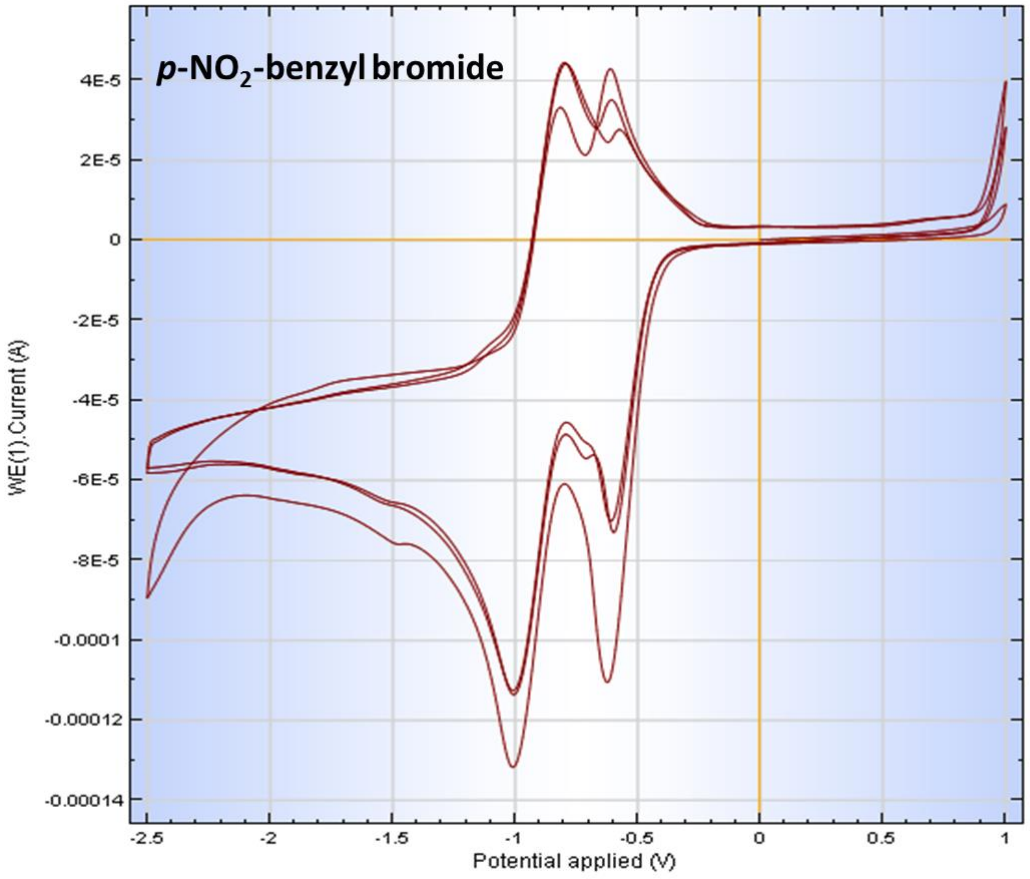

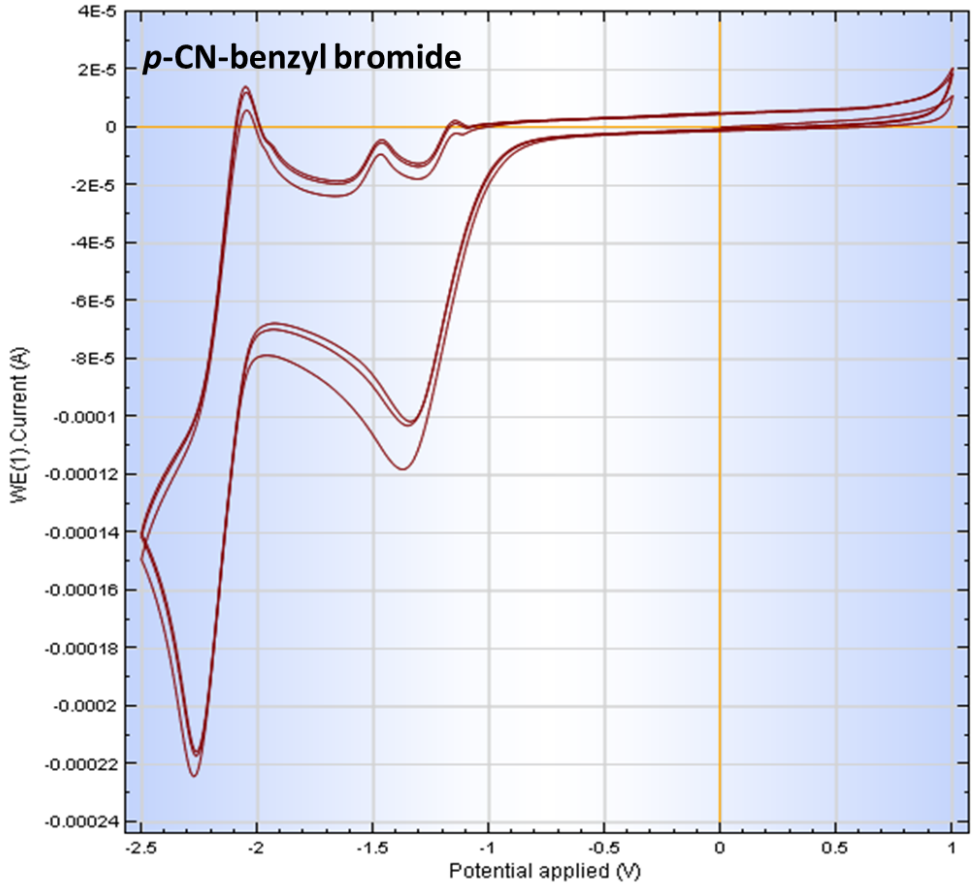
p-CN-benzyl bromide
WE(1).Current (A)
4E-5
2E-5
0
-2E-5
-4E-5
-6E-5
-8E-5
-0.0001
-0.00012
-0.00014
-0.00016
-0.00018
-0.0002
-0.00022
-0.00024
-2.5
-2
-1.5
-1
-0.5
0
0.5
1
Potential applied (V)

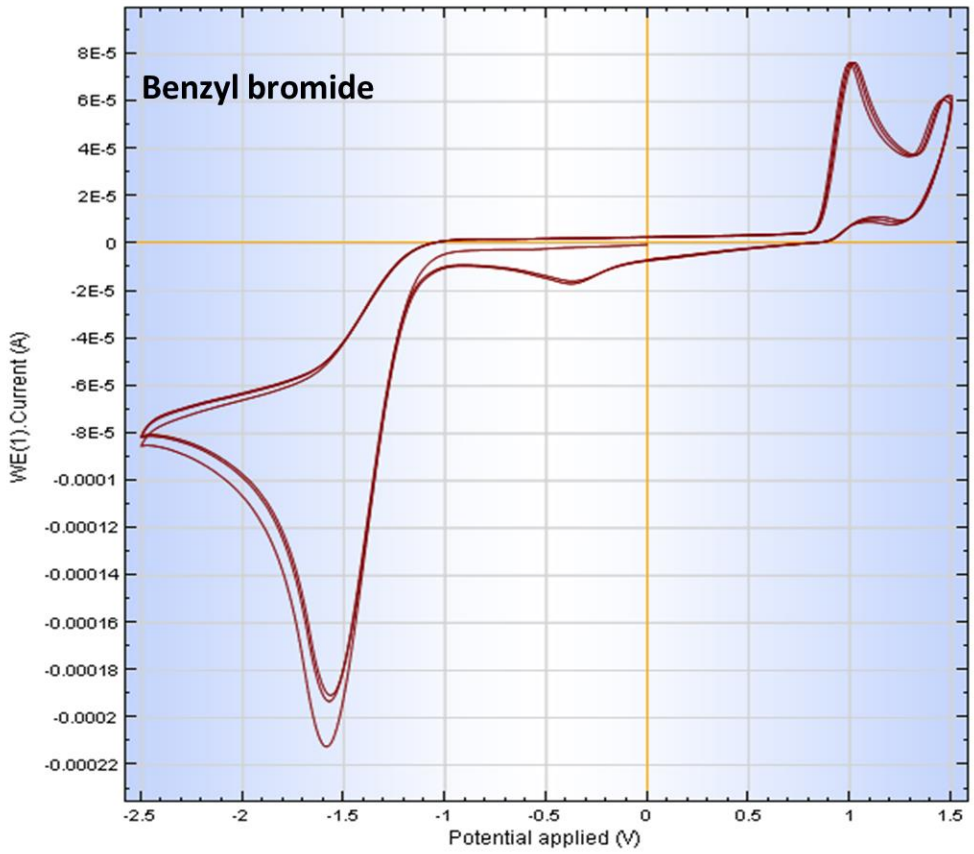
Benzyl bromide
WE(1).Current (A)
8E-5
6E-5
4E-5
2E-5
0
-2E-5
-4E-5
-6E-5
-8E-5
-0.0001
-0.00012
-0.00014
-0.00016
-0.00018
-0.0002
-0.00022
-2.5
-2
-1.5
-1
-0.5
0
0.5
1
1.5
Potential applied (V)

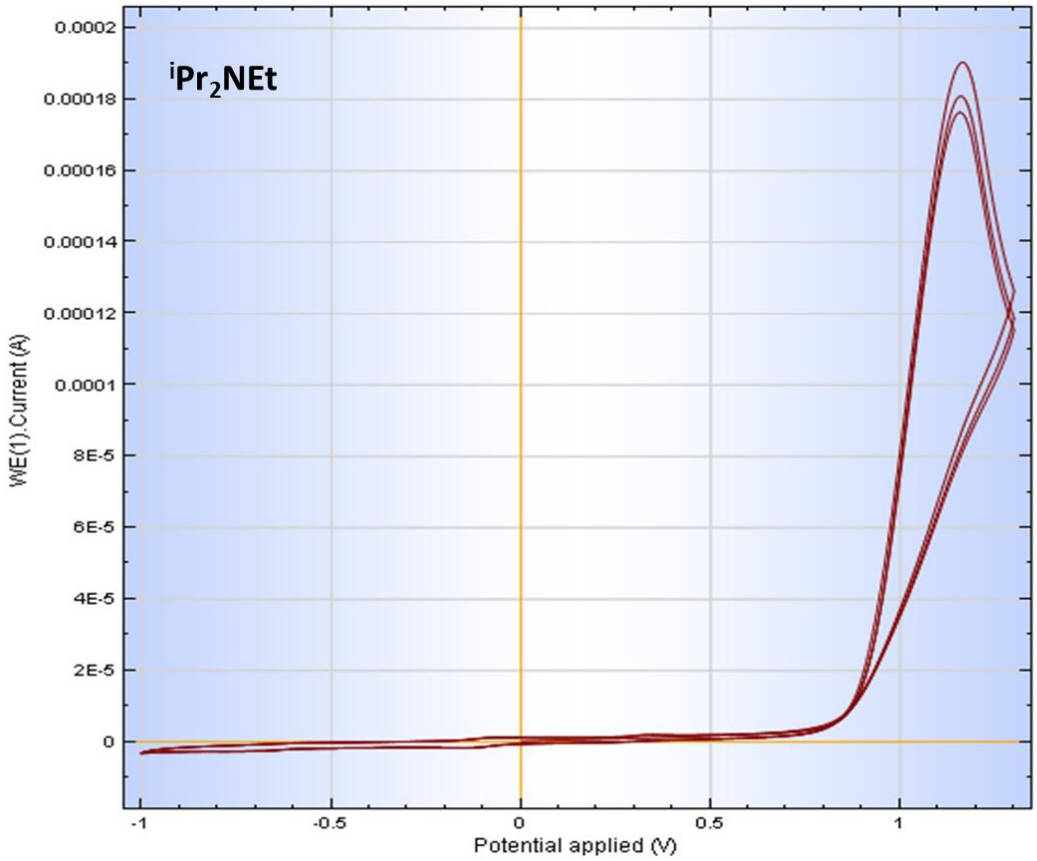
$^{i}Pr_2NEt$
WE(1).Current (A)
0.0002
0.00018
0.00016
0.00014
0.00012
0.0001
8E-5
6E-5
4E-5
2E-5
0
-1
-0.5
0
0.5
1
Potential applied (V)

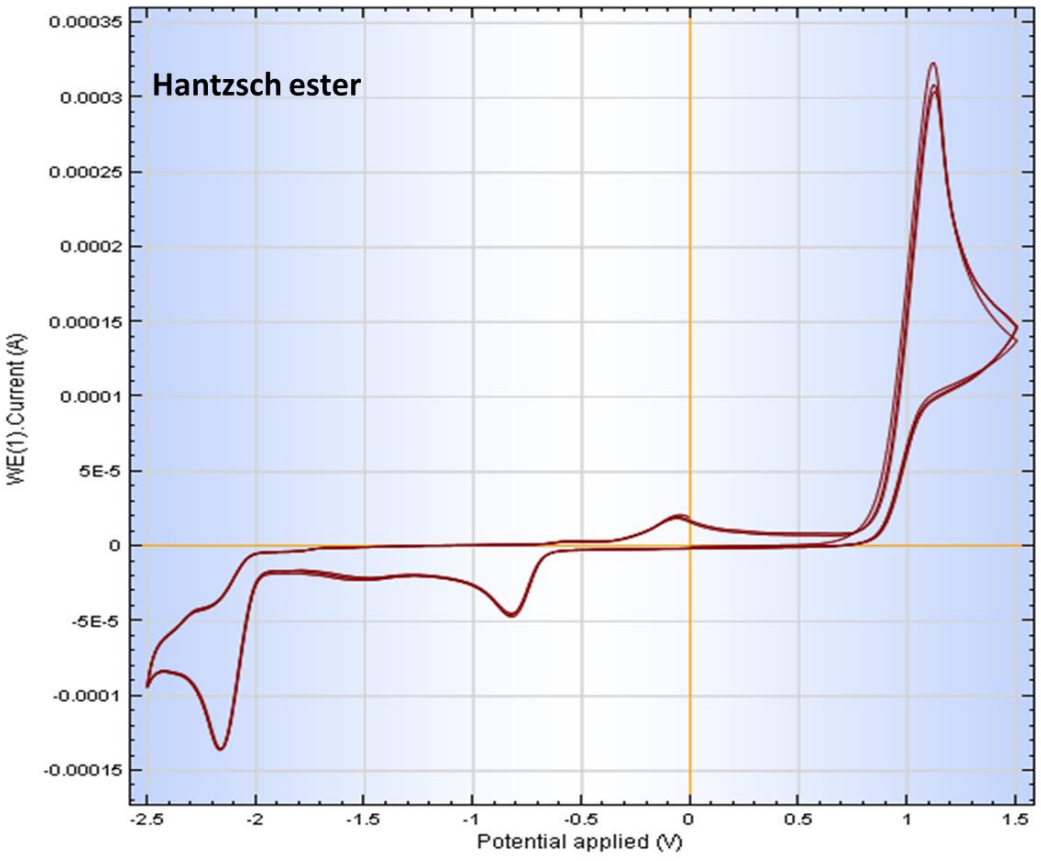
Hantzsch ester
WE(1).Current (A)
0.00035
0.0003
0.00025
0.0002
0.00015
0.0001
5E-5
0
-5E-5
-0.0001
-0.00015
-2.5
-2
-1.5
-1
-0.5
0
0.5
1
1.5
Potential applied (V)

4.6 REFERENCES

1. M Neumann, S Füldner, B König, K Zeitler. *Angew. Chem. Int. Ed.* **2011,** *50***,** 951

2. D P Hari, B König. *Org. Let.* **2011**, *13***,** 3852

3. H Shih, M N Vander Wal, R L Grange, D W MacMillan. *J. Am. Chem. Soc.* **2010**, *132***,** 13600

4. D A Nicewicz, D W C MacMillan. *Science* **2008**, *322***,** 77

5. Z Lu, T P Yoon. *Angew. Chem. Int. Ed.* **2012**, *51,* 10329

6. A E Hurtley, M A Cismesia, M. A. Ischay, T P Yoon. *Tetrahedron* **2011**, *67,* 4442

7. M Cherevatskaya, S Füldner, C Harlander, M Neumann, S Kümmel, S Dankesreiter, A Pfitzner, K Zeitler, B König. *Angew. Chem. Int. Ed.* **2012**, *51***,** 4062

8. G Grampp. *Berichte der Bunsengesellschaft für physikalische Chemie* **1994**, *98*, 1349.

9. T Hofbeck, H Yersin. *Inorg. Chem. (Washington, DC, U. S.)* **2010**, *49*, 9290

10. H Yersin, A F Rausch, R Czerwieniec, T Hofbeck, T Fischer. *Coord. Chem. Rev.* **2011**, *255*, 2622

11. E Baranoff, J Yum, M Graetzel, M K Nazeeruddin. *J. Organomet. Chem.* **2009**, *694*, 2661

12. J D Nguyen, E M D'Amato, J M R Narayanam, C R J Stephenson. *Nature Chem.* **2012**, *4*, 854

13. D A Koch, B Henne, C Bartak . *J. Electrochem. Soc.* **1987,** *134,* 3062

14. C Andrieux, A Gorande, J-M Saveant. *J. Am. Chem. Soc.* **1992,** *114,* 6892

15. J Narayanam, J Tucker, C R J Stephenson. *J. Am. Chem. Soc.* **2009**, *131*, 8756

16. G Grampp. *Berichte der Bunsengesellschaft für physikalische Chemie* **1994**, *98*, 1349.

17. A Schaap, S Siddiqui, G Prasad, E Palomino, L Lopez. *J. Photochem.* **1984**, *25*, 167

18. S Paul. *Chemistry and Light*. (The Royal Society of Chemistry, 1994), page 98.

19. Y S Park, R D Little. *J. Org. Chem.* **2008**, *73*, 6807

20. N Zhang, C Zeng, C M Lam, R K Gbur, R. D Little. *J. Org. Chem.* **2013**, 78, 2104

5. SUMMARY

Chapter 1 provides an overview on the organic synthesis mediated by heterogeneous photocatalysts reviewing recent advances and discussing the underlying photocatalytic mechanisms. Heterogeneous photocatalysis is applicable for a wide range of organic transformations from oxidations and reductions to carbon-heteroatom and carbon-carbon bond forming reactions including enantioselective examples. The wide variety of accessible heterogeneous semiconductor photocatalysts with different redox potentials, photostability, availability and recyclability makes them suitable for synthetic applications. The available data of valence band and conduction band energies in different solvents are still limited, as well as the understanding of the detailed photocatalytic mechanisms. It is expected that with continuing progress in these different aspects of heterogeneous photoredox catalysis more applications for organic synthesiswill be develop.

Chapters 2 and 3 describe examples of applications of heterogeneous photocatalysis in organic synthesis. Chapter 2 reports the stereoselective bond formation combining heterogeneous photocatalysis and organocatalysis in α-alkylation of aldehydes and Aza-Henry reactions. Heterogeneous photocatalysis could definitely serve as an alternative to the previously reported homogeneous reactions using transition metal complexes or organic dyes giving the comparable yields and stereoselectivity. The conduction band energies of excited TiO_2 and $PbBiO_2Br$ semiconductors are essential and sufficient for α-alkylation of aldehydes whereas excited CdS provides the required valence band energy for the Aza-Henry reaction.

Chapter 3 discusses photocatalytic [4+2] cycloaddition reactions utilizing TiO_2 and $PbBiO_2Br$ semiconductors as heterogeneous photocatalysts. The readily availability of the photocatalysts and their possible recyclability and easy separation from reactants are advantageous. However, the reaction requires long reaction times in aqueous media and the formation of anisaldehyde as a by-product limits the yield of the target cycloaddition product to 50%.

5. SUMMARY

Chapter 4 reports the dehalogenation of benzyl bromides under photocatalytic conditions. There are two possible mechanistic pathways of the photocatalytic reaction utilizing an Ir(III) complex as a photocatalyst leading to the same products: Either the photoinduced electron transfer to the bezyl bromide occurs directly from the excited state of the iridium complex or the photoreduced complex in its ground state acts as the reducing reagent. The short lifetime of the complex excited state disfavors the electron transfer from the excited state, although sufficient redox potential difference. Our investigations have shown that the excited state redox potential of iridium complexes can be engineered by suitable ligand design, but their difficult to predict lifetime is of equal importance for the use as photocatalyst.

6. ZUSAMMENFASSUNG

Das erste Kapitel bietet einen Überblick über die Verwendung heterogener Photokatalyse in der organischen Synthese, dabei wird insbesondere auf die neuesten Entwicklungen sowie die zugrundeliegenden Mechanismen eingegangen. Heterogene Photokatalyse findet Anwendung in einer Vielzahl organischer Reaktionen, die Bandbreite reicht dabei von Oxidationen und Reduktionen über Kohlenstoff-Heteroatom-Bindungsknüpfungen bis hin zu Kohlenstoff-Kohlenstoff-Bindungsknüpfungen wobei sogar enantioselektive Beispiele bekannt sind. Die vielseitigen Eigenschaften wie unterschiedliche Redoxpotentiale, Photostabilitäten, Verfügbarkeit und die Möglichkeit das Material zu recyclen, machen heterogene Halbleitermaterialen interessant für die Verwendung als Photokatalysatoren. Allerdings ist das Wissen über Valenz- und Leitungsbandenergien in verschiedenen Lösungmitteln und das genaue Verständnis der zugrundeliegenden photokatalytischen Mechanismen noch begrenzt. Es ist jedoch anzunehmen, dass mit fortschreitendem Erkenntnisstand auf diesen Gebieten die heterogene Katalyse zunehmende Anwendung in der organischen Photosynthese finden wird.

Die Kapitel 2 und 3 befassen sich dann mit konkreten Anwendungen heterogener Photokatalyse in der organischen Synthese. Kapitel 2 beschreibt die Kombination von Organokatalyse und Photokatalyse zur α-Alkylierung von Aldehyden sowie für die Aza-Henry-Reaktion. Heterogene Photokatalyse kann durchaus als Alternative zu den bereits beschriebenen homogenen Photokatalysen unter Verwendung von Übergangsmetallkomplexen oder organische Farbstoffen dienen, da sie vergleichbare Ausbeuten und Stereoselektivitäten liefert. Die Energien des Leitungsbandes von TiO_2 und $PbBiO_2Br$ sind ausreichend und entscheidend für die α-Alkylierung von Aldehyden, wohingegen CdS im angeregten Zustand die benötigte Valenzbandenergie für Aza-Henry-Reaktionen aufweist.

Das Kapitel 3 beschreibt TiO_2 und $PbBiO_2Br$ katalysierte [4+2] Zykloadditionen. Von Vorteil in diesen Reaktionen ist die leichte Verfügbarkeit sowie Rückgewinnung durch Abtrennen von den Reagenzien der heterogenen Halbleiterkatalysatoren. Es werden jedoch lange Reaktionszeiten benötigt, zudem limitiert die als Nebenreaktion auftretende Bildung von Anisaldehyd die Ausbeute der Photoreaktion auf 50%.

6. ZUSAMMENFASSUNG

Kapitel 4 diskutiert die photokatalytische Dehalogenierung von Benzylbromiden. Für den Mechanismus der durch einen Ir(II)- Komplex katalysierten Photoreaktion gint es zwei mögliche Wege, die jeweils zum selben Produkt führen: Zum einen kann der photoinduzierte Elektronentransfer auf das Benzylbromid direkt aus dem angeregten Zustand des Iridiumkomplexes stattfinden, zum anderen kann der vorher photochemisch reduzierte Komplex im Grundzustand als Elektronendonor fungieren. Der direkte Elektronentransfer aus dem angeregten Zustand wird durch dessen kurze Lebensdauer unwahrscheinlicher, obwohl er eine ausreichende Reduktionskraft besitzen würde. Unsere Untersuchungen konnten zeigen, dass das Reduktionspotential des angeregten Zustandes von Iridiumkomplexen durch Ligandendesign gezielt gesteuert werden kann, allerdings ist für die Photokatalyse auch die nur schwer vorhersagbare Lebensdauer des angeregten Zustandes von entscheidender Bedeutung.

7. APPENDIX

7.1 ABBREVIATIONS

°C	Degree Celsius
µL	Micro liter
^{13}C	Carbon NMR
^{1}H	Proton NMR
$CDCl_3$	Deuterated chloroform
CH_3CN	acetonitrile
DCB	1,4-Dicyanobenzene
DMF	Dimethylformamide
DMSO	Dimethyl sulfoxide
e^-	Electron
EI	Electron impact ionization
En	Dienophile
ET	Electron transfer
EtOAc	Ethyl acetate
eV	Electron volts
H^+	Proton
H_2O	Water
HRMS	High resolution mass spectrometry
LED	light-emitting diode
M	Molar concentration
MHz	Mega hertz
Min	Minute
mL	Milli liter
mm	Milli meter
mmol	Milli mole
nm	nano meter
NMR	Nuclear magnetic resonance
OLED	Organic light-emitting diode
PE	Petrol ether
PET transfer	Photoinduced electron
R_f	Retention factor
sat.	saturated
SC	Semiconductor
Sens	Sensitizer
TEMPO	(2,2,6,6-Tetramethyl-piiperidin-1-yl)oxyl
TLC	Thin layer chromatography
TPP^+	2,4,6-Triphenylpyrylium tetrafluoroborate
UV	Ultra violet
V	Volt

7.2 CONFERENCE CONTRIBUTIONS AND PUBLICATIONS

Conference Contributions

22.07 – 23.07.2011 **HFMC** in Heidelberg

Poster-presentation: “Heterogeneous Photocatalysis in organic synthesis”

07.08 – 12.08.2011 **ICP 2011: 25th Internation Congress on Photochemistry** in Beijing (China)

Poster-presentation: “Heterogeneous Photocatalysis in organic synthesis”

02.04 – 04.04.2012 **502. WE-Heraeus-Seminar on Harvesting Light** in Bad Honef

Poster-presentation: “Applying Heterogeneous Photocatalysis on Enantioselective Organic Chemistry"

13.07 – 21.07.2012 **XXIV IUPAC Symposium on Photochemistry** in Lissabon (Portugal)

Oral presentation: "Applying heterogeneous Photocatalysis on Enantoselective organic Synthesis"

26.08 – 30.08.2012 **4th EuCheMS Chemistry Congress** in Prague (Czech Republic)

Poster-presentation: “Applying Heterogeneous Photocatalysis on Enantioselective Organic Chemistry"

15.09 – 27.09.2012 **ICCOS 2012** in Moscow (Russia)

Oral presentation: "Heterogeneous Photocatalysis in Organic Synthesis"

7. APPENDIX

10.04 – 11.04.2013 **FineCat 2013** in Palermo (Italy)

Oral presentation: "Heterogeneous Photocatalysis in Organic Synthesis"

Publications

"Visible light promoted stereoselective alkylation by combining heterogeneous photocatalysis with organocatalysis" Cherevatskaya, M., Neumann, M., Füldner, S., Harlander, C., Kümmel, S., Dankesreiter, S., Pfitzner, A., Zeitler, K., König, B. *Angew. Chem. Int. Ed.* **2012**, *51*, 4062-4066.

"On the properties of the anions derived from α-deprotonation of α-(o-carboran-1-yl)- and α-ferrocenyl-1-alkylbenzotriazoles" Moiseev, S. K.; Cherevatskaya, M. A.; Verbitskaya, T. A.; Glukhov, I. V.; Peregudov, A. S.; Kalinin, V. N. *Russian Chemical Bulletin* **2012**, *61*(10), 1933-1942.

"Heterogeneous semiconductor photocatalysts" Pfitzner, A., Dankesreiter, S., Eisenhofer, A., Cherevatskaya, M. *Chemical Photocatalysis* (De Gruyter) **2013,** 211-246

7.3 CURRICULUM VITAE

Personal data

Maria Alexandrovna Cherevatskaya

born on 05.02.1987 in Usinsk (Russian Federation)

unmarried

maria.cherevatskaya@gmail.com

Education

04/2010 – 09/2013

PhD supervised by Prof. Dr. Burkhard König at the Institute of Organic Chemistry, University of Regensburg, in the research area of Photocatalysis, sponsored by the *GRK 1626 "Chemical Photocatalysis"* with a *PhD scholarship*.

"Photocatalytic Transformations Catalyzed by Inorganic Semiconductors and Iridium Complexes"

- Application of heterogeneous photocatalysis in organic synthesis
- Application of new Ir(III) complexes in photocatalytic organic transformations

09/2004 – 02/2010

University studies in Mendeleev Russian University of Chemistry and Technology, Moscow, Russia

"On the properties of the anions derived from α-deprotonation of α-(o-carboran-1-yl)- and α-ferrocenyl-1-alkylbenzotriazoles"

07/2009 – 08/2009	Leipzig University Research stay with Prof. Dr. Eva-Maria Hey-Hawkins DAAD scholarship “Synthesis of Carborane Derivatives”
09/1997 – 05/2004	Secondary School in Usinsk, Russian Federation
09/1994 – 05/1997	Elementary School in Usinsk, Russian Federation

Additional qualifications

Languages	Russian (native speaker), English (business fluent), German (basic knowledge)
Chemical Analysis	NMR, UV-Vis spectrophotometer, Cyclic Voltametry, Chromatography
EDP	ChemDraw, MestreNova, MS Office, Corel Draw

7.4 ACKNOWLEDGEMENTS

First and foremost I would like to thank my supervisor Prof. Dr. Burkhard König. I want to express my sincere gratitude to him for giving me an opportunity to visit Germany and work in his research group and for all kind of help and support he offered me throughout these years and possibility independently try my ideas. I am very happy to stay in Regensburg for my PhD in his group.

I am very thankful to Prof. Dr Arno Pfitzner and Prof. Dr. Axel Jacobi von Wangelin for being the doctoral committee members of my thesis. I thank Prof. Dr. Robert Wolf for being the Chairman in my PhD defence.

I express my gratitude to Prof. Dr. Arno Pfitzner and Prof. Dr. Kirsten Zeitler for the fruitful collaborative projects.

I thank all members of the central analytical department, especially Fritz Kastner and Georgine Stühler for recording 2D NMR spectra, Wolfgang Söllner, Carola Prockl and Josef Kiermair for recording mass spectra. I thank Peter Kreitmeier for developing microreactor technik and providing help in technical questions.

I would like to thank Dr. Rudi Vasold and Simone Strauβ for HPLC, Ernst Lautenschlager for his help in all technical questions. I thank Susanne Schulze for being so nice and kind and fast regarding chemical orderings. I would like to gratefully thank Regina Hoheisel for helping in CV measurements and Britta Badziura and Petra Hilgers for help in organizational questions with GRK 1626 " Chemical Photocatalysis".

I thank GRK 1626 " Chemical Photocatalysis" for the financial support during my stay in Regensburg and giving the possibility to take part in all conferences I participated. And of course I am thankful to all guys from Graduate College for efficient meetings and funny moments, I learned a lot.

I am grateful to Stefan Dankesreiter for the collaboration and successfully bringing two different fields of chemistry in one fruitful project.

I owe my thanks to all my present and past co-workers in the König group and who made my stay in Regensurg colourful and exciting. Thank you for coffee breaks and after work beers and getting together and PhD parties.

I am deeply thankful to my lab mates Tascha, Tanja, Stefan and Thomas – we have shared a good time together, I was happy to see you first right in the morning during my stay in the lab 32.1.27.

7. APPENDIX

Thank you….:

Durga: for being a close friend, I found support every time I asked you something and I was soothing every time we talked.

Andi: for interesting discussions and support in scientific and personal questions. Thank you for being a close friend. And of course for joint car trips.

Sanne: for the enjoyable beer evenings with long discussions and training my german language, I promise to continue….

Tascha: for seeing you every morning and being my friend-lab mate. I am so thankful for that month leaving in your apartment! You helped a lot!

Thea: for being so kind and helpful, thank you for the last experiment!

Anna: for sharing the lab course and help.

Majkl: thank you for being a kind person and always being ready to help.

Tanja and Evgeny: for supporting me in the beginning of my stay here.

I would like to thank Andi and Durga for proofreading parts of the manuscript for this thesis and Thea for helping in translating the Zusammenfassung to german language.

My grateful thanks to my colleagues and friends whom I am not personally mentioning here, everyone has put a significant part to make my stay in Regensburg unforgettable. And especially the ski trips with you guys deserve special thanks!

I will be eternally grateful to my parents for raising me to be the person I am now and for loving and supporting me in every way I could ever think of for the last 26 Years. I am happy to see you both together, you are the fundamental for me. I cannot thank you enough! I am thankful to my sister Nastya, you are with me from my birth, we are close even living in different places, I am happy to have you in my life.

Vitalik: there will not be enough words. Thank you for support and love, thank you for changing my life and bringing me to the point I am in now and the future events and the time being together and our unexpected *a priori* successful project. I am happy to meet you and have you in my life. I love you.